UNIVERSITÀ DEGLI STUDI DELLA TUSCIA DI VITERBO

DIPARTIMENTO DI SCIENZE ECOLOGICHE E BIOLOGICHE

Corso di Dottorato di Ricerca in

GENETICA E BIOLOGIA CELLULARE – XXVIII

"*Analysis of the role of Werner Helicase Interacting Protein 1 in response to replication stress*"

(s.s.d. BIO / 11)

Tesi di dottorato di:

Dott. Giuseppe Leuzzi

Coordinatore del corso

Prof. (Giorgio Prantera)

Tutore

Dott.ssa (Annapaola Franchitto)

Data della discussione

06/05/2016

Dedicated to

my grandparents

INDEX

SUMMARY **1**

1. INTRODUCTION **3**

THE BASIC OF EUKARYOTIC DNA REPLICATION 4

Initiation of DNA Replication 5

Origins firing and chain elongation 5

Termination of DNA Replication 7

DNA REPLICATION STRESS 8

Causes of Replication Stress 8

Consequences of Replication Stress 11

RESPONSE TO REPLICATION STRESS 12

DNA Damage Checkpoint 12

The Replication Checkpoint 14

ATR signaling 16

RESTARTING MECHANISMS OF STALLED FORKS 18

Fork Repriming and Translesion Synthesis 20

Fork Reversal 21

Regulation of replication fork restart mechanisms 22

STABILIZATION AND PROTECTION OF STALLED FORKS 24

Fork Protection Factors 24

Cellular nucleases involved in fork degradation 27

Physiological function of fork protection 28

THE WERNER HELICASE INTERACTING PROTEIN 1 (WRNIP1/WHIP1) 29

Evidences supporting WRNIP1 role during Replication Stress 30

2. AIM **33**

3. RESULTS **34**

WRNIP1 IS REQUIRED FOR PROTECTION AND RESTART OF STALLED FORKS UPON REPLICATION STRESS 34

MRE11 DEGRADATES NASCENT DNA STRAND AT STALLED FORKS IN ABSENCE OF WRNIP1 41

WRNIP1 DEPLETION PRODUCES PARENTAL-STRAND ssDNA ACCUMULATION AND RAD51 DESTABILIZATION AFTER FORK STALLING 43
RAD51 AND MRE11 ARE DIFFERENTLY RECRUITED TO STALLED REPLICATION FORKS IN WRNIP1-DEFICIENT CELLS ... 49
RAD51 PROTECTS NASCENT DNA STRAND FROM DEGRADATION AFTER REPLICATION STALLING IN WRNIP1-DEFICIENT CELLS ... 51
WRNIP1 STABILIZES RAD51 ON STALLED FORKS ... 54
LOSS OF WRNIP1 OR ITS ATPase ACTIVITY LEADS TO DNA DAMAGE ACCUMULATION AND CELL DEATH AFTER REPLICATION STALLING ... 58
UNPROTECTED STALLED FORKS LEAD TO CHROMOSOMAL INSTABILITY IN WRNIP1-DEFICIENT CELLS ... 61

4. DISCUSSION ... 66

5. MATERIALS AND METHODS ... 72
CELL LINES AND CULTURE CONDITIONS ... 72
CHEMICALS ... 72
SITE-DIRECT MUTAGENESIS AND CLONING ... 72
PLASMIDS AND RNA INTERFERENCE ... 73
DNA FIBER ANALYSIS ... 73
IN SITU PLA ASSAY ... 74
CO-IMMUNOPRECIPITATION, CELL FRACTIONATION AND WESTERN BLOT ... 74
CldU CO-IMMUNOPRECIPITATION OF PROTEINS AT STALLED FORKS ... 76
NEUTRAL AND ALKALINE COMET ASSAY ... 77
IMMUNOFLUORESCENCE ... 77
LIVE/DEAD STAINING ... 78
CHROMOSOMAL ABERRATION ANALYSIS ... 78
STATISTICAL ANALYSIS ... 79

6. REFERENCES ... 82

7. ACKNOWLEDGMENTS ... 96

SUMMARY

Genome instability is a common feature of cancer cells. Most of the chromosomal abnormalities arising in tumours come from defective DNA replication (Abbas et al., 2013; Aguilera and Gómez-González, 2008; Branzei and Foiani, 2010; Zeman and Cimprich, 2014). For this reason, accurate handling of stalled replication forks is of paramount importance for the maintenance of genome stability. Recently, it has been demonstrate that RAD51 recombinase is involved in protecting stalled replication forks from nucleolytic attack by MRE11, which otherwise can seriously threaten genome stability (Hashimoto et al., 2010; Schlacher et al., 2011). However, the identity of other factors that can collaborate with RAD51 in this task and how this pathway operates are still poorly elucidated.

In this study, we have identified a previously uncharacterized function of the human Werner helicase interacting protein 1 (WRNIP1) as a factor working in conjunction with the RAD51 recombinase in response to replication stress.

We show that WRNIP1 is directly involved in protection and restart of stalled replication forks following replication stress. We also demonstrated that WRNIP1 is required for preventing uncontrolled MRE11-mediated degradation of nascent DNA strand at stalled replication forks. WRNIP1 depletion results in a large enhancement of parental-strand ssDNA accumulation produced by the action of MRE11 nuclease activity, but it does not lead to a greater amount of RAD51 bound to chromatin. Thus, WRNIP1-deficient cells show an overt RAD51 destabilization after fork stalling.

We establish that WRNIP1 is directly recruited to stalled replication forks and cooperates with RAD51 to safeguard fork integrity, by promoting RAD51 stabilization on ssDNA. We further demonstrate that replication fork protection does not require the ATPase activity of WRNIP1 that is however essential to achieve the recovery of perturbed replication forks. Loss of WRNIP1 or its catalytic activity exhibit high sensitivity to HU-induced fork stalling, leading to DNA damage accumulation and cell death, and that unprotected stalled forks is responsible for chromosomal instability arising, after fork stalling, specifically in WRNIP1-deficient cells. Interestingly, downregulation of the anti-recombinase FBH1, which promotes the removal of RAD51 from chromatin, can compensate for loss of WRNIP1 activity. Indeed, attenuation of replication fork degradation and chromosomal aberrations have been observed in WRNIP1-deficient cells after FBH1 depletion, due to

enhancement of the amount of RAD51 chromatin-bound. Consistently, over-expression of RAD51 in WRNIP1-deficient cells counteracts stalled replication fork degradation. Therefore, our results clearly indicate that WRNIP1 plays a crucial role in stabilizing RAD51 to stalled forks, protecting them from the MRE11-dependent degradation. Furthermore, we establish that WRNIP1 is implicated in the stalled fork resumption through its ATPase activity.

Altogether, our work suggests a molecular basis for the role of human WRNIP1 in safeguarding genome stability in response to replication stress. In particular, they unveil a unique role for WRNIP1 as a replication fork-protective factor in maintaining genome stability.

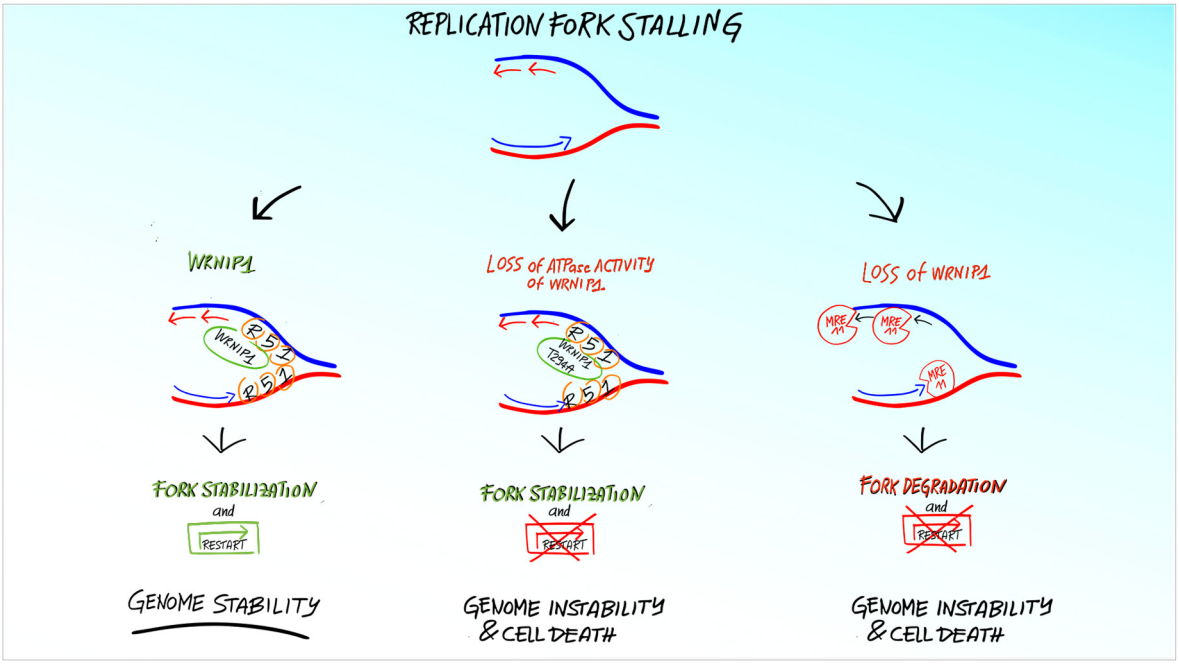

Highlights:

- WRNIP1 protects stalled replication forks from degradation;
- ATPase activity of WRNIP1promotes stalled replication forks restart;
- WRNIP1 contributes to the stabilization of RAD51 on stalled replication forks;
- FBH1 downregulation compensates for loss of WRNIP1 activity.

1. INTRODUCTION

DNA replication is a highly complex cellular process by which eukaryotic cells accurately and efficiently duplicated their genome, generating identical sets of chromosomes, thereby transmitting genetic information to daughter cells. Efficient and error-free DNA replication is the key for faithful duplication of chromosomes before their segregation. Moreover, DNA replication is tightly monitored to ensure that the genome is replicated just once per cell cycle, before mitosis begins (Branzei and Foiani, 2010).

DNA replication is not only crucial to cellular division but also plays a crucial role in the maintenance of genomic integrity (Watanabe and Maekawa, 2010). Both exogenous and endogenous damaging agents constantly urge DNA, so that DNA lesions frequently occur. Thus, cells need to deal with DNA lesions during replication by activating an adequate cellular response. If not properly repaired, these lesions may hinder replication fork progression leading to fork arrest (*fork stalling*), which causes alterations of DNA replication dynamic known as "*replication stress*" (Zeman and Cimprich, 2014).

Since replication stress has considered the primary source of genome instability, cells must monitor fork integrity and they need to match DNA replication with other cellular processes, such as chromatin reassembly and the establishment of cohesion between sister chromatids. The success of all these processes is crucial to avoid DNA breaks, chromosomal rearrangements, and mutations that can cause not only the loss of cell viability, but also a large number of human syndromes, including premature aging, various cancer predispositions and genetic abnormalities (Branzei and Foiani, 2010). Therefore, it seems logical that studying DNA replication and the pathways that suppress the instability of replication fork is directly relevant to understanding the mechanisms by which cancers and other pathological disorders arise.

THE BASIC OF EUKARYOTIC DNA REPLICATION

DNA replication is the mechanism by which DNA polymerases synthesize a DNA strand complementary to the original template strand. This process allows the cell to duplicate a single DNA double helix into two DNA helices, so that the high-fidelity passage of genetic information from parental cell to daughter cells is assured. For this reason, DNA replication has to occur without errors. In G_1 phase of the cell cycle, many of the DNA replication regulatory processes are initiated. In eukaryotes, the vast majority of DNA synthesis occurs during S phase of the cell cycle, and the entire genome must be unwound and duplicated to form two daughter copies. During G_2 phase, any damaged DNA or replication errors are corrected. Finally, one copy of the genomes is segregated to each daughter cell at mitosis (M) phase (Leman and Noguchi, 2013). Each of these daughter copies contains one strand from the parental duplex DNA and one nascent antiparallel strand. This mechanism, conserved from prokaryotes to eukaryotes, is known as semiconservative DNA replication (Meselson and Stahl, 1958) and it is organized into three distinct phases: initiation, elongation and termination (Fig. 1).

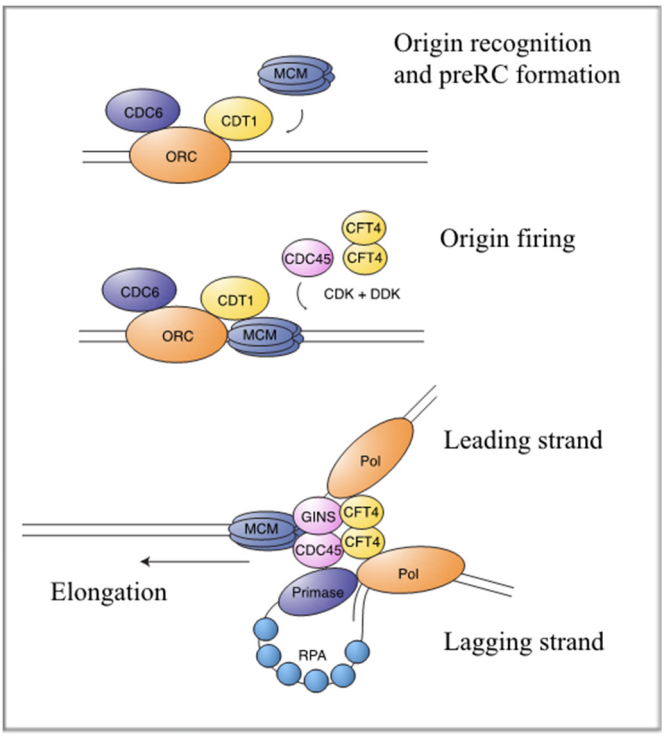

Figure 1. Schematic representation of different steps in eukaryotic DNA replication. Origin recognition and formation of the preRC complex comprises binding of ORC to DNA and subsequent recruitment of the Mcm2-7 helicase complex by Cdc6 and Cdt1. Firing of origins is brought about by the loading of Cdc45 and other firing factors and requires CDK and DDK activity and (see text). Subsequently, ORC, Cdc6 and Cdt1 dissociate from DNA and replication chain elongation occurs by the coordinated action of polymerases and other components of the replication complex. Modified from (Claus Storgaard Sørensen, 2011).

Initiation of DNA Replication

In eukaryotes, replication initiates from multiple regions distributed along chromosomes, know as *replication origins.* In budding yeast, replication origins have been efficiently mapped owing to clear consensus sequences (Wyrick et al., 2001). However, this is more difficult in higher eukaryotes. Although origin sequences are not clearly defined in mammals, they have been associated with certain features, which help to predict potential replication initiation sites, such as AT rich sequences (Altman and Fanning, 2004; Paixão et al., 2004) and matrix attachment regions.

Replication initiation begins when the origins are marked by the formation of a pre-replicative complex (preRC) in G1, before DNA replication, through the binding of the origin recognition complex (ORC). After ORC, additional replication factors, such as Cdc6, Cdt1 and the hexameric MCM2-7 complex, are loaded onto chromatin (Masai et al., 2010). Because the preRC cannot be assembled later in the cell cycle, the maximum number of origins available for a single S phase is determined during the licensing state, which occurs in G1 when the preRC is formed. Thus, preRCs mark "potential" origins, but only a subset is licensed for use during each round of replication (Edwards et al., 2002; Hyrien et al., 2003).

Origins firing and chain elongation

The *replisome* complex, which is a massive complex coordinating many proteins, assembles at replication origins and subsequently initiates bidirectional DNA synthesis in S phase in a process called *origins firing* (Leman and Noguchi, 2013).

The critical step for DNA replication is the conversion of pre-RC into initiation complex (IC). This step requires phosphorylation activity of CDK and CDC7 (Hoang et al., 2007; Sclafani, 2000), which mediate activation of preRC allowing the loading of RPA, MCM10 and CDC45 onto chromatin to carry out origins firing (Zhu et al., 2007). Importantly, not all licensed origins are fired. Indeed, most of them, defined *"dormant origins",* remain quiescents during normal replication although they have a crucial role during replication stress (Chen et al., 2015).

At the molecular level, the geometry of DNA replicating site is a *fork-like DNA structure*, where the DNA double helix is open or unwound, exposing unpaired DNA nucleotides for

recognition and base pairing for the incorporation of free nucleotides into double-stranded DNA (Leman and Noguchi, 2013).

Parental DNA is unwound by the CMG helicase complex. CMG is composed of the CDC45 protein, the mini-chromosome maintenance 2-7 complex (MCM2–7) and the tetrameric GINS complex (Ilves et al., 2010). CMG moving in the 3'-5' direction translocates along the leading strand while physically displacing the complementary strand by steric exclusion (Costa et al., 2014). DNA synthesis on the leading and lagging strands is performed by the Pol ε and Pol ε polymerases respectively, which make contact with CMG and PCNA (proliferating cell nuclear antigen). Polymerase ε (epsilon) synthesizes DNA in continuous manner, as it follows the same direction of DNA unwinding. This strand is known as "leading strand". Polymerase δ (delta) synthesizes DNA on the opposite template strand in a discontinuous fashion and this strand is termed "lagging strand". Because DNA polymerases require a primer on which to begin DNA synthesis, first, polymerase (Polα) acts as a replicative primase. Polα is associated with an RNA primase, and this complex accomplishes the priming task by synthesizing a primer. Importantly, this priming action occurs at replication initiation to begin leading and lagging strands synthesis (Georgescu et al., 2015) (Fig. 2).

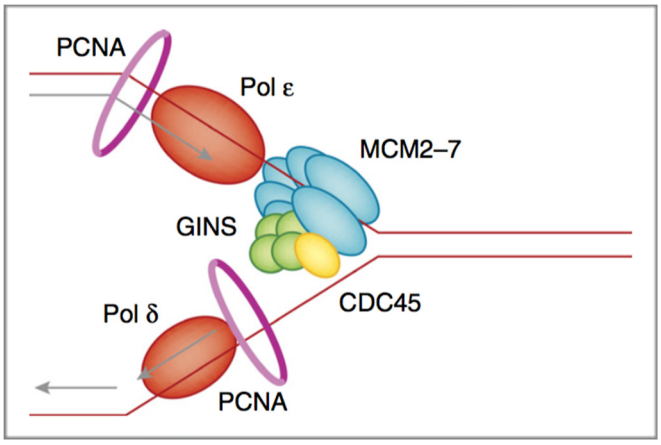

Figure 2. Illustration of replication fork and key components of replisome. Parental DNA is unwound by the CMG helicase complex. CMG is composed of the CDC45 protein (yellow), the minichromosome maintenance 2–7 complex (MCM2–7, blue) and the tetrameric GINS complex (green). CMG encircles the ssDNA on the leading strand and unwinds DNA by steric exclusion, moving in the 3′-to-5′ direction. DNA synthesis on the leading and lagging strands is performed by the Pol ε and Pol δ (orange) polymerases, respectively, which make contact with CMG. The sliding clamp PCNA (pink circle) acts as a processivity factor for the polymerases. From (Berti and Vindigni, 2016)

Termination of DNA Replication

Owing to stochastic origin firing and variable rates of replisome progression, the location and timing of eukaryotic termination is variable, making this process difficult to study. Little is known about termination process of DNA synthesis and most of our knowledge comes from studies on plasmid replication in *Xenopus* egg extracts or yeast chromosomal replication. Eukaryotic DNA replication terminates when converging replication forks meet (Santamaria, 2000). This process involves local execution of DNA synthesis, decatenation of daughter molecules and replisome break up, not necessarily in the following order. A large amount of evidence from simian virus 40 (SV40) and yeast systems suggests that sister chromatids become intertwined (catenated) at replication termination sites, and that the resolution of these structures, for successful completion of termination requires DNA topoisomerase II (TOPII) (Dewar et al., 2015).

Given the complexity of replication process, cells need to balance accuracy, speed, and the consumption of relevant resources, such as nucleotides and replication factors, to complete replication and to limit replicative stress events, which are considered the primary source of genome instability.

DNA REPLICATION STRESS

A wide variety of factors, such as DNA replication errors, spontaneous chemical reactions, reactive metabolic products, exogenous environmental agents or some anticancer therapeutics can cause DNA damage. It is estimated that DNA damage occurs at a rate of 1.000 to 1.000.000 molecular lesions per cell per day (Hoeijmakers, 2009). Furthermore, cells are particularly vulnerable to DNA damage during DNA replication, because virtually all forms of DNA damage block DNA replication, causing *replication stress* (Allen et al., 2011), which can compromise genome integrity if not properly processed.

Replication stress is defined as a phenomenon that arises when genetic or environmental conditions lead to the replicative polymerase to move slowly and/or stall, potentially leading to fork collapse and generating genome instability. It can be generated by a wide range of physical obstacles, and usually results in physical structures, namely stretches of single-stranded DNA (ssDNA), which represents a hallmark of replication stress (Zeman and Cimprich, 2014).

Causes of Replication Stress

Although, replication stress arises from many different sources, one of the most commonly recognized sources of replication stress is down-regulation of limiting replication factors . Indeed, faithful DNA replication requires numerous factors, and their limitation can result in the slowing of replication fork progression and, ultimately, in stalling of replication fork. These replication factors include components of the replication machinery, histones, histone chaperones that package replicated DNA and the pool of nucleotides (dNTPs) (Aguilera and García-Muse, 2013). Nucleotides are the building blocks for DNA synthesis and their titration is one of the key aspects during replication. Indeed, the reduced level of dNTPs slows down the progression of the forks and increases the chance of fork stalling per se (Anglana et al., 2003; Poli et al., 2012). Hydroxyurea (HU), a drug used to treat resistant chronic myelocytic leukemias and other tumors (Madaan et al., 2012; Patnaik and Tefferi, 2016), inhibits ribonucleotide reductase (RNR) and creates imbalances in the cellular dNTPs, which affect DNA polymerases and contribute to replication stress (Yarbro, 1992).

An excess of replication origin firing can also be a source of replication stress, through the exhaustion of factors essential for DNA synthesis and for the maintenance of fork integrity,

including RPA protein, which protects single-strand DNA (ssDNA). Indeed, the level of RPA becomes limiting when the number of replication origins increases. As a result, new ssDNA stretches cannot be protected by RPA, and therefore, the replication forks become more susceptible to collapse and breakage (Toledo et al., 2013).

In addition to limiting replication factors, a wide variety of obstacles can hamper replication fork progression leading to replication stress. These obstacles include DNA lesions, DNA-protein complexes and DNA sequences that can form secondary structures (Gelot et al., 2015). Some DNA sequences are intrinsically challenging for the replication machinery. For instance, common fragile sites (CFS) are normal components of human genome, unusually prone to breakage. These human genomic regions are difficult-to-replicate and display frequent events of fork stalling (Debatisse et al., 2012; Franchitto and Pichierri, 2011, 2014). In addition, trinucleotide repeats can form secondary DNA structures (hairpins, triplexes, etc) that are thought to block replication fork progression (Kim and Mirkin, 2015; McMurray, 2010). Recently, G-quadruplexes, secondary structures which form in GC-rich DNA, have also been highlighted as a significant source of DNA damage (Bochman et al., 2012; Paeschke et al., 2013).

In response to base damage, such as abasic site, stretches of ssDNA can be exposed at replication forks as a consequence of replicative helicases continuing to unwind the parental DNA while the replicative DNA polymerases are stalled. This uncoupling between helicase and polymerase activities is probably not the sole cause of accumulation of ssDNA at stalled forks. Indeed, agents that create physical blocks to helicase movement, such as inter-strand cross-links (ICLs) or torsional stress induced by the DNA topoisomerase I cleavage complex, are not expected to promote uncoupling. However, ssDNA can be detected in presence of these agents, suggesting a degradation process of newly-synthesized DNA, through the combined action of nucleases and DNA helicases, thereby creating ssDNA at fork junction (Berti and Vindigni, 2016).

Some studies have suggested that replication stress events can occur when replication forks and transcription complexes collide. Indeed, replication and transcription machineries both operate on DNA, so that, it is not unusual that the two processes interfere with each other, and that collision between replication and transcription complex occurs (Bermejo et al., 2012; Helmrich et al., 2013). Moreover, it has been proposed that replication stress can be induced by nucleotide misincorporation. Indeed, rNTPs stall the replicative polymerases,

and bypass of these rNTPs requires the DNA damage tolerance (DDT) pathways (Nick McElhinny et al., 2010) discussed above.

In the context of tumorigenesis, the oncogene-induced replication stress is an important matter (Gorgoulis and Halazonetis, 2010; Negrini et al., 2010). Oncogene activation alters DNA replication dynamic leading to increased replication stress and DNA breaks. There are several proposed mechanisms for the induction of replication stress upon oncogene activation. Two of the proposed mechanisms are related to an inappropriate/insufficient or excessive-usage of replication origins (Hills and Diffley, 2014). Overexpression of cyclin E reduces the number of replication origins that are licensed during G1 (Ekholm-Reed et al., 2004). As a consequence, replication stress increases in S-phase due to the shortage of back-up origins to cope with stalled forks. In contrast, the overexpression of certain oncogenes, such as MYC and RAS, has the opposite effect since it increases the origins firing (Dominguez-Sola et al., 2007) leading to a depletion of the cellular dNTPs (Fig. 3).

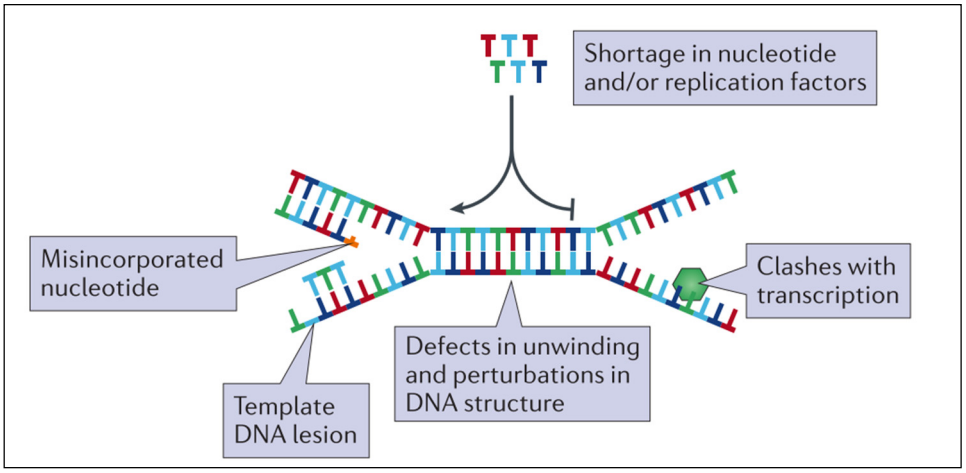

Figure 3. Schematic representation replication stress causes. Replicative stress results from endogenous or exogenous obstacles to DNA replication. These include the incorporation of incorrect nucleotides or defects in DNA unwinding, each of which results in a structural hindrance to fork progression; other similar obstacles include lesions in the template DNA or the presence of protein complexes that are involved in transcription. A shortage of nucleotides or replication factors can also impair the progression of ongoing DNA replication. Modified from (Dobbelstein and Sørensen, 2015)

Consequences of Replication Stress

Genome instability is a common feature of cancer cell. Most of the chromosomal abnormalities founded in tumors arise from defective DNA replication, pointing out the role of replication stress in cellular transformation process (Gaillard et al., 2015).

In silico analysis of homozygous and heterozygous focal deletions in cancer samples and cell lines revealed that most of the heterozygous deletions in transformed cells are found in already defined CFS or in large genes (Rajaram et al., 2013). Similar deletions can be induced by the treatment of cells with aphidicolin (Aph), an inhibitor of replicative DNA polymerases alfa, delta and epsilon, which induces replication stress (Baranovskiy et al., 2014; Krokan et al., 1981). These data indicate that replication stress is likely the source of most of the passenger deletions during transformation, suggesting a major role for replication stress in cancer genome development.

Another evidence supporting replication stress as driving force of malignant transformation is oncogene activation, which suggests that mild levels of replication stress allow the accumulation of genome instability that help to develop tumorigenesis. In addition, the connection between replication stress and tumorigenesis is further strengthened by the findings that the treatment of mice with hydroxyurea promotes leukemogenesis.

Lastly, replication stress might also lead to chromosomal instability (CIN) through an increase in defects on chromosome segregation. Consistently, the analysis of CIN+ versus CIN- colon adenocarcinoma cells reveals the presence of replication stress only in CIN+ cells, along with corresponding chromosome segregation defects (Burrell et al., 2013).

Since replication stress has deleterious effects on genome stability, cells replicating their DNA must be able to initiate an adequate replication stress response to minimize the risk of chromosomal rearrangement accumulation.

RESPONSE TO REPLICATION STRESS

To reduce replication stress, eukaryotic cells are well equipped of a genomic maintenance apparatus. This sophisticated apparatus allows the *replication stress response*, and it includes a set of DNA surveillance mechanisms called the DNA damage checkpoints (Jossen and Bermejo, 2013). The importance of the cellular response to replication stress is highlighted by the array of genetic diseases, as well as increased cancer predisposition, associated with alterations in the genes that participate in the response (Zeman and Cimprich, 2014).

Given the complexity of the DNA replication stress response, here, a brief overview of the network will be provided, and only proteins and pathways immediately relevant to the present study will be described in detail.

DNA Damage Checkpoint

The DNA damage checkpoint network is considered a signal transduction cascade consisting of three major groups of proteins (sensors, transducers and effectors) that act in concert to promote cell-cycle arrest, DNA repair, transcription and apoptosis (Friedberg et al., 2006) (Fig. 4).

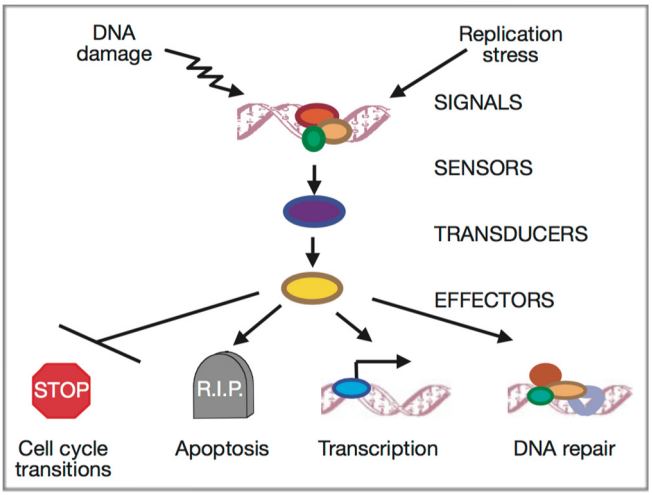

Figure 4. Conceptual organization of the signal transduction of checkpoint responses. DNA damages are recognized by sensor proteins. The signals are transmitted to transducers (mainly kinases) and the regulated transducer molecules activate effector kinases, which in turn promote cell-cycle arrest, DNA repair, transcription and apoptosis. (Zhou and Elledge, 2000)

The DNA damage checkpoint network is under control of members of the phosphoinositide 3-kinase-related kinase (PIKK) family. In mammals, signals initiated by the sensor very rapidly transduce to ATM and ATR kinases, which, in turn, phosphorylate a great number of substrates. ATM is 350 kDa oligomeric protein that exhibits significant homology to the PIKK. In humans, mutations in ATM cause ataxia telangiectasia, a rare autosomal recessive human disorder, characterized by genome instability, immunodeficiency and cancer predisposition (Shiloh, 1997). Cells lacking ATM are viable and patients and mice survive, suggesting that ATM is not essential for normal cell-cycle progression and cell differentiation. Activated ATM phosphorylates many proteins, including BRCA1, NBS1, CHK2 and p53, including itself (Shiloh and Kastan, 2001).

ATR was discovered in the human genome database as a gene with sequence homology to ATM and Rad3, hence the name ATR. The gene encodes a protein of 303 kDa with a C-terminal kinase domain and regions of homology to other PIKK family members. Unlike ATM, ATR null mice are embryonic lethal and mutations causing a partial loss of its activity have been reported to be associated with the human autosomal recessive disorder Seckel syndrome (O'Driscoll et al., 2003). As ATM, ATR is capable of phosphorylating serine or threonine residues in SQ/TQ sites (Abraham, 2001). Once the active ATR is translocated to replication foci, it can phosphorylate and activate CHK1. This model is consistent with the observation that CHK1 is also essential for embryonic cell viability (Liu et al., 2000).

In response to DNA damage, the PIKK family kinases ATM and ATR phosphorylate target proteins on serine and threonine residues, thereby activating the DNA damage checkpoint. The ATM pathway responds to the presence of double-strand breaks (DSBs), and acts during all phases of the cell cycle. The ATR pathway can respond to agents that interfere with the function of DNA replication forks, such as ultraviolet light (UV) and HU. DNA-alkylating agents might activate both pathways, although these types of DNA damage impose stress on progressing replication forks, they clearly also could elicit strand breaks under some circumstances (Zhou and Bartek, 2004) (Fig. 5).

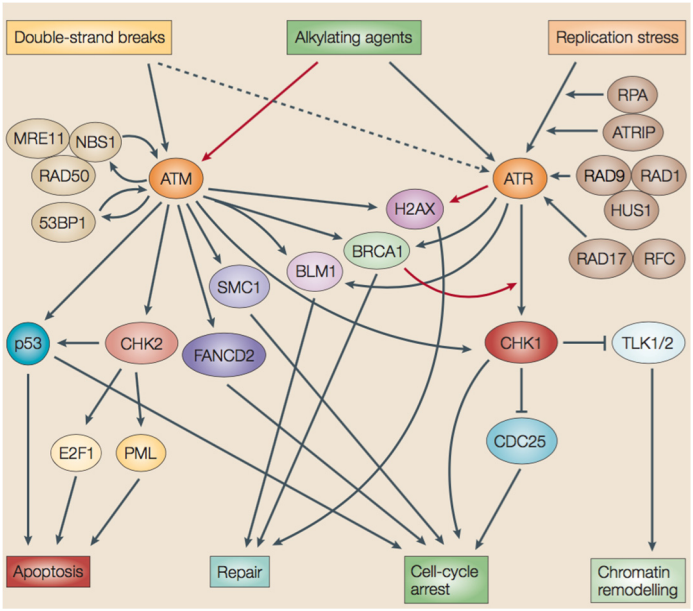

Figure 5. DNA damage response signal-transduction network (Zhou and Bartek, 2004).

The Replication Checkpoint

In eukaryotic cells there are multiple checkpoints that operate along the entire cell cycle. G1 and G2 phases of the cell cycle are under the control of a single checkpoint pathway, while at least three checkpoint activities can be founded associated with S-phase (Bartek et al., 2004). This difference can be explained with the high susceptibility of DNA during replication as well as the intrinsic difficulties to duplicate, in efficient manner, complex genome as that of human cells. So, the S-phase is under the control of multiple and, in some ways, redundant checkpoints pathways. There is a replication-independent checkpoint pathway that is activated by the presence of DSBs and the replication-dependent checkpoint, which can be divided in two different sub-pathways: replication checkpoint and S/M checkpoint. These pathways respond to replication stress, thus, to stalling of replication machinery that can be caused by several factors as discussed below (Branzei and Foiani, 2005).

The replication checkpoint is required to preserve stability of stalled forks until the causes of replication stress have been removed/resolved; whereas the S/M checkpoint is needed to prevent premature entry in mitosis with unreplicated or damaged chromosomes. To slow-down S-phase progression, the replication checkpoint targets kinases responsible for origin firing, while the S/M checkpoint inhibits the Cyclin1/CDK1 activity.

Since these two replication-dependent checkpoints are triggered by the same signal at stalled fork, they can be considered as two facets of a common pathway, so that in this work they will be collectively referred to as replication checkpoint (Fig. 6).

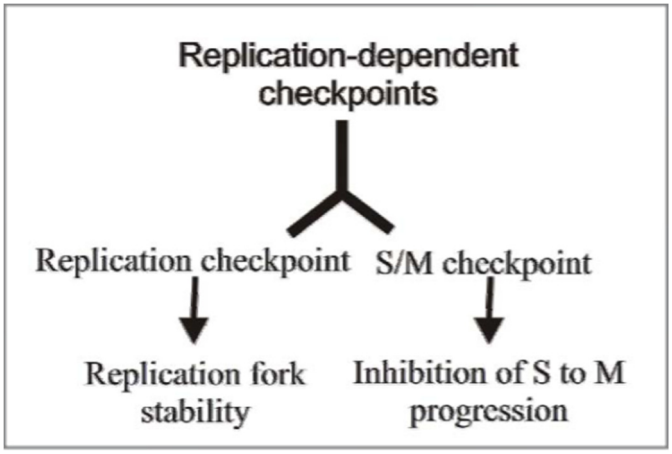

Figure 6. Schematic representation of the replication-dependent checkpoint operating in s-phase of cell cycle.

The two main functions of the replication checkpoint are maintenance of the integrity of the stalled forks and inhibition of the S/M transition. The first activity is not only important for prompt resumption of DNA synthesis once the arresting stimuli are relieved, but also to restrict access to recombination enzymes that could process replication intermediates at the fork after replisome disassembly, i.e. after replication fork collapse. On the other hand, the control of the S to M progression is essential to prevent mitotic entry with incompletely replicated DNA, a condition resulting in mitotic catastrophe and loss of cell viability. In addition, the replication checkpoint prevents firing of late origins, thus reinforcing the S/M blockage (Branzei and Foiani, 2005).

ATR signaling

The replication checkpoint is entirely controlled by the ATR kinase (Ataxia telangiectasia and Rad3-related), which "senses" replication blockage and propagates the checkpoint signal to replication, repair and cell cycle proteins, either directly or through the checkpoint kinase CHK1 (Cimprich and Cortez, 2008; Zou et al., 2003).

ATR responds to a broad spectrum of genotoxic agents that include UV, topoisomerase inhibitors, alkylating and cross-linking agents, as well as chemicals that interfere with DNA polymerization, such as Aph and HU (Byun et al., 2005; Cortez et al., 2001; Zhou and Elledge, 2000).

A lot of data obtained in different model systems indicates that when the polymerase encounters a lesion its progression is blocked, while the helicase keeps unwinding the DNA. The uncoupling between the stalled polymerase and the helicase generates a segment of ssDNA (Byun et al., 2005; Tercero et al., 2003).

ATR and its regulatory subunit ATRIP can sense fork stalling through their direct interaction with the ssDNA binding protein RPA (Ball et al., 2005; Zou et al., 2003). Association of ATR/ATRIP complex with chromatin leads to phosphorylation of several downstream targets, most notably the RAD9/RAD1/HUS1 complex (9.1.1 complex) that is recruited to stalled forks independently from ATR/ATRIP, but through another protein factor, RAD17, which binds directly to RPA (Abraham, 2001; Zou and Elledge, 2003). Recruitment of the RAD17/9.1.1 complex cooperates with ATR/ATRIP to determine full replication checkpoint activation and ATR-dependent phosphorylation of other targets (Zou et al., 2002). The 9.1.1 complex provides a docking station to other factors implicated in the replication checkpoint, facilitating subsequent phosphorylation by ATR. In other words, the 9-1-1 complex recognizes a DNA end that is adjacent to RPA-ssDNA stretch. Phosphorylation of several of the ATR targets also requires additional "mediators", such as Claspin and BRCA1. Claspin is necessary for CHK1 phosphorylation by ATR (Gottifredi and Prives, 2005). CHK1 is the downstream checkpoint kinase in response to fork stalling or DNA damage originated at the replication fork, and directly contributes to maintain integrity and competence of stalled forks (Feijoo et al., 2001; Lopes et al., 2001). Indeed, CHK1 induces cell cycle arrest by its inhibitory phosphorylation of CDC25, the phosphatase activating CDK1 and CDK2 . ATR activation has both a positive and negative effect on replication-origin firing in response to replication stress: it prevents new origin

firing by inhibiting replication initiation, through CHK1-mediated inhibition of the CDC7 kinase activity, but it also promotes firing of dormant origins within preexisting replication factories, thus allowing completion of DNA synthesis in the vicinity of perturbed replication forks (Fig. 7) (Costanzo and Gautier, 2003; Shechter et al., 2004).

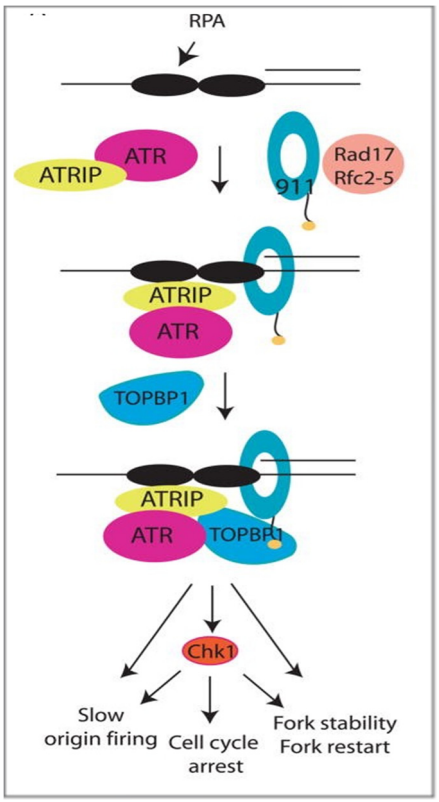

Figure 7. Schematic representation of ATR signaling activation. The ATR-ATRIP complex and the 9-1-1 complex are recruited to the ssDNA-5′ primer junction independently. RPA binds ATRIP and directs the Rad17-RFC complex to load the 9-1-1 checkpoint clamp at the 5′ primer junction. Loading of 9-1-1 brings the ATR activator TopBP1 to the damage site through an interaction involving two BRCT domains of TopBP1 and the phosphorylated C-terminal tail of Rad9 (see text). TopBP1 binds and activates ATR in an ATRIP-dependent manner, leading to phosphorylation of the downstream kinase Chk1 and other ATR effectors. In response to DNA damage or replication stress, ATR and its effectors ultimately slow origin firing and induce cell cycle arrest as well as stabilize and restart stalled replication forks. (Cimprich and Cortez, 2008)

Studies using Xenopus egg-extracts indicate that ATR/ATRIP and the 9.1.1. complexes are loaded to active origins also during unperturbed S phase, probably to supervise accurate timing of origin firing (Hekmat-Nejad et al., 2000). Likewise, the CHK1 kinase seems instrumental to normal S-phase progression. Consistently, biochemical data support in vivo evidence of an essential role of ATR and CHK1 during unperturbed cell growth, as shown by the embryonic lethal phenotype of ATR and CHK1-null mice (Brown, 2004; Sørensen et al., 2003).

If the large amount of work performed unveiled a lot of the mechanisms at the basis of the checkpoint activation and induction of cell cycle arrest, little is known about the branch of the checkpoint involved in maintaining stalled fork stability and restart. Indeed, how stalled forks are handled by eukaryotic cells and how DNA synthesis is recovered under different conditions is basically unclear.

RESTARTING MECHANISMS OF STALLED FORKS

Replication forks are vulnerable to stalling or collapse as they encounter obstacles on the DNA template, which can be unrepaired DNA damage, DNA-bound proteins or secondary structures. Similarly, chemical agents, like HU and Aph, inhibit replication elongation, leading to fork stalling or collapse (Kotsantis et al., 2015).

Because of redundancy in number of potential replication origins, higher eukaryotes including mammals, could easily overcome replication fork arrest by passive replication from a convergent fork (Kawabata et al., 2011). However, cells also possess several independent mechanisms that allow restart of replication from stalled forks, which are particularly important whenever passive replication is not possible (Yeeles et al., 2013).

In recent years, single-molecule analyses of replication, by using DNA combing or the DNA fibre technique and electron microscopy, have led to a better understanding of mammalian replication fork restart (Berti and Vindigni, 2016; Petermann and Helleday, 2010). Various proteins that are not part of the core replication machinery promote efficient replication fork restart through different modes. In mammalian cells, fork repriming, translesion synthesis (TLS) and fork reversal seem to response a wide range of stimuli that cause replication fork arrest allowing fork restart (Fig. 8) (Berti and Vindigni, 2016; Petermann and Helleday, 2010).

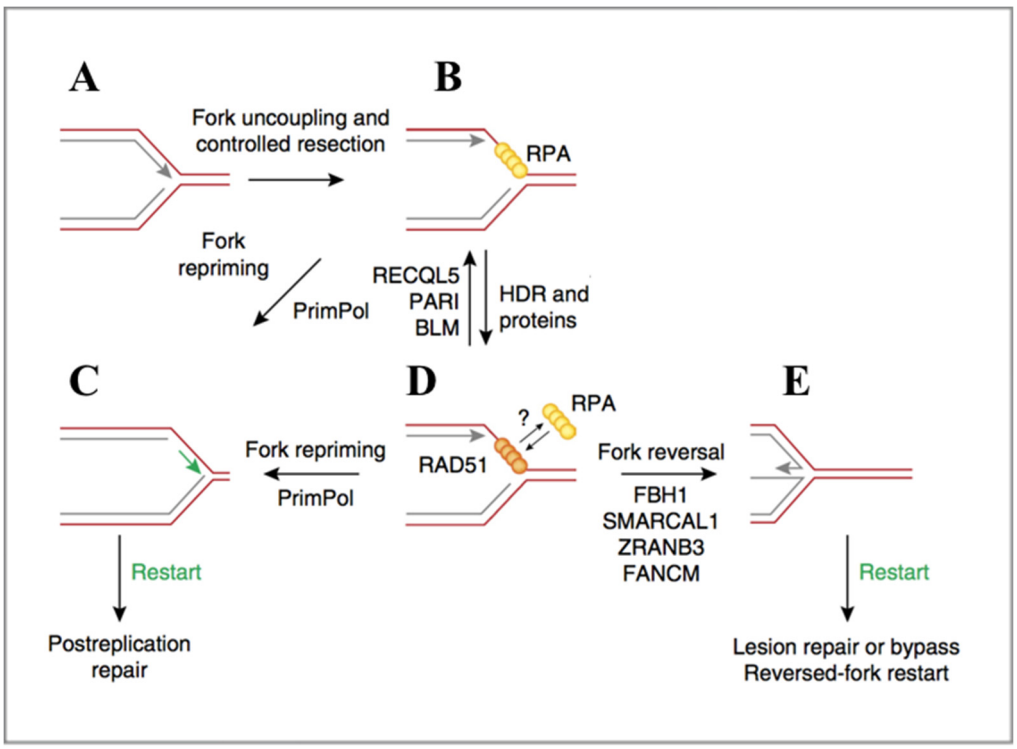

Figure 8. Mechanisms of replication-fork processing and restart. Different mechanisms may resume DNA synthesis when replication forks are stalled. **(A-B)** Replication-fork uncoupling leads to ssDNA accumulation at the fork junction through functional dissociation of the MCM helices and the stalled polymerase. Alternatively, fork uncoupling may result from nuclease-mediated resection of stalled forks. ssDNA is rapidly coated by the ssDNA-binding protein RPA (yellow spheres). **(C)** Fork repriming. DNA synthesis can be reprimed (green arrow) and reinitiated ahead of a lesion or block. The resulting gaps are repaired post replicatively by a recombination-based mechanism or by specific translesion synthesis (TLS) polymerases. TLS polymerases may also function at stalled replication forks to ensure continued DNA synthesis through damaged templates (not shown). **(D)** Fork reversal. A controlled resection and uncoupling event at stalled forks promotes loading of RAD51 (orange spheres) and primes fork reversal **(E)**. The exact location of RAD51 binding within forks is not known. Fork reversal prevents collisions between the moving fork and a block or lesion, allowing the lesion to be repaired by the DNA repair machinery. Modified from (Berti and Vindigni, 2016)

Fork Repriming and Translesion Synthesis

Base modifications limited to one strand of the DNA template do not produce a physical block for the moving replicative helicase, but can stall polymerases and uncouple helicase unwinding from DNA synthesis. In contrast, lagging-strand DNA lesions are well tolerated because of the inherently discontinuous nature of Okazaki-fragment synthesis and maturation, leading strand lesions represent a major obstacle for processive DNA synthesis (Yeeles et al., 2013). In these cases, DNA-damage tolerance (DDT) mechanisms ensure that replication continues with a minimal effect on fork elongation, either by using specialized DNA polymerases or by postponing repair. Fork progression may be facilitated by specialized polymerases called TLS polymerases, which have the ability to replicate through a damaged template, albeit with lower fidelity (Sale et al., 2012). Alternatively, the replisome may skip the damaged DNA, thus leaving an unreplicated ssDNA gap to be repaired after replication. The bacterial replisome is able to reinitiate DNA synthesis downstream of a leading-strand lesion by de novo priming and recycling or exchange of stalled replicative polymerases (Heller and Marians, 2006; Yeeles et al., 2013). This mechanism also appears to efficiently restart replication in eukaryotes, and proteins capable of 'repriming' DNA synthesis beyond a lesion have recently been identified (Elvers et al., 2011; Lopes et al., 2006). The human primase PrimPol ensures resumption of DNA synthesis after UV irradiation and under conditions of dNTPs shortage. Interestingly, PrimPol has also TLS activity, although it is currently uncertain whether its fork-repriming or lesion-bypass activity is important for fork restart (Mourón et al., 2013). Thus, it is clear that define the mechanisms that orchestrate the choice between repriming and TLS is an important matter for future investigation.

After repriming, the replisome resumes DNA synthesis, leaving an ssDNA gap behind it. This gap is usually filled by an error-free, homology-directed repair (HDR)-mediated process or by specialized TLS polymerases (Ghosal and Chen, 2013). In this context, an important role is played by Proliferating cell nuclear antigen (PCNA) mono-ubiquitination and poly-ubiquitination that may coordinate the repair of these ssDNA gaps by TLS synthesis or HDR, respectively (see below). Post-replicative gap repair is crucial for genome stability because unrepaired ssDNA gaps may be converted to DSBs (Toledo et al., 2013).

Recent studies suggest that unreplicated regions lead to aberrant mitotic structures, probably due to an excess of ssDNA gaps, which might overpower the repair and filling mechanisms operating in G2, thus leading to chromosomal aberrations and breaks during mitosis or during the following replicative round (Chan et al., 2007; Harrigan et al., 2011).

Fork Reversal

Fork reversal is an alternative DDT mechanism in which stalled replication forks reverse their course to support DNA damaged repair through remodeling of replication forks. In particular, a typical replication fork (three-way junction) is converted into a four-way junction by the coordinated annealing of the two newly synthesized strands and the re-annealing of the parental strands, to form a fourth 'regressed' arm at the fork elongation point (Neelsen and Lopes, 2015). Recent findings in higher eukaryotic systems established fork reversal as an evolutionarily conserved response to various types of DNA replication stress, including topological constraints, DNA lesions, DNA secondary structures, template discontinuity, deregulated initiation of replication and imbalance in the dNTPs (Follonier et al., 2013; Ray Chaudhuri et al., 2012; Zellweger et al., 2015).

Currently, the knowledge in the formation of fork-reversal mechanism is very limited. *In vitro* studies have demonstrated that several DNA translocases, including RAD54, SMARCAL1, FANCM, ZRANB3, can promote fork reversal (Bétous et al., 2012; Blastyák et al., 2007; Bugreev et al., 2011; Ciccia et al., 2012; Gari et al., 2008). However, the same *in vitro* reaction can be catalyzed by different helicases, including human F-box DNA helicase protein 1 (FBH1), the RecQ helicase family members BLM and WRN. However, the *in vivo* function of these helicases has thus far been confirmed only for FBH1 in conditions of low nucleotide availability, in which its function is presumably the unwinding of the lagging strand (Fugger et al., 2015). The recombinase RAD51 seems to be important for converting uncoupled forks (forks with extended ssDNA stretches) into reversed forks following nucleotide depletion and topoisomerase inhibition. Thus, fork reversal may be primed by RAD51 loading at the extended ssDNA regions, which promotes the re-annealing of parental strands (Zellweger et al., 2015).

The restart of reversed-fork has been elucidated in more detail. Notably, the human RECQ1 helicase drives the restart of reversed replication forks, and its function is regulated by the poly (ADP-ribose) polymerase 1 (PARP1), which suppresses RECQ1 activity until the damage is repaired. For this reason, PARP1 is considered a molecular

switch to control transient fork reversal and replication fork restart following different sources of genotoxic stress (Berti et al., 2013). Recently, a second human DNA2 and WRN-dependent mechanism of reversed-fork processing and restart has been identified. The DNA2 nuclease and WRN helicase cooperate in resecting reversed replication forks with a 5′-to-3′ polarity and mediating fork restart (Thangavel et al., 2015). In particular, it has been postulated that the 3' tail generated by resection may be specifically recognized by a protein that drives a branch migration to reestablish functional replication fork. A good candidate for this reaction is the DNA translocase SMARCAL1, which efficiently converts four-way junctions into functional replication fork when 3′-ssDNA tail is coated by RPA (Bétous et al., 2013). Alternatively, partially single-stranded DNA structures may activate an HDR-like mechanism of reversed-fork restart. In this scenario, the 3′ overhang on the regressed arm might be coated by RAD51, which would mediate invasion of the duplex ahead of the fork, thus resulting in a Holliday junction structure that could be resolved by specific resolvases (Bizard and Hickson, 2014; Issaeva et al., 2010).

Fork reversal has been proposed as a mechanism for DNA damage bypass in human cells, during which one newly synthesized strand serves as a transient alternative template for continued DNA synthesis in the face of lesions on the template DNA. It can be considered to be an 'emergency brake' that provides time and the correct DNA template, to allow the DNA repair machinery to repair damage before replication resumes (Neelsen and Lopes, 2015). However, it should keep in mind that fork reversal could also have pathological consequences. Indeed, under specific circumstances, such as checkpoint defects (Couch et al., 2013; Neelsen et al., 2013), the nucleolytic cleavage of reversed forks could contribute to genome instability in neurodegenerative syndromes and cancer.

Regulation of replication fork restart mechanisms

As above mentioned, fork repriming, translesion synthesis and fork reversal are the main mechanisms that allow the restart of stalled fork, in response to a wide range of stimuli that cause replication stress. However, it is not entirely clear how cells choose between these molecular mechanisms. Interestingly, repriming mechanisms at stalled forks limit extensive fork uncoupling and ssDNA gap formation, which instead are necessary to trigger fork reversal, thus suggesting that these mechanisms are mutually exclusive (Fumasoni et al., 2015).

On the basis of emerging evidence, it has been suggest that PCNA post-translational modifications may be a key regulator of pathway choice. For example, PCNA poly-ubiquitination might promote fork reversal through the recruitment of translocases with reported fork-regression activity, such as ZRANB3 (Ciccia et al., 2012). Alternatively, PCNA mono-ubiquitination may promote TLS by recruiting specific TLS polymerases to stalled forks (Mailand et al., 2013; Moldovan et al., 2007). In addition, RAD51 supports both the TLS activation *via* PCNA mono-ubiquitination (Chen et al., 2016) and the early stages of fork reversal (Zellweger et al., 2015), indicating that RAD51 may also act as a switch to balance fork reversal and TLS or repriming events. For this reason, a key objective for future research will be to identify specific RAD51 partner, mediators or signaling processes that promote one pathway *versus* the other.

STABILIZATION AND PROTECTION OF STALLED FORKS

As described above, multiple pathways work in the restarting of stalled replication forks to allow DNA replication completion. Beyond the importance of restarting stalled forks, replication fork protection seems to be equally important to assure genomic stability, as it is underscored by the increasing number of proteins identified as being part of this process. Recent studies have underlined a crucial role for proteins involved in the Fanconi Anaemia (FA)/homologous recombination (HR) pathway in maintaining genome stability during replication stress (Costanzo, 2011). Components of this pathway have traditionally been associated with the HR-dependent repair of inter-strand crosslinks (ICLs), and mutations in these genes give rise to Fanconi Anaemia, a rare human disorder characterized by severe developmental abnormalities and tumor predisposition (Lord and Ashworth, 2007; Wang and Gautier, 2010). In addition to their importance in promoting the repair of ICLs, it is now apparent that several FA/HR proteins also play a role in protection and stabilization of stalled replication forks from uncontrolled nucleolysis (Hashimoto et al., 2010; Schlacher et al., 2011, 2012). If left unprotected, excessive nucleolytic processing (fork degradation) renders such forks unrecoverable, and may perturb replication to such an extent that stretches of under-replicated DNA accumulate. Therefore, these fork protection factors represent important barriers to prevent genome instability.

Fork Protection Factors

Several FA/HR proteins are important to avoid replication fork over-processing by cellular nucleases, even if the DNA recombinase RAD51 seems to play a central role (Hashimoto et al., 2010; Schlacher et al., 2011, 2012). RAD51 is found over-expressed in many cancers, and mutations or polymorphysm in the RAD51 gene have been identified in several human tumors, including breast cancer and head and neck squamous cell carcinoma (Richardson, 2005). The most well-characterized function of RAD51 is to promote homologous DNA pairing and strand exchange in an ATP-dependent reaction, by displacing the single-stranded DNA binding protein RPA to form helical nucleoprotein filament preferentially assembling in the 3'-to-5' direction (Baumann et al., 1996; Kowalczykowski, 2015). This RAD51 function play a central role in HR, which, in turn, is critical to recovery from double strand breaks (DSBs), one of the most deleterious lesions.

However, recent findings, obtained by using different model systems, have highlighted that the loading of RAD51 to replication forks also functions to assist continuous DNA synthesis by stabilizing replication fork intermediates and preventing deleterious nucleolytic over-processing. Moreover, it seems that this protective function of RAD51 depends on its ability to form nucleofilaments at stalled replication forks (Hashimoto et al., 2010; Schlacher et al., 2011).

In addition to RAD51, Breast cancer type 2 susceptibility protein (BRCA2), one of the two genes frequently found mutated in hereditary breast cancers (Petrucelli et al., 2013), also suppresses genomic instability upon replication fork stalling, by preventing the degradation of nascent DNA (Schlacher et al., 2011). Human BRCA2 has eight conserved RAD51 interaction motifs termed BRC repeats, which are essential for HR. The importance of HR for survival is reflected in the observation that truncations of BRCA2, including the BRC repeats, are lethal in mice during embryogenesis. In addition to the BRC repeats, a RAD51 interaction site has been identified in the C-terminal (C-ter) of BRCA2, which is distinct in sequence from the BRC repeats. Although BRCA2 truncations involving only the BRCA2 C-ter region appear developmentally normal, however, they confer shorter life spans, increased tumorigenesis, and hematopoietic dysfunction (Donoho et al., 2003; Lord and Ashworth, 2007; McAllister et al., 2002; Navarro et al., 2006). These RAD51 interaction domains have been shown to promote localization of RAD51 to DSBs, and stabilization of RAD51 oligomers bound to DNA. Since BRCA2 is required to load RAD51 onto single-strand DNA (ssDNA) at stalled replication forks, it is natural to assume that its ability to protect replication forks from degradation is due to its role in this process. Schlacher and colleagues (2011) found that a BRCA2 mutant, lacking the C-ter RAD51 binding domain, is defective for its stalled fork-protective function, but retains intact HR repair of DSBs. Therefore, after its loading onto nascent ssDNA, the stabilization of RAD51 by BRCA2 is crucial in preventing excessive nucleolytic processing. Indeed, the stabilization of RAD51 nucleofilaments on ssDNA by preventing its ATP-dependent dissociation protects against the over-processing of forks when BRCA2 is truncated for C-ter. These observations, together with other experiments reported in the same work, suggest that BRCA2 has a ‘stalled fork-protective’ function mediated by its stabilizing effect on the RAD51 nucleoprotein filament, but distinct from its role in traditional DSBs repair by HR (Schlacher et al., 2011).

Other factors seem to be involved in stalled fork protection. For instance, FANCD2 protein stabilizes and protects damaged forks from nucleolytic attack, even if this does not seem to be connected to the recruitment/stabilization of RAD51 to stalled forks (Schlacher et al., 2012).

On the contrary, the helicase/nuclease WRN and the TLS polymerase REV1 are deemed to prevent fork resection at nascent DNA by stabilizing RAD51 nucleoprotein filaments (Iannascoli et al., 2015; Su et al., 2014; Yang et al., 2015). In this scenario, the regulation of a RAD51 nucleoprotein filaments formation would be an important matter. Indeed, since RAD51 is a key player in replication-associated HR and in fork protection pathway, controlling the binding of RAD51 to its potential DNA substrates or to chromatin more generally, is an effective manner to preserve genome stability.

Several DNA helicases have been identified that can control the stability of a RAD51 nucleoprotein filaments (Bugreev et al., 2007; Hu et al., 2007). Many of these belong to the UvrD family of proteins, such as Srs2 in yeast and PARI in mammals (Moldovan et al., 2012; Veaute et al., 2003). Mammalian cells express an UvrD family member, FBH1, which combines a helicase function with the ability to ubiquitylate target proteins and it is considered the mammalian functional counterpart of Srs2 (Chiolo et al., 2007). FBH1 has been reported to suppress RAD51 nucleoprotein filaments formation and consistent with this, the level of RAD51 nuclear foci is greatly increased in FBH1-deficient cells (Simandlova et al., 2013). Recently, it has been proposed a mechanism of action according to which FBH1 translocates along DNA, where a physical interaction with RAD51 causes the dissociation of RAD51 from the developing nucleofilaments. Following this displacement of RAD51, the SCF^{FBH1} targets RAD51 for ubiquitination, preventing its re-association with the DNA (Chu et al., 2015).

In certain contexts, RAD51 filament dissolution may also be crucial in maintaining replication fork stability. Indeed, the loss of RECQL5 helicase leads to fork degradation, although it works to dissolve RAD51 nucleofilaments (Hu et al., 2007), pointing out that both destabilization and over-stabilization of RAD51 nucleofilaments are deleterious to replication fork integrity and chromosomal stability.

Cellular nucleases involved in fork degradation

Nucleases have key roles in restarting stalled forks after genotoxic stress. However, excessive and uncontrolled nucleolytic activity is clearly detrimental to genome stability. Thus, it is important to distinguish the limited degradation of nascent DNA strands required for efficient fork restart from the extensive degradation of stalled replication intermediates, which underlies the pathological effects observed in FA/HR-deficient cells.

Over the past decade much progress has been made in understanding the role of different nucleases involved in the replication stress response. MRE11, CtIP, DNA2, and EXO1 have been implicated in processing DSBs and in DNA end resection. It is thought that MRE11 and CtIP act together to perform short-range resection, whilst EXO1 and DNA2/BLM act independently to execute 5'-3' long-range processing (Nimonkar et al., 2011).

The MRE11 possesses the 3' to 5' exonuclease activity and endonuclease activity, and it is involved in homologous recombination, telomere length maintenance, and DNA double-strand break repair (Liao et al., 2012; Paull and Gellert, 1998). Recently, MRE11 has been implicated in the uncontrolled resection, which leads to fork degradation, observed in the absence of FA/HR protection factors (Hashimoto et al., 2010; Schlacher et al., 2011, 2012). Indeed, MRE11-dependent fork resection underlies the increased chromosome breakage exhibited by BRCA2 null cells. Moreover, a direct inhibition of MRE11 nuclease, with the chemical inhibitor mirin, suppresses the over-processing of stalled fork and genomic instability (Dupré et al., 2008a; Schlacher et al., 2011). Thus, it seems that these FA/HR factors specifically restrict the activity of MRE11 at stalled replication forks to prevent over-processing. However, since MRE11 has limited nucleolytic processing activity, other nucleases acting downstream of MRE11 might promote the extensive degradation observed in these studies. In addition to MRE11, DNA2 and EXO1 also play important roles in fork processing. DNA2 knockdown, but not depletion of EXO1 or MRE11, has been shown to alleviate fork processing after HU treatment (Thangavel et al., 2015). Furthermore, RNAi-mediated depletion of DNA2 in FANCD2-deficient cells rescues their hypersensitivity to ICLs (Costanzo, 2011). Finally, EXO1 has also been directly implicated in fork over-resection (Iannascoli et al., 2015). Therefore, it seems that different fork protection factors act to antagonize the actions of different nucleases.

Physiological function of fork protection

The pathological consequences arising from the inability to protect stalled replication forks underline a pivotal physiological role of fork protection pathway during replication stress.
Firstly, during oncogene-induced replication stress, fork protection factors would be crucial to prevent chromosomal aberrations, which would otherwise promote cellular transformation. Since most fork protection factors also promote DNA replication and/or HR repair, which are important tumor suppressor functions, it is difficult to assess the impact of fork protection on tumorigenesis directly. Nevertheless, mutations affecting a CDK phosphorylation site in the C-terminus of BRCA2, which is important for regulating fork protection (but not HR), are found in individuals affected with breast cancer (Esashi et al., 2005; Schlacher et al., 2011), suggesting that fork degradation-dependent mechanism may contribute to tumorigenesis.
Secondly, it is likely that the presence and function of these protective proteins influence an individual's response to chemotherapeutic treatment, particularly in response to agents, such as HU that induces high levels of replication stress. In this case, loss of fork protection likely contributes to tumor progression by permitting wide-ranging genomic rearrangements. Moreover, in cells lacking these components, transient treatment with chemotherapeutics, which induce replication stress, would likely lead to further mutagenesis and genome instability.
Lastly, given that defects in replication stress response genes give rise to developmental abnormalities and microcephaly, it is likely that loss of the fork protection function contributes to the development of some of these clinical defects (Zeman and Cimprich, 2014).
Although many fork protection factors have been identified, it is possible that more novel factors remain to be discovered. In addition, it is currently unclear how these factors suppress deleterious nucleolytic over-processing, so that further studies are necessary to define a deeper understanding of the molecular mechanisms underlying fork protection pathway. Investigation of this mechanism could reveal an exciting area of research as it may provide new therapeutic approaches for diseases associated with an aberrant replication stress response.

THE WERNER HELICASE INTERACTING PROTEIN 1 (WRNIP1/WHIP1)

Among proteins participating in the maintenance of genome stability, whose function is still poorly characterized, is the human Werner helicase interacting protein 1 (WRNIP1), previously called WHIP1. The WRNIP1 protein was originally identified, through the yeast two-hybrid method, as mouse protein that physically interacts with the WRN protein (WRN) (Kawabe Yi et al., 2001), a member of the RecQ family of DNA helicases that plays a crucial role in response to replication stress, and significantly contributes to the recovery of stalled replication forks (Franchitto and Pichierri, 2011; Petermann and Helleday, 2010). WRNIP1 belongs to the AAA+ class of ATPase family proteins that is evolutionary conserved and whose central region is similar to Escherichia coli RuvB, a Holliday junction branch migration motor protein (Hishida et al., 2001; Kawabe et al., 2001). The human amino acid sequence of WRNIP1 has homology with the replication factor C (RFC) family of clamp loader proteins and possesses an ATPase domain containing a Walker A and B motif for ATPase activity in the middle of the molecule (Kawabe Yi et al., 2001). For WRNIP1 ATPase activity is required threonine on amino acid position 294. Indeed, a mutant protein of human WRNIP1 in which threonine 294, a conserved residue in the nucleotide-binding motif of AAA+ family proteins, was substituted with alanine led to suppression of ATPase activity (Tsurimoto et al., 2005). In addition to ATPase domain, WRNIP1 contains a nuclear localization signal, leucine zipper DNA binding domains, and an ubiquitin-binding zinc finger domain (UBZ domain-RAD18 type) that can bind ubiquitin (Fig. 9).

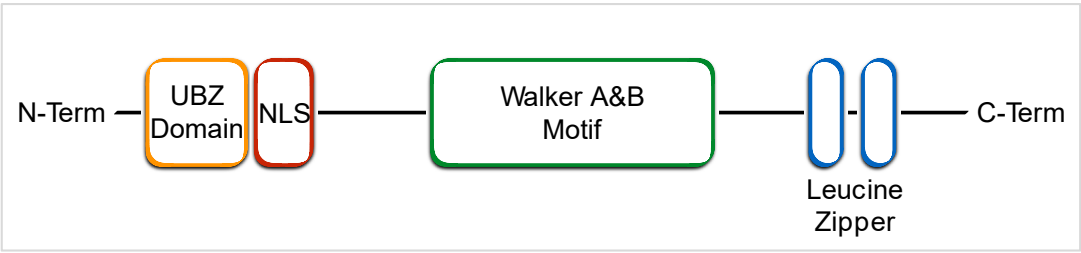

Figure 9. Schematic representation of human WRNIP1 structure. From left to right: UBZ domain-RAD18 type; Nuclear Localization Signal (NLS); Walker A & B motif; Leucine zippers.

A conserved aspartate residue in the zinc finger domain is essential to bind ubiquitin and polyubiquitin. Consistently, a single point mutation of aspartate on amino acid position 37 in alanine completely abolished ubiquitin binding in vitro (Bish and Myers, 2007). In

addition, WRNIP1 is one of many proteins whose ubiquitin-binding domain directs its own ubiquitination. WRNIP1 is heavily ubiquitinated, with 12 sites identified and several of these ubiquitination sites lie near critical conserved motifs within the ATPase domain, suggesting that ubiquitination may regulate WRNIP1 ATPase activity by directly interfering with nucleotide binding or hydrolysis (Bish and Myers, 2007).

Evidences supporting WRNIP1 role during Replication Stress

Little is known about the WRNIP1 function in human cells. On the contrary the Maintenance of Genome Stability 1 protein (MGS1), the budding yeast homolog of WRNIP1, has been extensively studied. MGS1 is involved in the maintenance of DNA topology and in the post-replication repair (Branzei et al., 2002; Hishida and Ohno, 2002). Mutations of the MGS1 can enhance aging processes in budding yeast (Hishida et al., 2002; Kim et al., 2005). Furthermore, genetic analysis using MGS1 mutants reveals that it is required for preventing the genome instability caused by replication arrest, but it is not involved in DNA lesions repair (Hishida et al., 2002). Over-expression of MGS1 is lethal or very toxic in combination with mutations in genes that encode proteins involved in DNA replication, such as DNA polymerase δ (Polδ), RFC, PCNA and RPA (Branzei et al., 2002). MGS1 physically and functionally interacts *in vivo* with budding yeast Pol31, the second subunit of Polδ (Vijeh Motlagh et al., 2006). Consistently, *in vitro* studies have demonstrated that human WRNIP1 forms homo-oligomeric complex that physically interacts with DNA Polδ. This interaction stimulates Polδ DNA synthesis activity, mainly increasing the frequency of DNA replication initiation events (Tsurimoto et al., 2005). These findings provide the first biochemical evidence that WRNIP1 is involved in a eukaryotic replication fork complex, and that it modulates Polδ activity. However, the exact function and regulation of WRNIP1 in human cell remains to be elucidated. WRN protein interacts with Polδ subunits p66 and p50 (Szekely et al., 2000), and human WRNIP1 interacts with three Polδ subunits except the p66. This means that they can interact simultaneously with Polδ through their common target p50. Therefore, taking into account their functional interaction and their possible simultaneous association with Polδ, it has been proposed a model in which WRN, WRNIP1 and Polδ form a ternary complex in functional situations. This model proposes that WRNIP1 may be a modulator for initiation or re-initiation events of DNA Polδ-mediated DNA synthesis. In particular, WRNIP1, through its ATPase activity, may function as a sensor of DNA damage or arrested

replication fork regulating the extent of DNA synthesis (Tsurimoto et al., 2005). According to this model, the WRNIP1 protein might play a crucial role during perturbed replication to avoid replication stress accumulation (Fig. 10).

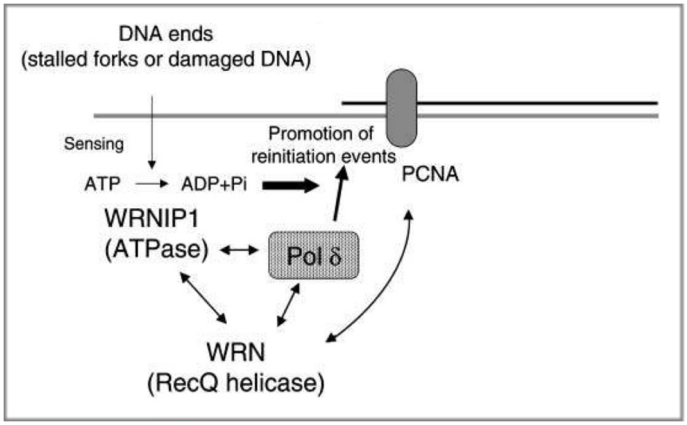

Figure 10. Model of a ternary complex containing WRNIP1, WRN and polδ at an arrested replication fork. WRNIP1, WRN and polδ may form a ternary complex. WRN and polδ also interact with PCNA. This complex may function to regulate pol δ-mediated DNA synthesis when the replication fork complex is stalled by DNA damage or structural stress. The ATPase activity of WRNIP1 functions as a sensor of DNA ends, and ATP hydrolysis regulates the stimulation of polδ. Thus, complex formation plays a crucial role in the re-initiation of stalled replication forks. (Tsurimoto et al., 2005)

Accordingly, *in vitro* investigations reveal that WRNIP1 binds in an ATP-dependent manner to forked DNA that mimics stalled replication forks (Yoshimura et al., 2009).

A further study in human cells has demonstrated that WRNIP1 resides in DNA replication factories, since it localizes either with RPA and PCNA (Crosetto et al., 2008). Interestingly, this localization seems to specifically require its UBZ domain (Crosetto et al., 2008). Upon treatments with UVC light-induced stalled fork, the amount of chromatin-bound WRNIP1 significantly increases (Crosetto et al., 2008). In addition to the amount of chromatin-bound WRNIP1, also the percentage of WRNIP1 foci co-localizing with replication factories increases, suggesting that human WRNIP1 may deal with stalled forks, as inferred from earlier yeast studies.

Very recently, human WRNIP1 protein has been implicated in the activation of ATM-mediated checkpoint after replication stress induced by low-dose Aph, further supporting the hypothesis that WRNIP1 may be directly involved in response to mild replication stress (Kanu et al., 2015). Furthermore, WRNIP1 has been found de-regulated in a subset of

human tumours (Lukk et al., 2010), underscoring its possible role in maintenance of genome stability.

As discussed above, replication stress response is an intricate multi-step pathway, and we are only beginning to understand how the different steps integrate and how key proteins of the response are controlled. Although several evidences indicate the involvement of WRNIP1 during replication stress response, the exact molecular function that WRNIP1 accomplishes is not yet determined. Thus, a more detailed knowledge of the WRNIP1 function could help us to better understanding of the complex network of replication stress response, and it could also provide further insights into the molecular mechanisms underlying the chromosome instability phenotype of human WRNIP1-deficient cancer cells.

2. AIM

It is well established that the proper execution of DNA replication is an essential aspect of cellular life. However, proliferating cells are constantly subjected to a wide variety of threats originating by the action of exogenous and endogenous agents that can hinder replication fork progression. Several studies have clearly demonstrated that inaccurate handling of stalled replication forks can lead to genomic instability, a well-known source of human diseases and cancer onset (Abbas et al., 2013; Aguilera and Gómez-González, 2008). To minimize such a risk, cells have evolved a sophisticated mechanism, called replication stress response, to cope with perturbed replication forks (Branzei and Foiani, 2009, 2010; Yeeles et al., 2013; Zeman and Cimprich, 2014). Replication stress response is considered an intricate multi-step pathway, in which the importance of stabilizing and restarting stalled replication forks is also evidenced by the increasing number of proteins identified as being part of these mechanisms. Recently, it has been proposed that homologous recombination (HR) proteins take part to a pathway deputed to the maintenance of stalled fork stability. Based on these works, a current model has been proposed in which BRCA2 and RAD51 may act in preventing rather than repairing lesions at stalled replication forks, in order to protect nascent DNA strand from degradation mediated by the exonucleolytic activity of MRE11 (Hashimoto et al., 2010; Schlacher et al., 2011; Ying et al., 2012). However, despite extensive research, it is still not completely understood how these HR proteins operate during the resolution of fork stalling, and which are their partners.

Among proteins participating in the maintenance of genome stability, whose function is still poorly characterized, is the human Werner helicase interacting protein 1 (WRNIP1). Although the yeast homolog of WRNIP1, MGS1, is required to prevent genome instability caused by replication arrest (Branzei et al., 2002), little is known about the function of human WRNIP1.

The aim of this study was to investigate the function of human WRNIP1 during normal and perturbed DNA replication, to gain more insights into the function of the protein. In particular, we characterized the role that human WRNIP1 may play during replication stress response by analysing its involvement both in restart of stalled forks and in the HR-related fork-protection pathway.

3. RESULTS

WRNIP1 IS REQUIRED FOR PROTECTION AND RESTART OF STALLED FORKS UPON REPLICATION STRESS

To investigate the function of human WRNIP1 during DNA replication, we monitored replication genome-wide at single-molecule level by performing DNA fiber assay. Firstly, we generated MRC5SV cells stably expressing WRNIP1-targeting shRNA (shWRNIP1). Next, isogenic cell lines stably expressing the RNAi-resistant full-length wild-type WRNIP1 (shWRNIP1^{WT}) or its ATPase-dead mutant form of WRNIP1 (shWRNIP1^{T294A}) (Tsurimoto et al., 2005), were created using the shWRNIP1 cells (Fig. 11A). To determine whether WRNIP1 affects replication under normal growth conditions (i.e. in the absence of any treatment), we measured the rate and symmetry of the replication fork progression in shWRNIP1^{WT}, shWRNIP1 and shWRNIP1^{T294A} cells. We sequentially labelled cells with the thymidine analogues 5-chloro-2'-deoxyuridine (CldU) and 5-iodo-2'-deoxyuridine (IdU) as described in the experimental scheme (Fig. 11B). Under these conditions, shWRNIP1^{WT}, shWRNIP1 and shWRNIP1^{T294A} cells showed almost identical fork velocity with an average fork progression rate of about 1.0 kb per minute (Fig. 11C). Moreover, the frequency of asymmetric replication tracks was similar in all cell lines (Fig. 11D), confirming that no elongation defect is triggered when WRNIP1 or its enzymatic activity was lost.

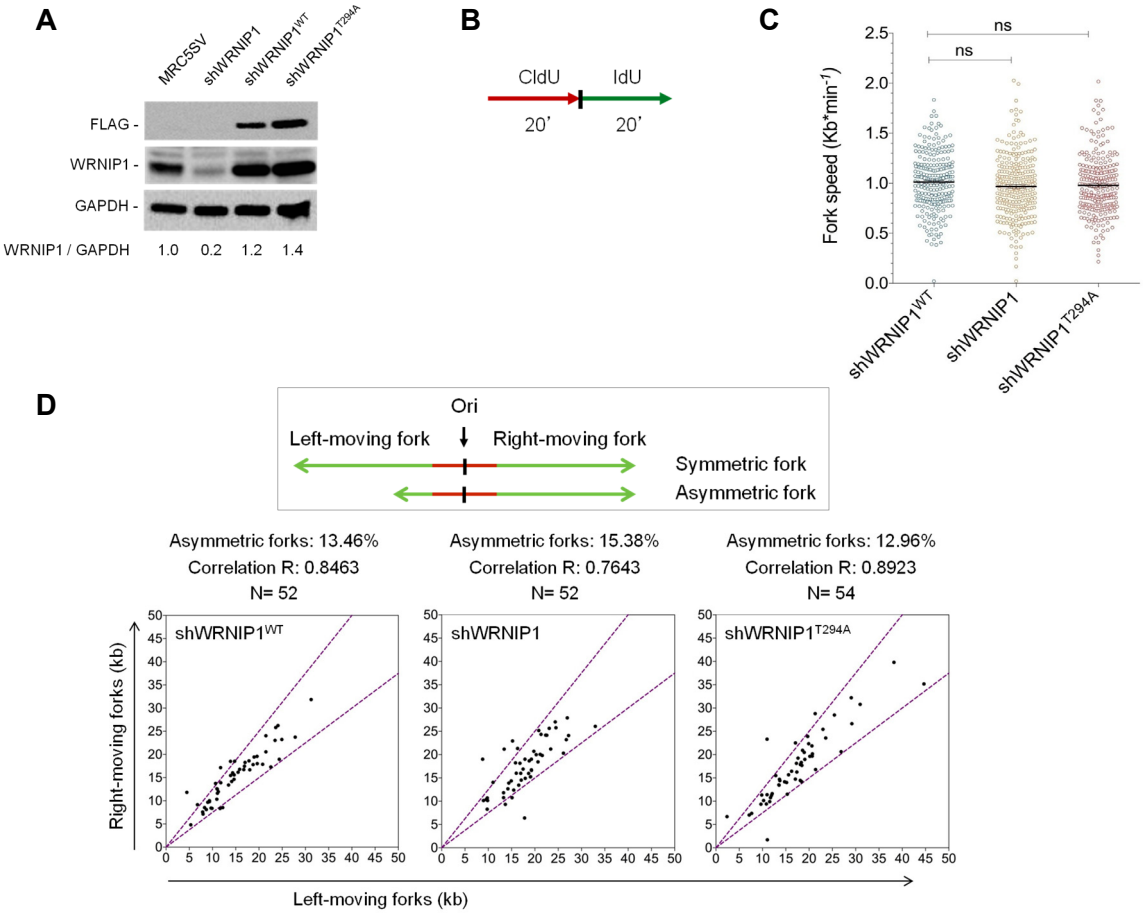

Figure 11. Analysis of replication dynamics in wild-type cells (shWRNIP1^{WT}) and WRNIP1-deficient (shWRNIP1) or mutant (shWRNIP1^{T294A}) cells. (**A**) Western blot analysis showing the expression of the WRNIP1 protein in wild-type cells (shWRNIP1^{WT}) and WRNIP1-deficient (shWRNIP1) or mutant (shWRNIP1^{T294A}) cells. MRC5SV fibroblasts were used as a positive control. The membrane was probed with an anti-FLAG or anti-WRNIP1. GAPDH was used as a loading control. Below each lane of the blot the ratio of WRNIP1 protein to total protein, then normalized to MRC5SV, is reported.
(**B**) Experimental scheme of dual labelling of DNA fibers in shWRNIP1^{WT}, shWRNIP1 and shWRNIP1^{T294A} cells. Cells were pulse-labelled with CldU, and then subjected to a pulse-labelling with IdU. (**C**) Analysis of replication fork velocity (fork speed) in the cells under unperturbed conditions. The length of the green tracks were measured. Mean values are represented as horizontal black lines (ns, not significant; Student's t-test). (**D**) Cells were treated as in (B). For each replication origin, the length of the right-fork signal was measured and plotted against the length of the left-fork signal. A schematic representation of symmetric and asymmetric forks is given. If the ratio between the left-fork length and the right-fork length deviated by more than 33% from 1 (that is, outside the violet dashed lines in the graphs), the fork was considered asymmetric. The percentage of asymmetric forks was calculated for all cell lines. N= number of forks counted for each cell line. R represents linear correlation coefficient.

To obtain a deeper insight into the role of WRNIP1 in replication, we explored whether loss of WRNIP1 influences fork progression after HU-induced replication stress. Thus, we pulse-labelled shWRNIP1^{WT}, shWRNIP1 and shWRNIP1^{T294A} cells with CldU and IdU as reported (Fig. 12A). DNA fiber analysis showed that WRNIP1 depletion resulted in a significant enhancement in the percentage of stalled forks induced by HU respect to wild-type cells (Fig. 12B). Similarly, the expression of the mutant form of WRNIP1 greatly affected fork progression after HU (Fig. 12B). Interestingly, comparing the percentage of restarting forks in all cell lines, we observed that loss of WRNIP1 reduced the ability of cells to resume replication after release from HU in the same extent as loss of its ATPase activity (Fig. 12B). All other replication parameters (Origins, Terminations and Interspersed fibers) were not significant different among the cell lines (Fig. 12C). These results implicate WRNIP1, through its ATPase activity, in restarting stalled forks.

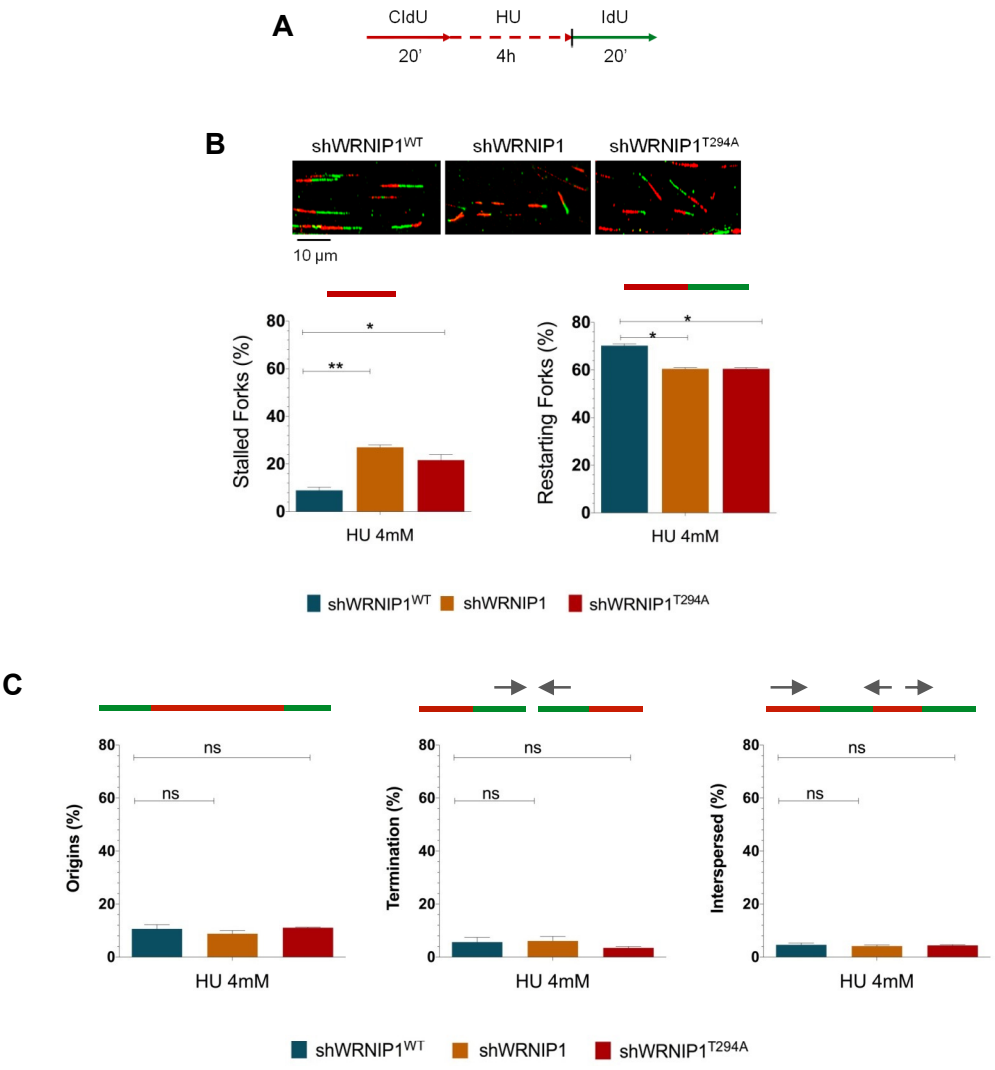

Figure 12. Analysis of replication dynamic in wild-type cells (shWRNIP1WT) and WRNIP1-deficient (shWRNIP1) or mutant (shWRNIP1T294A) cells after HU induced replication stress. (**A**) Experimental scheme of dual labelling of DNA fibers in shWRNIP1WT, shWRNIP1 and shWRNIP1T294A cells. Cells were pulse-labelled with CldU, treated with 4mM HU and then subjected to a pulse-labelling with IdU. (**B**) Graphs show the percentage of red (CldU) tracts (stalled forks) or red-green (CldU-IdU) contiguous tracts (restarting forks) in the cells. Mean shown, n = 2. Error bars represent standard error. (*, $p < 0.05$; **, $p < 0.01$; Student's t test). Representative DNA fiber images are shown. Scale bars, 10 μm. (**C**) Graphs show the percentage of green (ldU) tracts (new origins), red-green-red (IdU-CIdU-IdU) contiguous tracts (termination events) or multiple CldU and IdU labels (interspersed fibers) in the cells. Mean shown, n = 2. Error bars represent standard error. (ns, not significant; Student's t test).

We next verified whether WRNIP1 was involved in the protection of stalled forks, by examining the stability of nascent replication strands. To this aim, we changed the DNA labeling scheme. Thus, shWRNIP1^{WT}, shWRNIP1 and shWRNIP1^{T294A} cells were sequentially pulse-labelled with CldU and IdU to mark nascent replication tracts before fork stalling with HU (Fig. 13A). The maintenance of the IdU label after HU treatment measures the extent of fork stability on the stretched DNA fibers. The analysis showed that IdU tract length remained unchanged with or without HU treatment in cells expressing wild-type WRNIP1 (shWRNIP1^{WT}) (7.72 and 7.96 μm, respectively; Fig. 13B). On the contrary, in WRNIP1-deficient cells (shWRNIP1), fork stalling led to a significant shortening of IdU tract length compared to unperturbed replication (4.70 and 7.43 μm, respectively; Fig. 13B). Notably, in shWRNIP1^{T294A} cells, IdU tract length was left unaffected after HU as in wild-type cells, revealing that the ATPase activity is dispensable for protection of stalled forks (7.30 and 7.40 μm, with and without HU, respectively; Fig. 13B). Since nascent IdU tracts are formed before treatment with HU, it is plausible that the decreasing in length of the IdU tracts takes place during exposure to the drug, as previously demonstrated (Schlacher et al., 2011). Thus, we deduced that WRNIP1 is essential in avoiding degradation of nascent DNA strands at stalled forks.

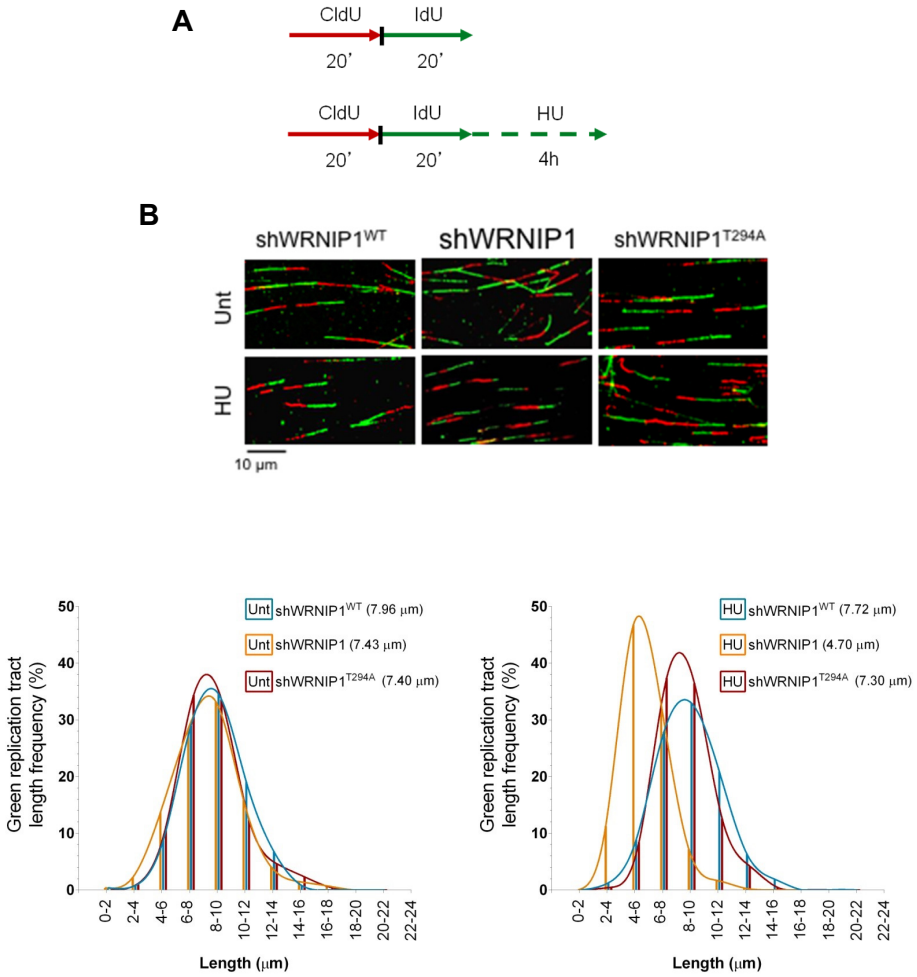

Figure 13. Loss of WRNIP1 leads to nascent DNA strand degradation after HU-induced replication stress. **(A)** Experimental scheme of dual labelling of DNA fibers in shWRNIP1^{WT}, shWRNIP1 and shWRNIP1^{T294A} cells. Cells were sequentially pulse-labelled with CldU and IdU as indicated, then treated or not with 4 mM HU. **(B)** Representative IdU tract length distributions in all cell lines under unperturbed conditions (left graph) or after HU treatment (right graph). Median tract lengths are given in parentheses. See also Appendix Tables 1 and 2 in Materials and Methods section for details on the data sets and statistical test. Representative DNA fiber images are shown. Scale bars, 10 µm.

To determine whether the phenotype of WRNIP1-deficient cells is a general response to replication arrest, we pulse-labelled shWRNIP1^{WT} and shWRNIP1 cells with IdU, followed by exposure to high dose of aphidicolin (Aph), a selective inhibitor of the replicative DNA polymerases (Fig. 14A). Since we observed that Aph showed substantial similarity to HU in the ability to reduce IdU tract length in the absence of WRNIP1 (7.34 and 4.83 µm, shWRNIP1^{WT} and shWRNIP1, respectively; Fig. 14B), we concluded that replication stress caused by various agents needs WRNIP1 to protect stalled forks.

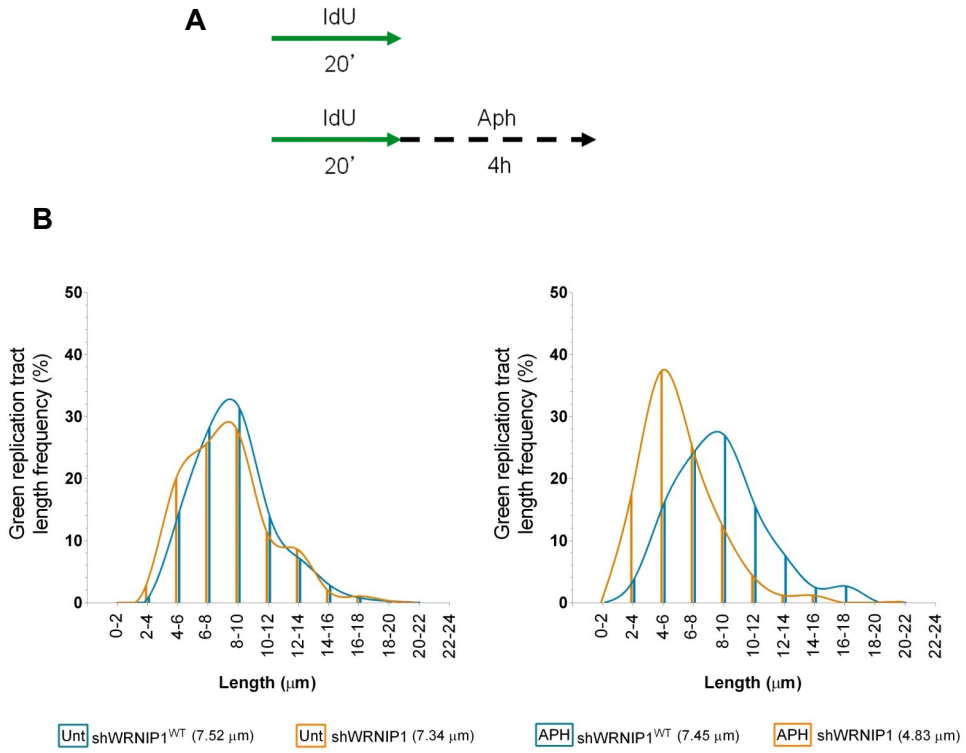

Figure 14. WRNIP1-deficient cells shows nascent DNA strand degradation after Aph-induced replication stress. (A) Scheme of DNA fiber tract analysis in wild-type (shWRNIP1^{WT}) and WRNIP1-deficient (shWRNIP1) cells. Cells were pulse-labelled with IdU and treated or not with 10 µM Aph. **(B)** Representative IdU tract length distributions in all cell lines under unperturbed conditions (left graph) or after Aph treatment (right graph). Median tract lengths are given in parentheses. See also Appendix Tables 1 and 2 in Materials and Methods section for details on the data sets and statistical test.

Moreover, to ascertain whether the role of WRNIP1 is kept in other cell types, we tested HEK293T cells transfected with control siRNA (HEK293T^{siCtrl}) or *WRNIP1* siRNA (HEK293T^{siWRNIP1}). After transfection, cells were pulse-labelled with IdU, and then exposed to HU (Fig. 15A). Although similar IdU tract length was observed in both cell lines under unperturbed conditions, however, WRNIP1-deficient cells (HEK293T^{siWRNIP1}) exhibited a defective maintenance of nascent length tracts after HU treatment as compared to the wild-type cells (HEK293T^{siCtrl}) (4.42 and 7.34 µm, respectively; Fig. 15B). This confirms that the fork-protective role of WRNIP1 is independent from the cell lines. Overall, our results suggest that, when replication is perturbed, WRNIP1 maintains the integrity of stalled forks and ensures their restart via its ATPase activity.

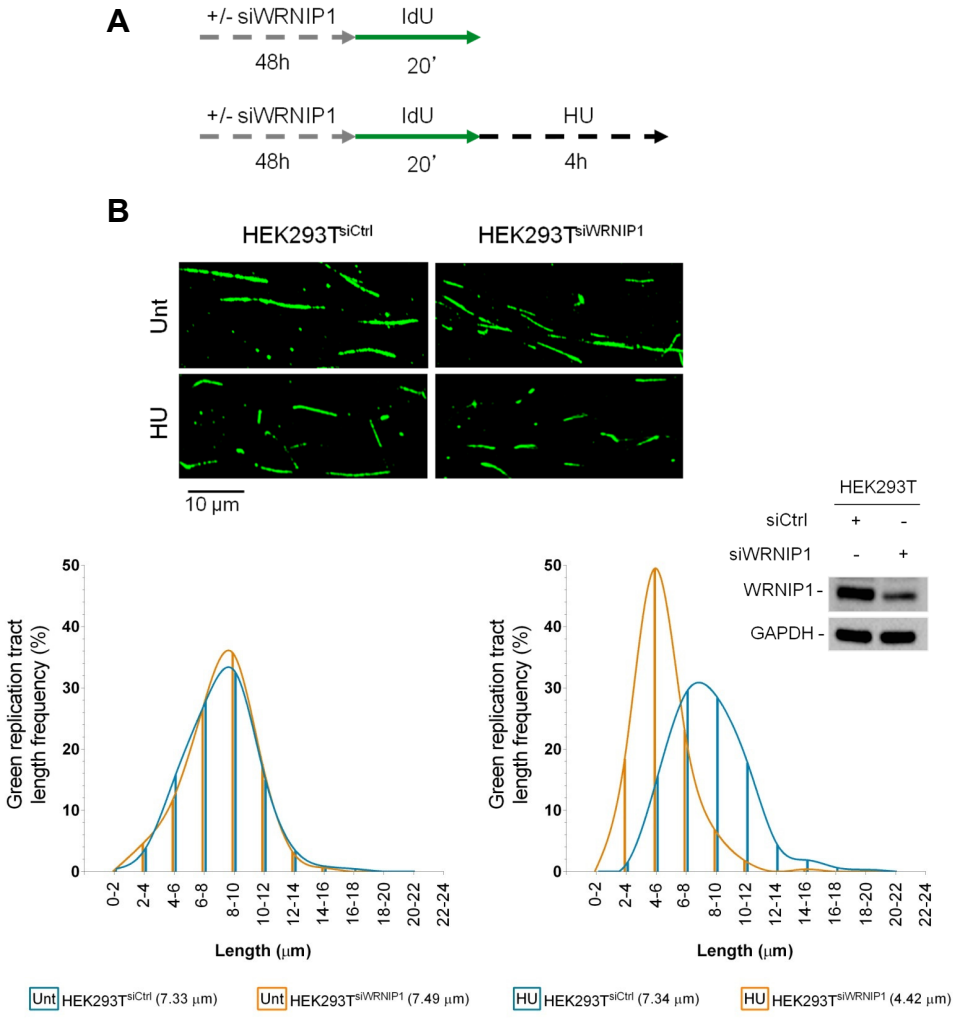

Figure 15. WRNIP1 interference in HEK293T cells results in nascent DNA strand degradation after replication stress. (A) Experimental scheme of pulse-labelling of DNA fibers in HEK293T cells transfected with control siRNA (HEK293T^{siCtrl}) or *WRNIP1* siRNA (HEK293T^{siWRNIP1}), and 48 h thereafter labelled with IdU. Next, cells were treated or not with 4 mM HU. **(B)** Representative IdU tract length distributions in HEK293T^{siCtrl} or HEK293T^{siWRNIP1} cells under unperturbed conditions (left graph) or after HU (right graph). Median tract lengths are given in parentheses. Representative DNA fiber images are reported. Scale bars, 10 µm. See Appendix Tables 1 and 2 in Materials and Methods section for details on the data sets and statistical test. Western blot shows the expression of the WRNIP1 protein in the cells. The membrane was probed with an anti-WRNIP1. GAPDH was used as a loading control.

MRE11 DEGRADATES NASCENT DNA STRAND AT STALLED FORKS IN ABSENCE OF WRNIP1

It has been reported that MRE11 activity is responsible for degradation of HU-stalled forks in BRCA2-defective cells (Schlacher et al., 2011; Ying et al., 2012). Since we proved that WRNIP1-deficient cells show instability of stalled forks, which is reminiscent of that observed in the absence of BRCA2, we asked whether MRE11 nuclease could similarly promote fork degradation in our cells. To test this hypothesis, we double-labelled shWRNIP1^{WT} and shWRNIP1 cells, followed by treatment with HU and mirin, a chemical inhibitor of MRE11 activity (Fig. 16A) (Dupré et al., 2008b), then we measured the length of the IdU tracts. As expected, mirin had no effect on HU-treated wild-type cells (Fig. 16B). However, we found that loss of MRE11 activity prevented IdU tract shortening by HU treatment in the absence of WRNIP1, reaching a value comparable to that of wild-type cells (7.89 and 4.95 µm, with or without MRE11 inhibition, respectively; Fig. 16B).

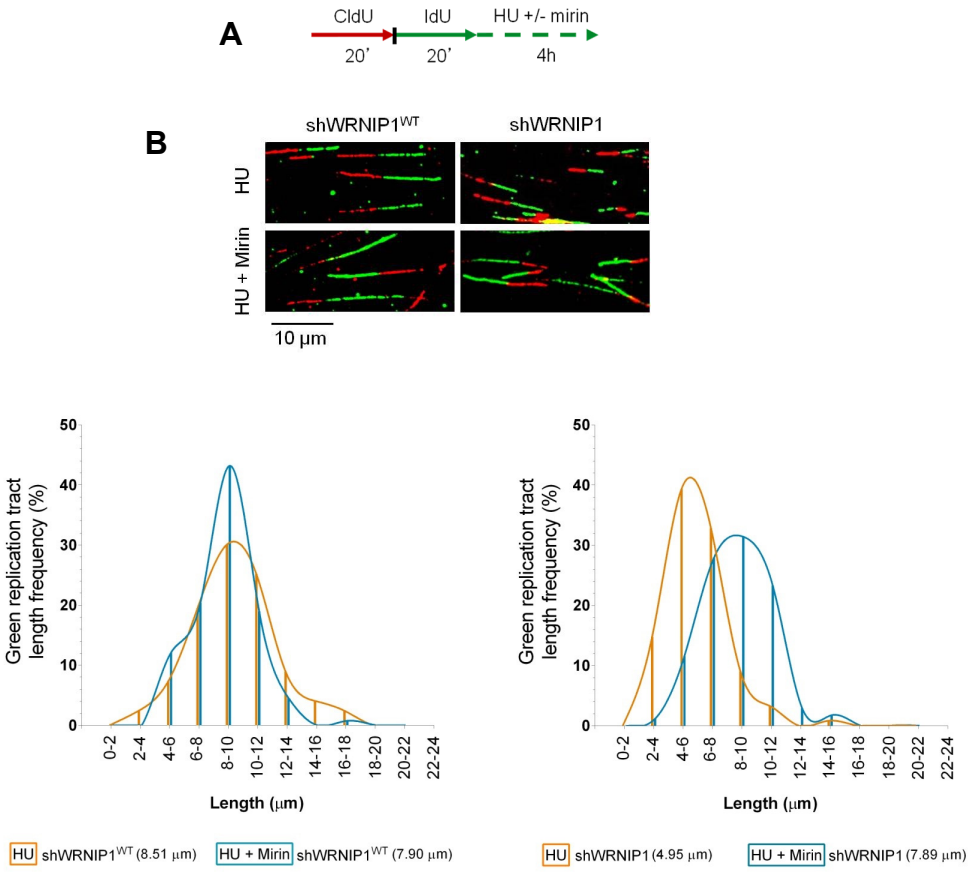

Figure 16. Inhibition of MRE11 exonuclease activity prevents nascent DNA strand degradation after replication stress. (A) Experimental scheme of dual labelling of DNA fibers in wild-type cells (shWRNIP1^{WT}) or WRNIP1-deficient cells (shWRNIP1). Cells were sequentially pulse-labelled with CldU and IdU as indicated, then left untreated or treated with 4 mM HU in combination or not with 50 μM Mirin. **(B)** Representative IdU tract length distributions in shWRNIP1^{WT} (left graph) or shWRNIP1 cells (right graph) after treatment. Median tract lengths are given in parentheses. See Appendix Tables 1 and 2 in Materials and Methods section for details on the data sets and statistical test. Representative DNA fiber images are shown. Scale bars, 10 μm.

Next, to exclude off-target effects produced by the MRE11 inhibitor, shWRNIP1 cells were transfected with siRNAs directed against MRE11, then labelled with IdU and treated with HU (Fig. 17A). Depletion of MRE11 resulted in a clear evidence of protection from nascent strand degradation during HU exposure, as IdU tract length was longer in HU-treated cells in which MRE11 was abrogated (7.43 and 4.72 μm, with or without MRE11 knockdown, respectively; Fig. 17B). Therefore, we conclude that MRE11 nuclease activity degrades stalled forks in the absence of WRNIP1.

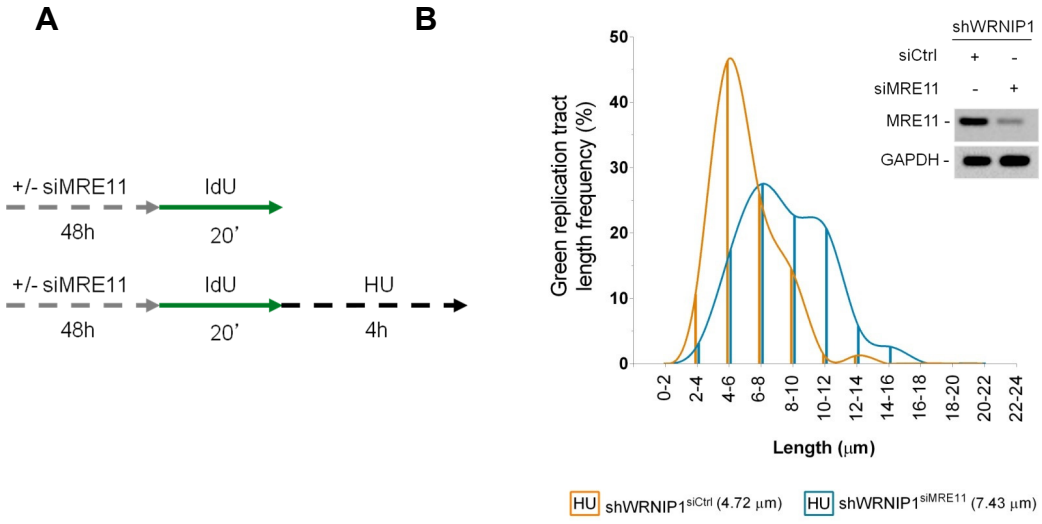

Figure 17. MRE11 interference in WRNIP1-deficient cells results in avoidance of nascent DNA strand degradation after replication stress. (A) Scheme of DNA fiber tract analysis in WRNIP1-deficient (shWRNIP1) cells. Cells were transfected with control siRNA (siCtrl) or *MRE11* siRNA (siMRE11), and 48 h thereafter labelled with IdU. Next, cells were treated or not with 4 mM HU. **(B)** Representative IdU tract length distributions in shWRNIP1 (shWRNIP1^{siCtrl}) cells or shWRNIP1 cells, in which MRE11 was depleted (shWRNIP1^{siMRE11}), treated or not with 4 mM HU. Median tract lengths are given in parentheses. See Appendix Tables 1 and 2 in Materials and Methods section for details on the data sets and statistical test. Western blot shows MRE11 depletion in shWRNIP1 cells. The membrane was probed with an anti-MRE11. GAPDH was used as a loading control.

WRNIP1 DEPLETION PRODUCES PARENTAL-STRAND ssDNA ACCUMULATION AND RAD51 DESTABILIZATION AFTER FORK STALLING

Next, we tested whether WRNIP1 depletion caused an increased parental-strand ssDNA accumulation at replication forks due to degradation of nascent DNA strand. We specifically visualized ssDNA by immunofluorescence using an anti-IdU antibody under non-denaturing conditions. To this aim, shWRNIP1^{WT} and shWRNIP1 cells were labelled with IdU for 24h, then released into fresh culture medium for 2h before stalling forks with HU (Fig.. 18). Moreover, to assess the dependence of ssDNA formed on MRE11 activity, parallel samples were exposed to mirin (Fig. 18). Our analysis showed that WRNIP1-deficient cells presented higher amount of ssDNA than wild-type cells under unperturbed and HU-treated conditions (Fig. 18). However, MRE11 inhibition substantially lowered the accumulation of ssDNA detected with or without fork stalling only in shWRNIP1 cells (Fig. 18).

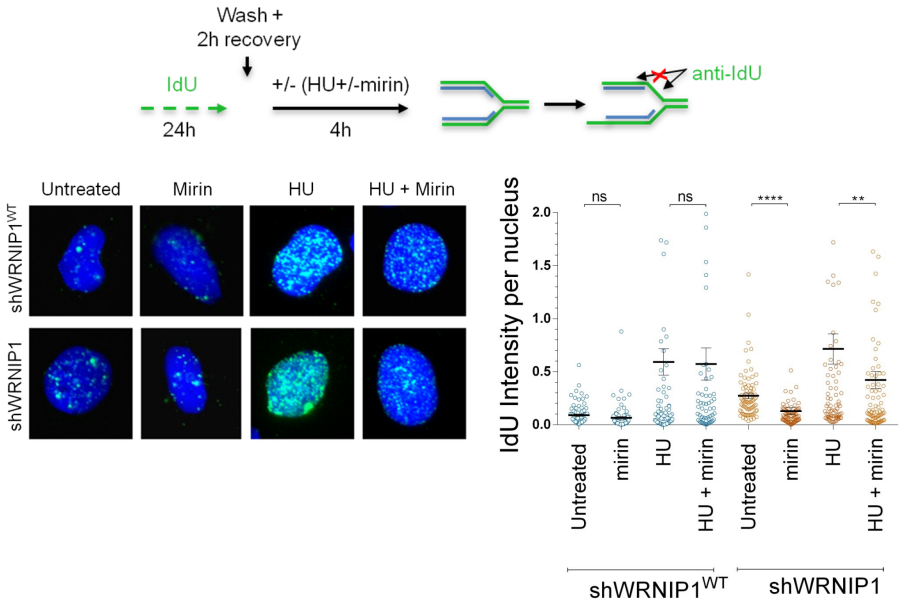

Figure 18. Analysis of parental ssDNA formation. Evaluation of ssDNA accumulation at parental-strand by immunofluorescence analysis in wild-type (shWRNIP1^{WT}) or WRNIP1-deficient (shWRNIP1) cells. Experimental design of ssDNA assay is shown. Cells were labelled with IdU for 24 h as indicated, washed and left to recover for 2 h, then treated or not with 4 mM HU. In parallel samples, the MRE11 activity is chemically inhibited with 50 μM Mirin, alone or in combination with HU-induced replication stress. After treatment, cells were fixed and stained with an anti-IdU antibody without denaturing the DNA to specifically detect parental ssDNA. Horizontal black lines represent the mean SE. Error bars represent standard error (ns, not significant; **, p<0.01; ****, p<0.0001; two-tailed Student's t test). Representative images are shown. DNA was counterstained with DAPI (blue).

Experiments with HU-treated shWRNIP1^{WT} and shWRNIP1 cells, in which MRE11 activity was disrupted by RNAi, confirmed the nuclease-dependent formation of ssDNA at parental strand in the absence of WRNIP1 (Fig. 19).

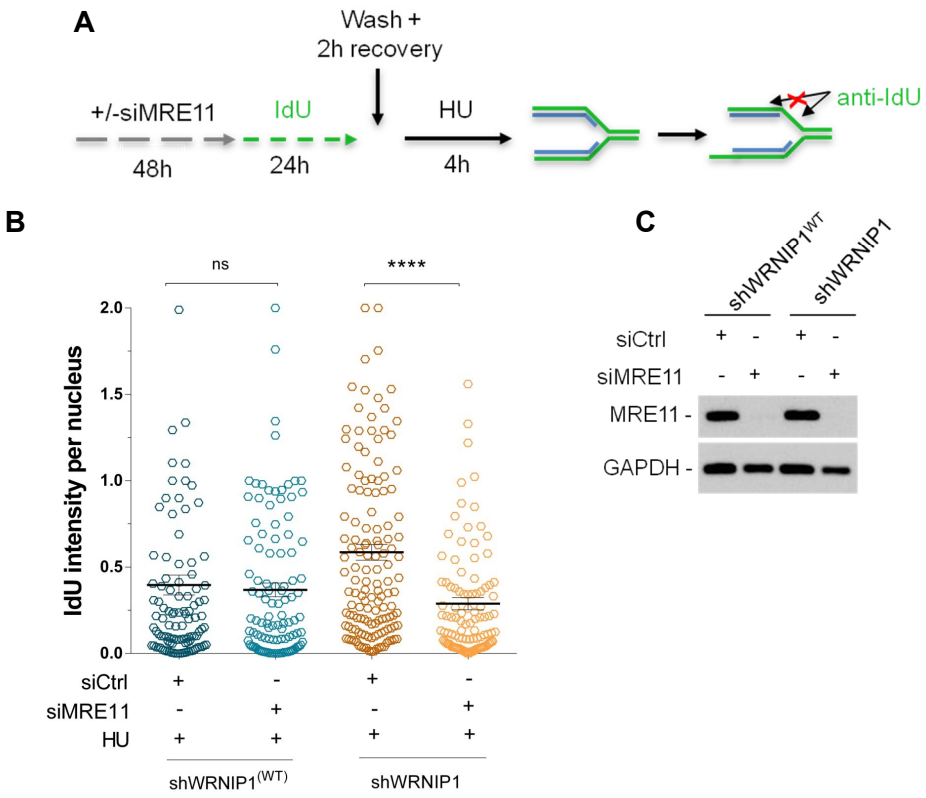

Figure 19. MRE11 depletion reduces ssDNA accumulation at parental-strand in WRNIP1-deficient cells. (**A**) Scheme of parental ssDNA assay. Wild-type (shWRNIP1^{WT}) and WRNIP1-deficient (shWRNIP1) cells were transfected with control siRNA (siCtrl) or *MRE11* siRNA (siMRE11), and 48 h afterward labelled with IdU for 24 h as indicated. Cells were washed and left to recover for 2 h, then treated with 4 mM HU. After treatment, cells were fixed and stained with an anti-IdU antibody without denaturing the DNA to specifically detect ssDNA at parental-strand. (**B**) Dot plot shows IdU intensity per nucleus. The intensity of the anti-IdU immunofluorescence was measured in at least 50 nuclei from two independent experiments. Horizontal black lines represent the mean SE. Error bars represent standard error (ns, not significant; ****, $p<0.0001$; two-tailed Student's t test). Western blot shows MRE11 depletion in shWRNIP1^{WT} and shWRNIP1 cells. (**C**) The membrane was probed with an anti-MRE11. GAPDH was used as a loading control.

Then, to verify whether nascent strand became single-stranded at stalled forks, shWRNIP1^{WT} and shWRNIP1 cells were shortly labelled with IdU immediately before HU treatment (Fig. 20). Immunofluorescence analysis showed little, but similar, IdU labelling in both shWRNIP1^{WT} and shWRNIP1 cells after HU treatment (Fig. 20).

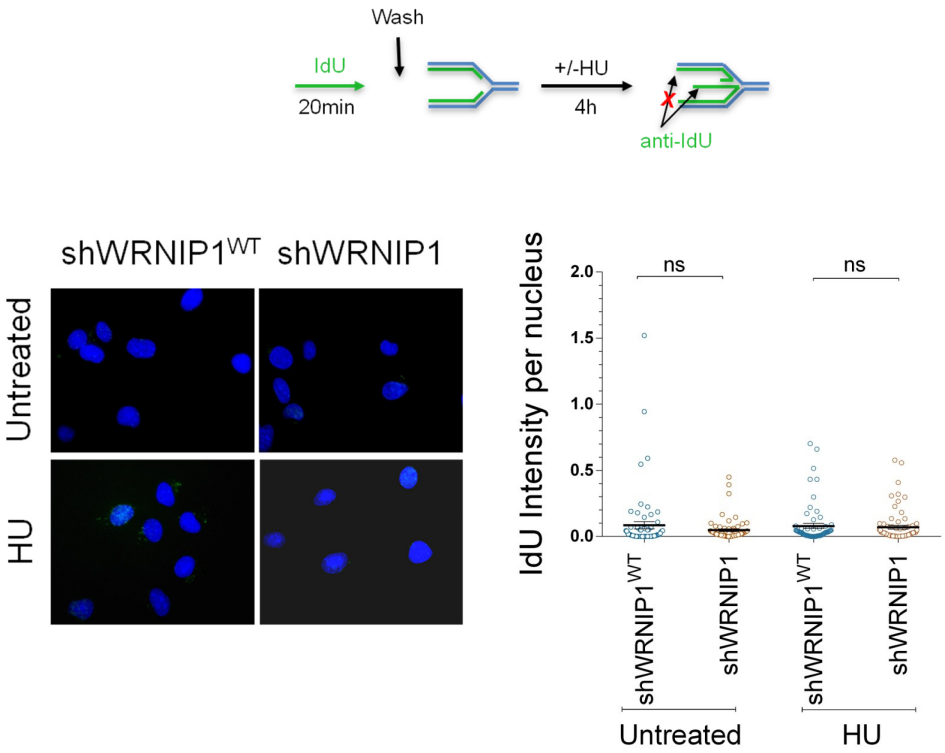

Figure 20. Analysis of nascent ssDNA accumulation in WRNIP1-deficient cells. Experimental design of ssDNA assay is reported. Wild-type (shWRNIP1^{WT}) and WRNIP1-deficient (shWRNIP1) cells were short-labelled with IdU, washed and treated or not with 4 mM HU for 4 h. After that, cells were fixed and stained with an anti-IdU antibody without denaturing the DNA to specifically detect nascent ssDNA. Dot plot shows IdU intensity per nucleus. Horizontal black lines represent the mean SE. Error bars represent standard error (ns, not significant; two-tailed Student's t test). Representative images are shown. DNA was counterstained with DAPI (blue).

Since RAD51-ssDNA complex is functionally relevant in protecting stalled replication forks from degradation (Schlacher et al., 2011), we wondered if the greater amount of ssDNA detected in WRNIP1-deficient cells could correlate with a larger amount of RAD51 bound to chromatin. To address this point, we performed a Western blot analysis after cellular fractionation in shWRNIP1^{WT} and shWRNIP1 cells treated or not with HU as indicated (Fig. 21A). As shown in Fig. 21A, the amount of chromatin-bound RAD51 was lower in shWRNIP1 than in shWRNIP1^{WT} cells under both unperturbed and fork-stalling conditions, suggesting that enhanced formation of ssDNA, in WRNIP1-deficient cells, is not accompanied by increased recruitment/stabilization of RAD51. Furthermore, as expected, in wild-type cells we observed an enhanced chromatin loading of MRE11 after fork stalling (Mirzoeva and Petrini, 2003), however, in WRNIP1-deficient cells, we detected a greater increase (Fig. 21A). In agreement with our biochemical fractionation experiments, immunofluorescence detection of RAD51 relocalization in shWRNIP1^{WT} and shWRNIP1 cells, treated or not with HU, showed a reduced percentage of RAD51 foci in the absence of WRNIP1 after fork stalling (Fig. 21B).

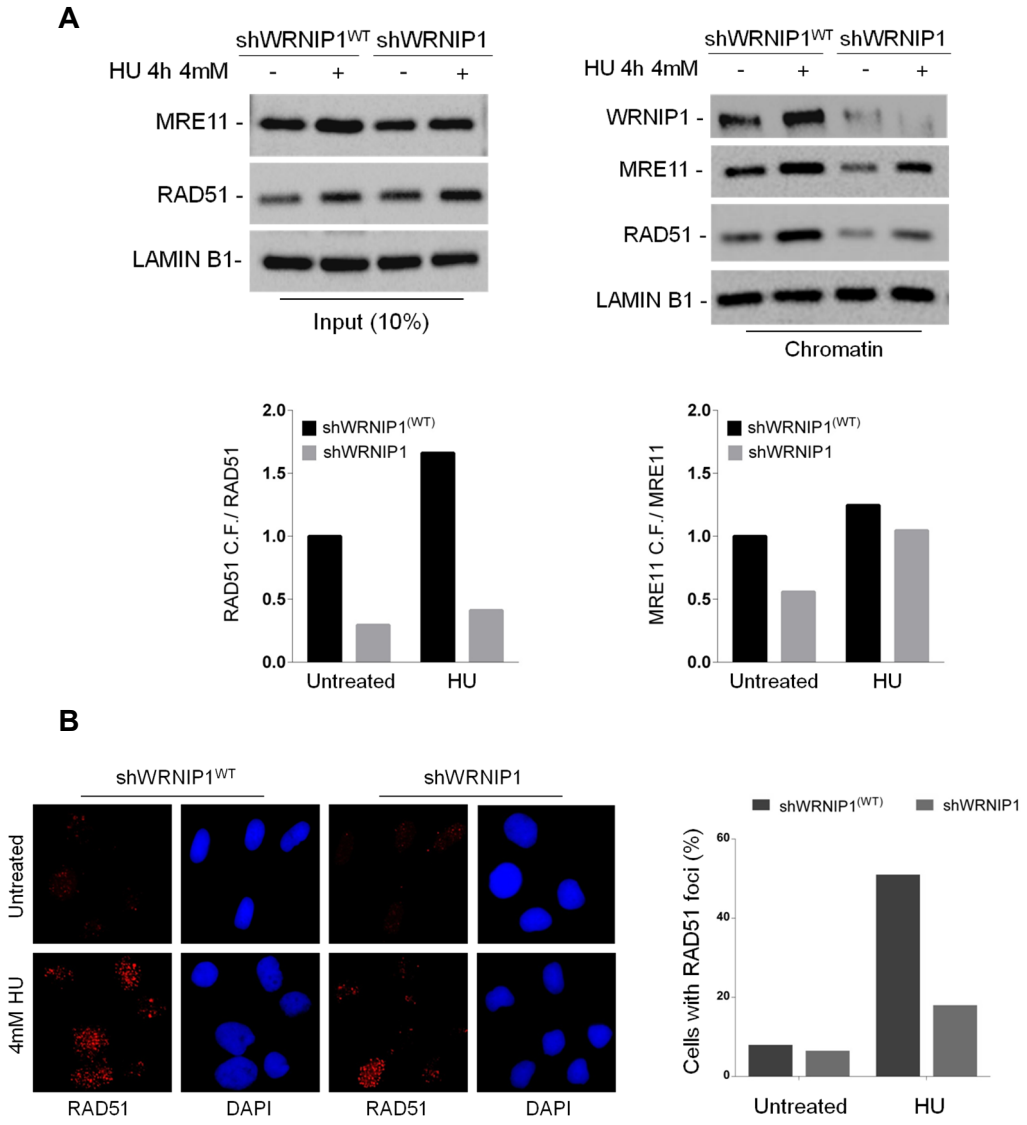

Figure 21. Analysis of RAD51 and MRE11 chromatin recruitment and RAD51 immunostaining (**A**) Analysis of chromatin binding of MRE11 and RAD51 in shWRNIP1^{WT} and shWRNIP1 cells. Chromatin fractions of cells, treated or not with 4 mM HU, were analysed by immunoblotting. The membrane was probed with the anti-WRNIP1, anti-MRE11 and anti-RAD51 antibodies. LAMIN B1 was used as a loading for the chromatin fraction. Total amount of RAD51 and MRE11 (Input) in the cells was determined with the relevant antibodies. LAMIN B1 was used as a loading control. In the graph, the fold increase respect to the wild-type untreated of the normalized ratio of the chromatin-bound RAD51 (or MRE11)/ total RAD51 (or MRE11) is reported for each cell line. (**B**) Wild-type (shWRNIP1^{WT}) or WRNIP1-deficient (shWRNIP1) cells were untreated or treated with 4 mM HU for 4 h, and then processed for immunofluorescence analysis with a specific anti-RAD51 antibody. The graph shows the percentage of cells with RAD51-foci. Representative images of cells stained for RAD51 are given. Nuclei were counterstained with DAPI (blue).

We further confirmed the presence of low levels of RAD51 in WRNIP1-deficient cells. Using a modification of the *in situ* proximity ligation assay (PLA), a fluorescence-based improved method that makes possible to reveal physical protein-protein interaction (Söderberg et al., 2008), to detect protein/DNA association (Iannascoli et al., 2015), we next investigated the co-localization of RAD51 at/near ssDNA. To this aim, shWRNIP1^{WT} and shWRNIP1 cells were treated or not with HU (Fig. 22). We found that the co-localisation between ssDNA (anti- IdU signal) and RAD51 significantly decreased in shWRNIP1 cells after replication stress (Fig. 22).

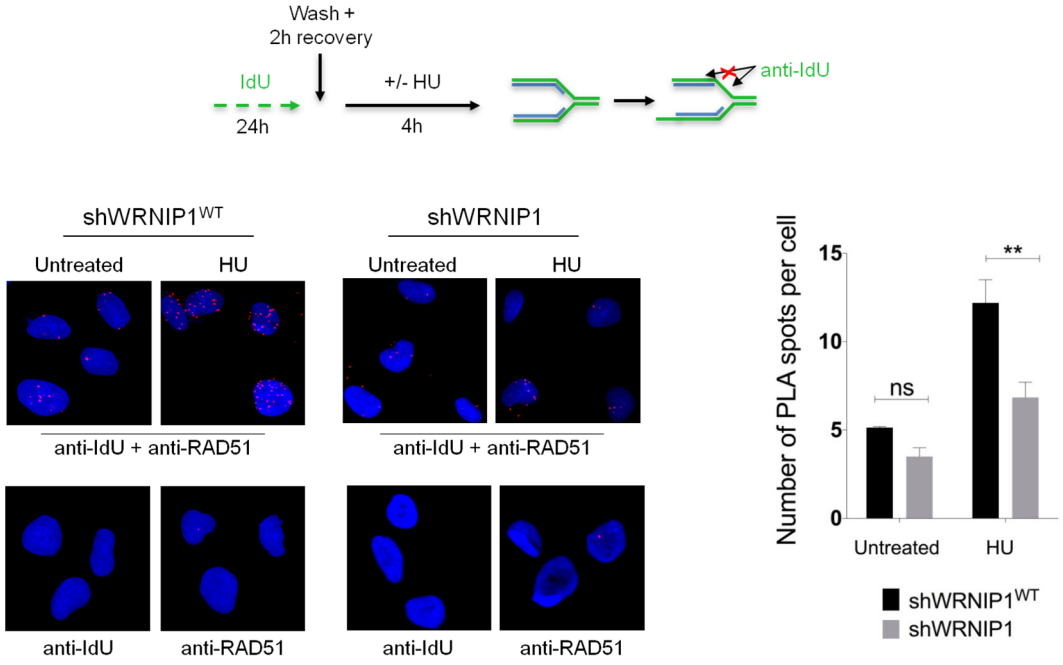

Figure 22. Analysis of DNA-protein interactions between ssDNA and endogenous RAD51 in shWRNIP1^{WT} and shWRNIP1 cells by *in situ* PLA assay. Experimental designed used for the assay is given. Cells were labelled with IdU for 24 h as indicated, washed and left to recover for 2 h, then treated or not with 4 mM HU for 4 h. Next, cells were fixed, stained with an anti-IdU antibody without denaturing the DNA to specifically detect parental-strand ssDNA, and subjected to PLA assay as described in the "Experimental procedures" section. Antibodies raised against IdU or RAD51 were used to reveal ssDNA or endogenous RAD51 respectively. Each red spot represents a single interaction between ssDNA and RAD51. No spot has been revealed in cells stained with each single antibody (negative control). DNA was counterstained with DAPI (blue). Representative images of the PLA assay are given. Graph shows the number of PLA spots per cell. Horizontal black lines represent the mean value (ns, not significant; **, $p < 0.01$; two-tailed Student's t test).

Since high amount of ssDNA formation was revealed in shWRNIP1 cells (Fig. 18), and given that visualization of a red spot in the cell requires the presence of both ssDNA (anti-IdU signal) and RAD51, the smaller number of PLA spots observed in the absence of WRNIP1 may correlate with the reduced levels of RAD51.

Finally, to exclude the possibility that, in shWRNIP1 cells, RAD51 was susceptible to proteasome-mediated degradation, we examined the amount of RAD51 upon MG132 treatment alone or in combination with HU. We found that proteasomal inhibition led to accumulation of RAD51 in unperturbed shWRNIP1 cells, but not after fork stalling (Fig. 23).

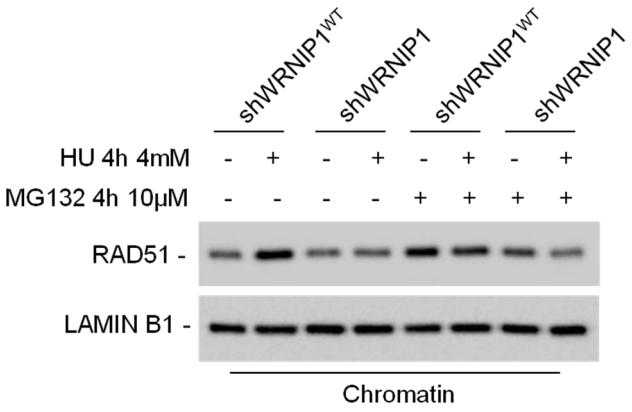

Figure 23. MG132 treatment does not accumulate RAD51 on chromatin after fork stalling. Analysis of chromatin binding of RAD51 in wild-type (shWRNIP1^{WT}) or WRNIP1-deficient (shWRNIP1) cells. Chromatin fractions of cells, treated or not with HU and proteasome inhibitor MG132 at the indicated times, were analysed by immunoblotting. The membrane was probed with an anti- anti-RAD51 antibody. LAMIN B1 was used as a loading for the chromatin fraction**.**

Therefore, we concluded that, under replication stress, RAD51 is not degraded but likely not properly stabilized in the absence of WRNIP1. Altogether these findings indicate that, when cells are depleted for WRNIP1, fork stalling results in a large enhancement of ssDNA at template DNA strand produced by the action of MRE11 nuclease activity, which does not lead to a greater amount of RAD51 bound to chromatin.

RAD51 AND MRE11 ARE DIFFERENTLY RECRUITED TO STALLED REPLICATION FORKS IN WRNIP1-DEFICIENT CELLS

Since our experiments suggest that loss of WRNIP1 results in reduced RAD51 loading to chromatin and MRE11-dependent nascent strand degradation after fork stalling, we wanted to ascertain whether RAD51 and MRE11 were differently recruited to stalled replication forks in the presence or absence of WRNIP1. To this end, shWRNIP1^{WT} and shWRNIP1 cells were pulse-labelled with CldU to mark newly replicated DNA, and exposed or not to HU. Co-immunoprecipitation of RAD51 or MRE11 with CldU-labelled replication sites was performed from cross-linked chromatin to detect DNA-associated proteins at replication forks. In line with previous studies (Petermann et al., 2010; Somyajit et al., 2015), our CldU-IP suggested the loading of RAD51 at nascent strand in wild-type cells (Fig. 24). Notably, under replication stress, in shWRNIP1 cells, RAD51 was detected at replication sites at lower levels than in shWRNIP1^{WT} cells (Fig. 24). In contrast, after fork stalling, the amount of MRE11 present in the CldU-IP was higher in the absence of WRNIP1 (Fig. 24). Moreover, and in accordance with a previous study (Dungrawala et al., 2015), this experiment indicated that WRNIP1 co-immunoprecipitated with CldU-labelled replication sites after HU treatment in wild-type cells, proving that WRNIP1 is associated with stalled replication forks (Fig. 24). Consistently with the MRE11-mediated nascent strand degradation observed in WRNIP1-deficient cells, these results provide evidence for impaired recruitment of RAD51, but enhanced recruitment of MRE11, to stalled replication forks.

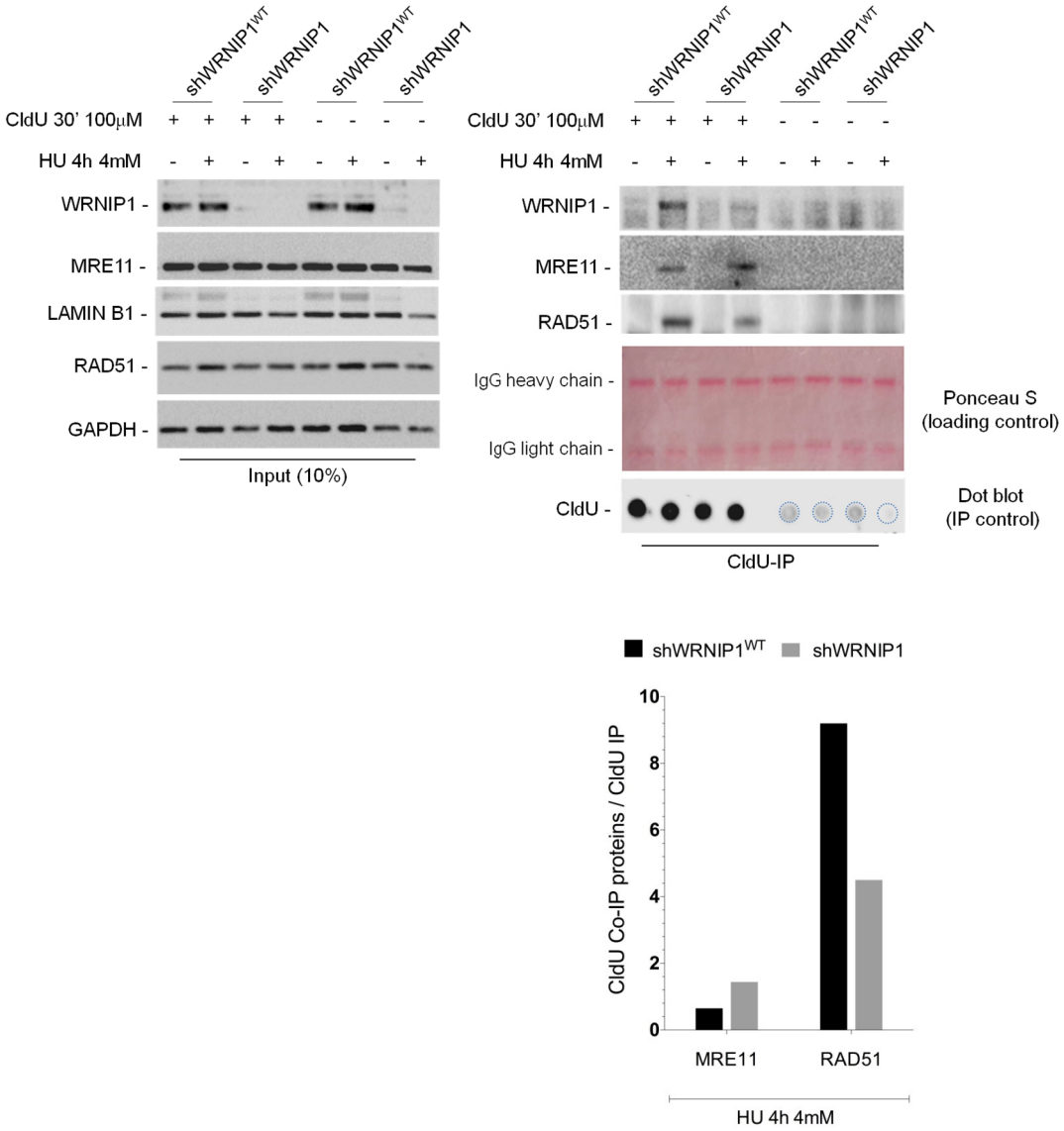

Figure 24. Localization of WRNIP1, MRE11 and RAD51 to stalled replication forks. Forks were isolated by CldU-co-immunoprecipitation (CldU-IP). shWRNIP1^{WT} or shWRNIP1 cells were pulse-labelled with CldU, then fixed or treated with HU. Cells were cross-linked, and the nuclear extracts were isolated (Input) and subjected to CldU-IP using an anti-CldU antibody (CldU-IP). The membranes were probed with the anti-WRNIP1 or anti-RAD51 antibodies. After stripping, the membranes were probed with an anti-MRE11 antibody. LAMIN B1 and GAPDH were used as loading controls (Input). Ponceau S was used as a loading control of CldU-IP. Dot blot analysis was performed to confirm that equal amounts of immunoprecipitated DNA from each sample. 10% of each IP was loaded on a nitrocellulose membrane. The membrane was probed with an anti-CldU antibody. The graph shows the normalized ratio of the proteins co-immunoprecipitated with CldU (CldU Co-IP proteins)/the total of labelled DNA immunoprecipitated with CldU (CldU IP) for each cell line after replication stress.

RAD51 PROTECTS NASCENT DNA STRAND FROM DEGRADATION AFTER REPLICATION STALLING IN WRNIP1-DEFICIENT CELLS

The RAD51 recombinase is directly implicated in the protection of nascent strand from MRE11-mediated degradation (Hashimoto et al., 2010; Schlacher et al., 2011), and BRCA2 stimulates RAD51 assembly on ssDNA (Jensen et al., 2010; Liu et al., 2010; Moynahan and Jasin, 2010). Since loss of WRNIP1 leads to a phenotype similar to that observed in BRCA2-defective cells, to identify the pathway in which WRNIP1 functions under replication stress, we examined whether chemical inhibition of RAD51, which disrupts RAD51 binding to DNA (Huang et al., 2012), could affect stabilization of stalled forks in WRNIP1-deficient cells. To this end, shWRNIP1^{WT} and shWRNIP1 cells were exposed to IdU and RAD51 inhibitor and treated with HU, then the length of the IdU tracts was measured (Fig. 25A). As expected, HU treatment resulted in IdU tract shortening in WRNIP1-deficient cells, but not in wild-type cells (5.31 and 7.40 μm, respectively; Fig. 25B). Moreover, as previously demonstrated (Schlacher et al., 2011), in wild-type cells treated with HU the inability to form RAD51 nucleoprotein filaments led to nascent strand degradation (Fig. 25B). However, our analysis showed that concomitant loss of WRNIP1 and RAD51 activity did not have a synergistic effect on degradation of nascent strand after HU (5.36 and 5.72 μm, shWRNIP1 and shWRNIP1^{WT} cells after HU+RAD51i, respectively; Fig. 25B). Moreover, DNA fiber analysis executed in wild-type and WRNIP1-deficient cells, in which RAD51 was downregulated by RNA interference, was comparable to that deriving from chemical inhibition of RAD51 (Fig. 25C-D).

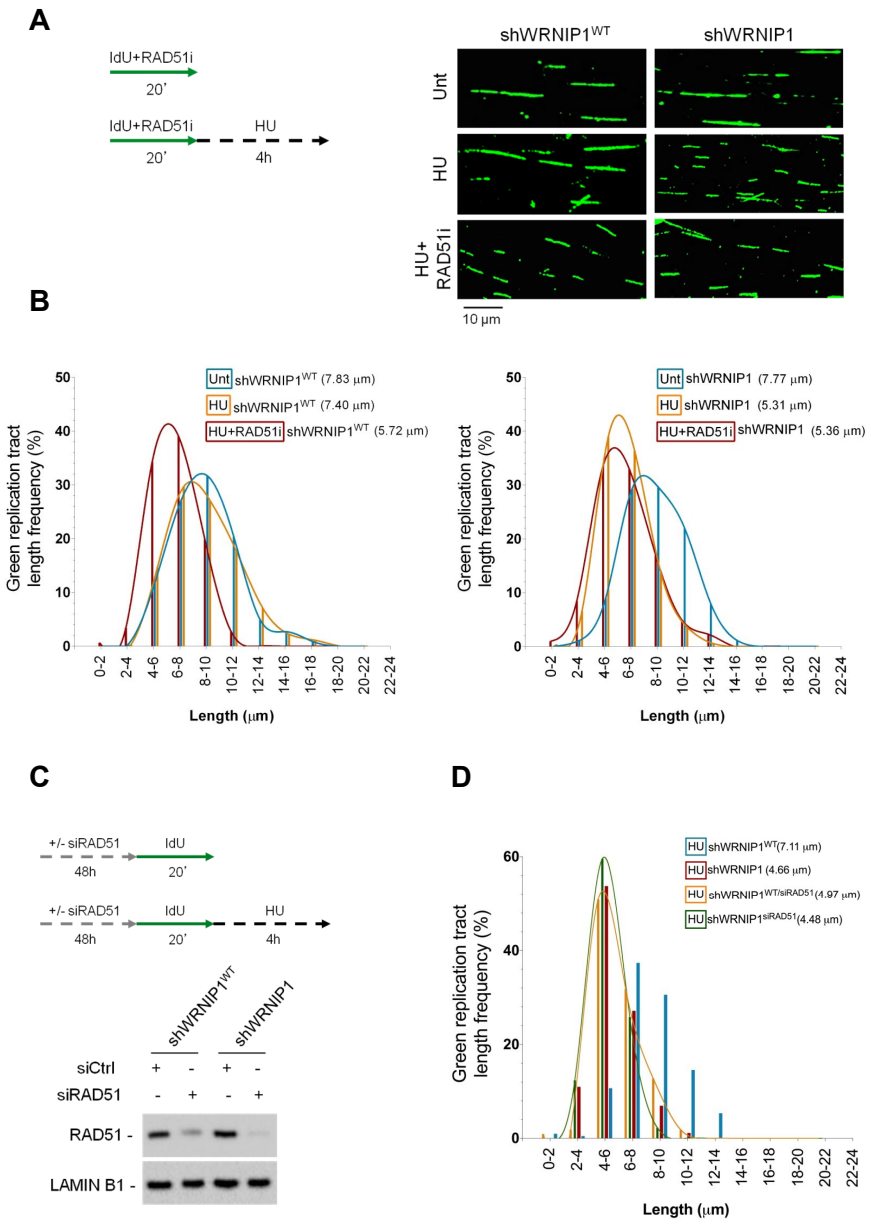

Figure 25. RAD51 chemical inhibition or interference in WRNIP1-deficient cells have not a synergistic effect on degradation of nascent DNA strand at stalled fork. (A) Experimental scheme of pulse-labelling of DNA fibers in wild-type cells (shWRNIP1^{WT}) or WRNIP1-deficient cells (shWRNIP1). Cells were labelled with IdU and exposed or not to 25 µM RAD51 inhibitor, then treated or not with 4 mM HU. **(B)** **R**epresentative IdU tract length distributions in shWRNIP1^{WT} cells (left graph) or shWRNIP1 cells (right graph). Median tract lengths are reported in parentheses. See Appendix Tables 1 and 2 in Materials and Methods section for details on the data sets and statistical test. Representative DNA fiber images are reported. Scale bars, 10 µm. **(C)** Scheme of DNA fiber tract analysis in wild-type (shWRNIP1^{WT}) or WRNIP1-deficient (shWRNIP1) cells. Cells were transfected with control siRNA (siCtrl) or *RAD51* siRNA (siRAD51), and 48 h thereafter labelled with IdU. Next, cells were treated or not with 4 mM HU. **(D)** Representative IdU tract length distributions in control shWRNIP1^{WT} or shWRNIP1 cells (shWRNIP1^{WT} or shWRNIP1, respectively), or cells in which RAD51 was depleted (shWRNIP1$^{WT/siRAD51}$ or shWRNIP1^{siRAD51}, respectively), treated or not with 4 mM HU. Median tract lengths are given in parentheses. See Appendix Tables 1 and 2 in Materials and Methods section for details on the data sets and statistical test. Western blot shows RAD51 depletion in the cells. The membrane was probed with an anti-RAD51. LAMIN B1 was used as a loading control.

Next, to directly test the requirement of RAD51 in the protection of stalled forks in the absence of WRNIP1, we over-expressed the wild-type human RAD51 in shWRNIP1 cells, and 48 h thereafter we treated them with HU (Fig. 26A). The over-expression of RAD51 in WRNIP1-deficient cells counteracted the shortening of IdU tracts upon HU (5.11 and 7.89 µm, with empty vector or wild-type RAD51, respectively; Fig. 26B). Therefore, WRNIP1 protects stalled replication forks by effective loading or retention of RAD51.

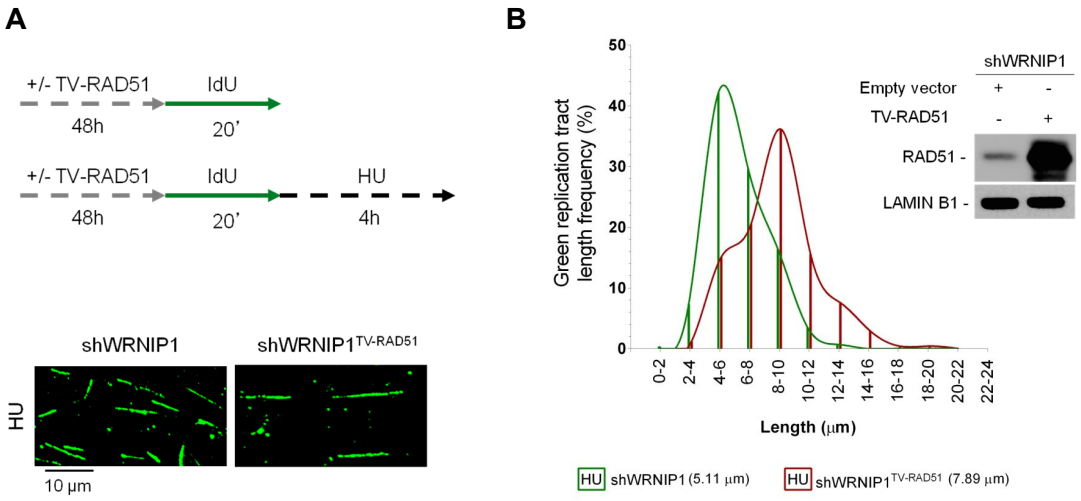

Figure 26. RAD51 overexpression protects nascent DNA strand from degradation after fork stalling in the absence of WRNIP1. (A) Scheme of DNA fiber tract analysis in shWRNIP1 cells. Cells were transfected with an empty vector or a plasmid expressing a wild-type human RAD51, and 48 h thereafter labelled with IdU and treated or not with 4 mM HU. **(B)** Representative IdU tract length distributions in shWRNIP1 cells or shWRNIP1 cells expressing exogenous wild-type RAD51 after HU exposure. Median tract lengths are given in parentheses. See Appendix Tables 1 and 2 in Materials and Methods section for details on the data sets and statistical test. Representative DNA fiber images are given. Scale bars, 10 µm. Western blot shows the expression of the RAD51 protein in shWRNIP1 cells. The membrane was probed with an anti-RAD51. LAMIN B1 was used as a loading control.

WRNIP1 STABILIZES RAD51 ON STALLED FORKS

To understand the functional correlation between WRNIP1 and RAD51, we investigated their possible interaction *in vivo,* by performing co-IP studies. HEK293T cells were transfected with the FLAG-tagged wild-type WRNIP1 and treated or not with HU. Our co-IP demonstrated that WRNIP1 associated with RAD51 both in the presence or absence of replication stress (Fig. 27A). In addition, we found that WRNIP1 immunoprecipitated also BRCA2 (Fig. 27A). To confirm the physical interaction of WRNIP1 with RAD51, we carried out the PLA analysis, a method allowing the detection of protein-protein interactions (Söderberg et al., 2008). To do this, shWRNIP1^{WT} cells were treated or not with HU, then subjected to the PLA. As shown in Fig. 27B, a fluorescent signal requiring the presence of both WRNIP1 and RAD51 was detected, showing their close localization *in situ*. Moreover, HU treatment increased the number of PLA spots per cell (Fig. 27B). Interestingly, similar results were obtained in shWRNIP1^{T294A} cells, suggesting that inhibition of catalytic activity of WRNIP1 does not hamper its interaction with RAD51 (Fig. 27B).

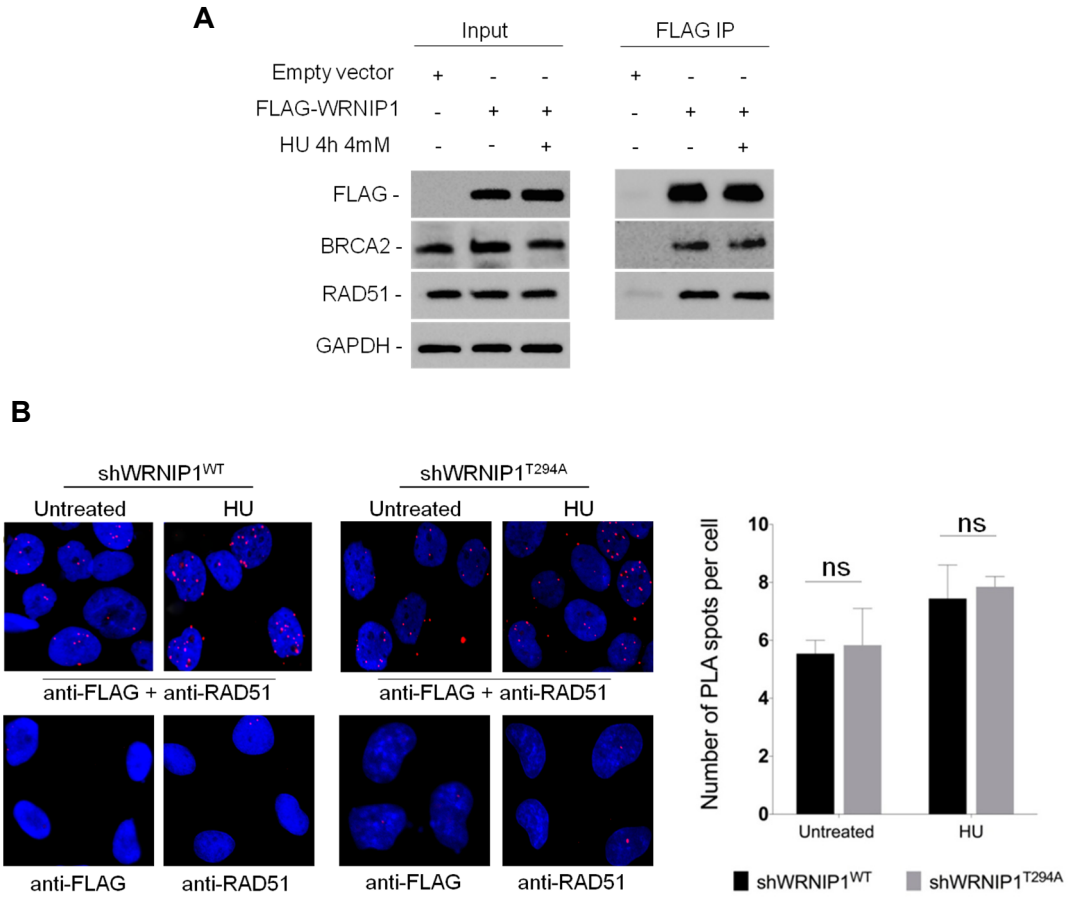

Figure 27 WRNIP1 and RAD51 physically interact both in the presence or absence of replication stress. (**A**) Co-immunoprecipitation experiments in HEK293T cells transfected with empty vector or FLAG-WRNIP1 plasmid. Cells were treated or not with HU. After treatment, cell lysates were immunoprecipitated (FLAG IP) using anti-FLAG antibody. The presence of WRNIP1, BRCA2 and RAD51 was assessed by immunoblotting using the anti-FLAG, anti-RAD51 and anti-BRCA2 antibodies, respectively. Whole cell extracts were analysed (Input). The membrane was probed with the same antibodies used for IP. GAPDH was used as a loading control. (**B**) Analysis of protein-protein interactions between WRNIP1 and endogenous RAD51 in wild-type (shWRNIP1^{WT}) or WRNIP1-mutant (shWRNIP1^{T294A}) cells by *in situ* PLA assay. Cells were labelled with IdU for 24 h, washed and left to recover for 2 h, then treated or not with 4 mM HU. Antibodies raised against FLAG-Tag and RAD51 were used to reveal FLAG-WRNIP1 or endogenous RAD51 respectively. Each red spot represents a single interaction between WRNIP1 and RAD51. No spot has been revealed in cells stained with each single antibody (negative control). DNA was counterstained with DAPI (blue). Representative images of the PLA assay are shown. Graph shows the mean number of PLA spots per cell SE. Error bars represent standard error (ns, not significant; two-tailed Student's t test).

To explore the link existing between WRNIP1 and the BRCA2/RAD51 complex in response to replication perturbation, DNA fiber assay was performed in HU-treated shWRNIP1^{WT} or shWRNIP1 cells, in which BRCA2 was downregulated by RNAi (Fig. 28A). In agreement with the observation that inhibition of RAD51 did not enhance the level of fork degradation at HU-stalled forks in WRNIP1-deficient cells (Fig. 25A), our analysis showed that concomitant depletion of WRNIP1 and BRCA2 did not result in further destabilization of stalled forks (4.56 and 4.67 µm, shWRNIP1$^{WT/siBRCA2}$ and shWRNIP1^{siBRCA2} cells after HU, respectively; Fig. 28B).

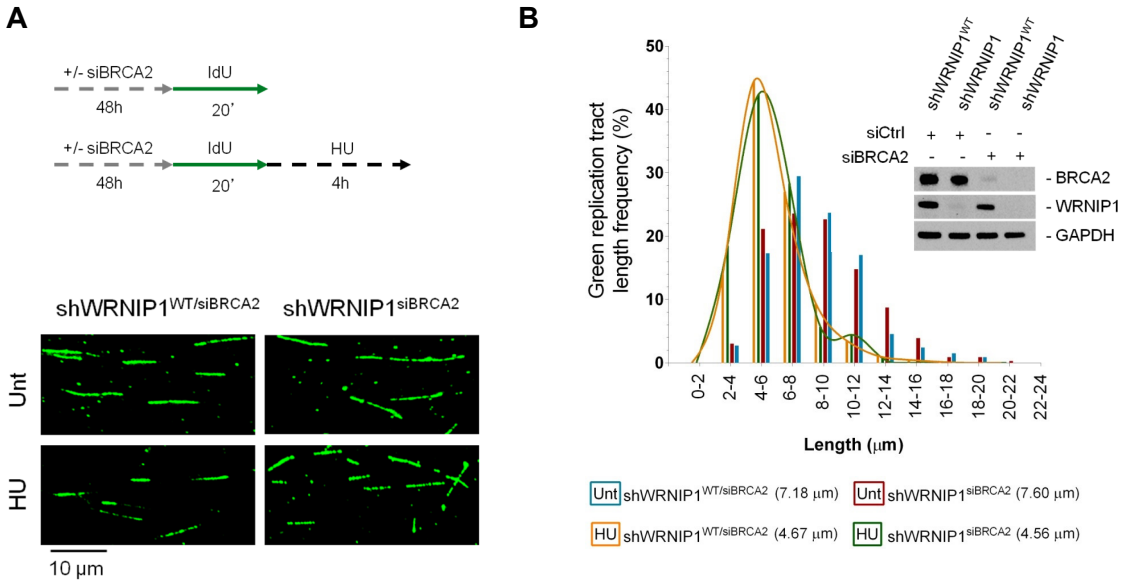

Figure 28. BRCA2 interference in WRNIP1-deficient cells has not a synergistic effect on degradation of nascent DNA strand at stalled fork. (**A**) Experimental scheme of pulse-labelling of DNA fibers in wild-type cells (shWRNIP1^{WT}) or WRNIP1-deficient cells (shWRNIP1). Cells were transfected with *BRCA2*

siRNA (siBRCA2), and 48 h thereafter labelled with IdU, then treated or not with 4 mM HU. (**B**) Representative IdU tract length distributions in shWRNIP1$^{WT/siBRCA2}$ or shWRNIP1^{siBRCA2} cells treated or not with HU. Median tract lengths are given in parentheses. See Appendix Tables 1 and 2 in Materials and Methods section for details on the data sets and statistical test. Representative DNA fiber images are reported. Scale bars, 10 μm. Western blot shows BRCA2 depletion in shWRNIP1^{WT} and shWRNIP1 cells. The membrane was probed with an anti-BRCA2 or anti-WRNIP1. GAPDH was used as a loading control.

This suggests that WRNIP1 and the BRCA2/RAD51 complex lie on a pathway involved in blocking degradation of newly synthesized DNA strand.

Since BRCA2 mediates RAD51 loading on ssDNA (Jensen et al., 2010; Liu et al., 2010; Moynahan and Jasin, 2010), we verified whether, in WRNIP1-deficient cells, the low amount of chromatin-bound RAD51 could depend on inefficient recruitment of BRCA2 upon replication stress. Immunofluorescence analysis showed no difference in the ability of shWRNIP1^{WT} and shWRNIP1 cells to relocalise BRCA2 after HU (Fig. 29).

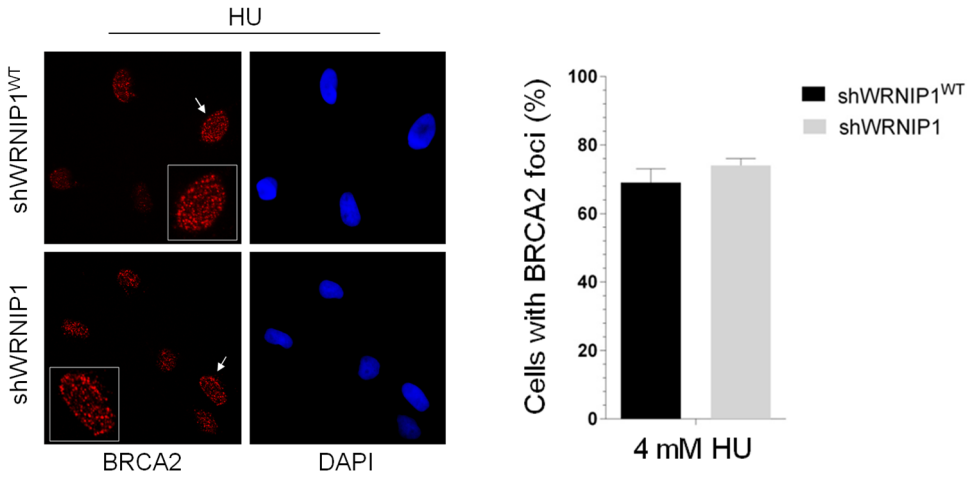

Figure 29. Loss of WRNIP1 does not affect BRCA2 relocalisation in foci after replication stress
Effect of loss of WRNIP1 on BRCA2 subnuclear relocalisation after treatment. Wild-type (shWRNIP1^{WT}) and WRNIP1-deficient (shWRNIP1) cells were treated or not with 4 mM HU for 4 h, then subjected to BRCA2 immunofluorescence. Graph shows the percentage of cells with BRCA2-positive foci after treatment. Error bars represent standard errors. (ns, not significant; two-tailed Student's t test). Representative images of cells with BRCA2 relocalised in foci after HU exposure are shown. Insets show enlarged nuclei for a better evaluation of BRCA2 relocalisation in the cells.

Thus, we asked whether the defective phenotype could derive from an uncontrolled translocase activity of the F-box DNA helicase 1 (FBH1) (Simandlova et al., 2013), leading to disruption of RAD51 filaments in the absence of WRNIP1. To this aim, we examined the stability of nascent strand in shWRNIP1 cells depleted for FBH1 using siRNA, and treated according to the scheme (Fig. 30A). Interestingly, DNA fiber analysis showed that abrogation of FBH1 prevented the shortening of IdU tracts after HU in WRNIP1-deficient cells (Fig. 30B). FBH1 is involved in extracting RAD51 from chromatin (Simandlova et al., 2013), and we found that its depletion restores DNA fiber length in the absence of WRNIP1. To test whether this phenotypic reversion could relate to stabilization of RAD51, we then performed cellular fractionation experiments in shWRNIP1 cells, in which FBH1 was downregulated. Our analysis showed that loss of FBH1 was associated with an increase in the proportion of RAD51 that is chromatin-bound under unperturbed and HU-treated conditions (Fig. 30C). Altogether, these experiments allow us to conclude that WRNIP1 serves to stabilize than recruit RAD51 to stalled forks, protecting them from the MRE11-dependent degradation.

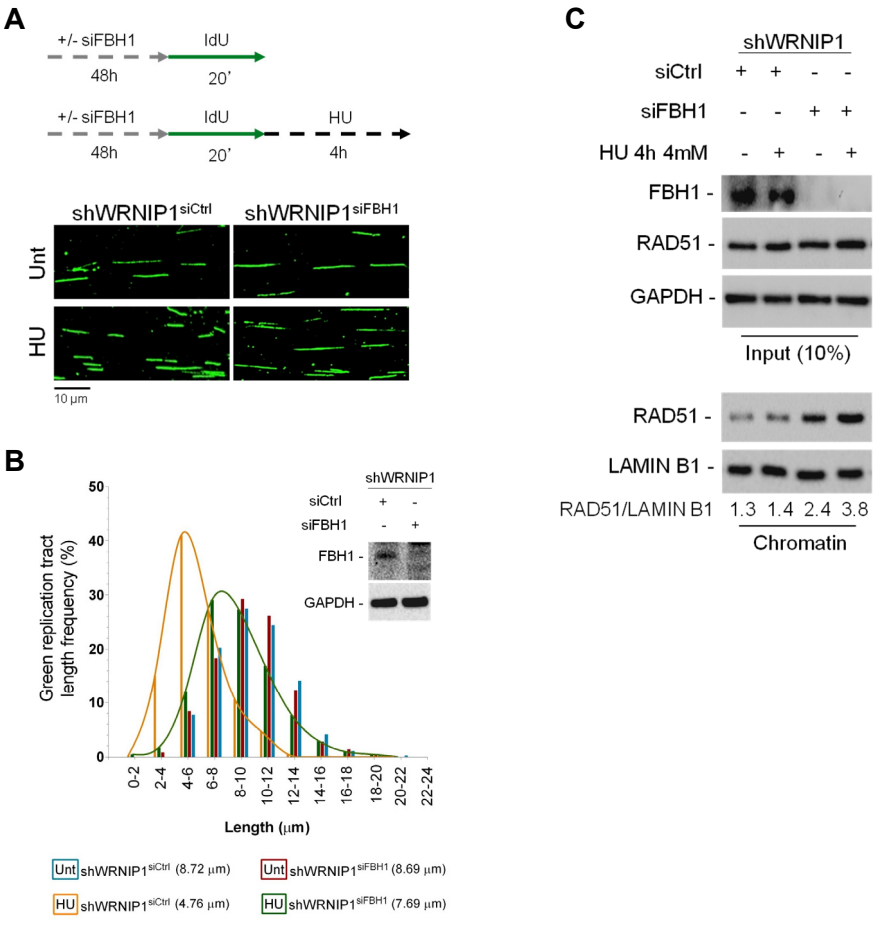

Figure 30. FBH1 depletion in WRNIP1-deficient cells stabilizes RAD51 onto chromatin preventing degradation of nascent DNA strand at stalled fork. (**A**) Experimental scheme of pulse-labelling of DNA fibers in shWRNIP1 cells. Cells were transfected with control siRNA (shWRNIP1siCtrl) or FBH1 siRNA (shWRNIP1siFBH1), and 48 h thereafter labelled with IdU, then treated or not with 4 mM HU. (**B**) Representative IdU tract length distributions in shWRNIP1siCtrl or shWRNIP1siFBH1 cells with or without HU treatment. Representative DNA fiber images are reported. Scale bars, 10 μm. Western blot shows FBH1 depletion in the cells. The membrane was probed with an anti-FBH1. GAPDH was used as a loading control. Median tract lengths are given in parentheses. See Appendix Tables 1 and 2 in Materials and Methods section for details on the data sets and statistical test. (**C**) Analysis of chromatin binding of RAD51 in shWRNIP1 cells depleted for FBH1. Cells were transfected with control siRNA (shWRNIP1siCtrl) or FBH1 siRNA (shWRNIP1siFBH1), and 48 h treated or not with HU for 4h. Chromatin fractions of cells were analysed by immunoblotting. The membrane was probed with the anti-FBH1 and anti-RAD51 antibodies. LAMIN B1 was used as a loading for the chromatin fraction. Total amount of RAD51 (Input) in the cells was determined with the relevant antibodies. GAPDH was used as a loading control. The ratio of the RAD51/LAMIN B1 signal (chromatin) is reported below each lane.

LOSS OF WRNIP1 OR ITS ATPase ACTIVITY LEADS TO DNA DAMAGE ACCUMULATION AND CELL DEATH AFTER REPLICATION STALLING

We next sought to characterize the physiological consequences of the inability of WRNIP1-deficient or mutant cells to preserve fork stability or promote fork restart after replication stress. We first examined the levels of DNA damage in wild-type (shWRNIP1^{WT}), WRNIP1-deficient (shWRNIP1) or mutant cells (shWRNIP1^{T294A}) under unperturbed cell growth conditions or upon HU-induced replication stress. We measured DNA damage accumulation at the single-cell level using anti-phospho-H2AX immunostaining. H2AX phosphorylation (γ-H2AX) is considered an early sign of DNA damage induced by replication stalling (Ward and Chen, 2001). Thus, shWRNIP1^{WT}, shWRNIP1 and shWRNIP1^{T294A} cells were treated or not with HU for 4 h, then immunostained with an anti-γ-H2AX antibody (Fig. 31). Our results showed that loss of WRNIP1 function or its ATPase activity resulted *per se* in about five-fold and three-fold increase in the percentage of γ-H2AX-positive foci-containing cells, respectively, relative to that of the control cells (Fig. 31).

In contrast, HU treatment led to enhanced accumulation of γ-H2AX-positive nuclei in all cell lines (Fig. 31). However, the increase in γ-H2AX foci formation appeared greater for shWRNIP1 and shWRNIP1^{T294A} cells, about 40% and 34%, respectively, versus 24% of wild-type cells (Fig. 31).

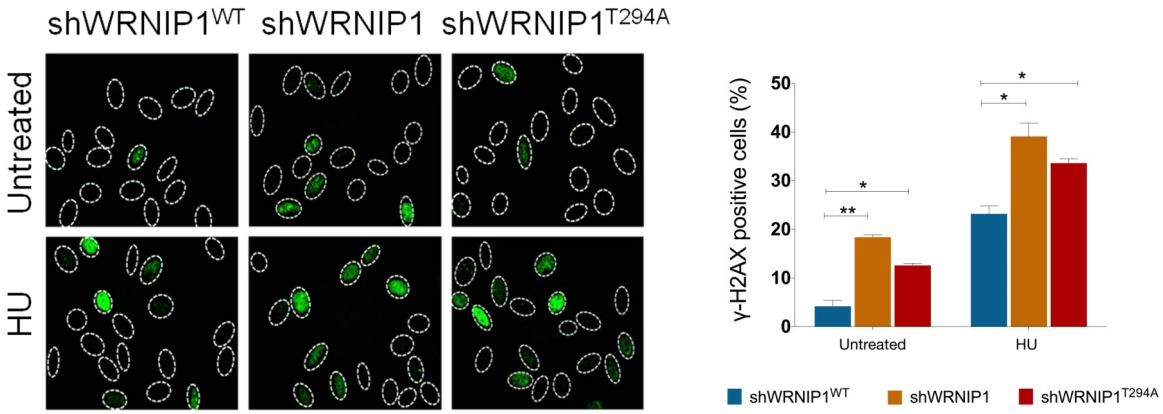

Figure 31. Analysis of DNA damage accumulation. Wild-type (shWRNIP1^{WT}), WRNIP1-deficient (shWRNIP1) or mutant (shWRNIP1^{T294A}) cells were treated or not with 4 mM HU for 4 h, then subjected to γ-H2AX immunofluorescence. Graph shows data presented as mean of γ-H2AX-positive cells SE from three independent experiments. Error bars represent standard error (*, $p < 0.1$; **, $p < 0.01$; two-tailed Student's t test). Representative images of nuclei showing the different number of foci per nucleus are reported.

As an alternative and sensitive method for the detection of DNA damage in individual cells, we used alkaline Comet assay. The experiments were performed under the same conditions as for -H2AX analysis. We found that loss of WRNIP1 or its ATPase activity increased the spontaneous level of DNA breakage compared with wild-type cells, similar to what observed by fluorescent data (Fig. 32A). Moreover, HU treatment caused a further enhancement of Comet tail moment reaching values significantly higher in shWRNIP1 and shWRNIP1^{T294A} cells than those in the control cells (Fig. 32A). To verify whether double-strand breaks (DSBs) were formed under our experimental conditions, we performed the neutral Comet assay in parallel samples. Comparing the Comet tail moment in the different cell lines tested, we did not notice appreciable amounts of DSBs (Fig. 32B).

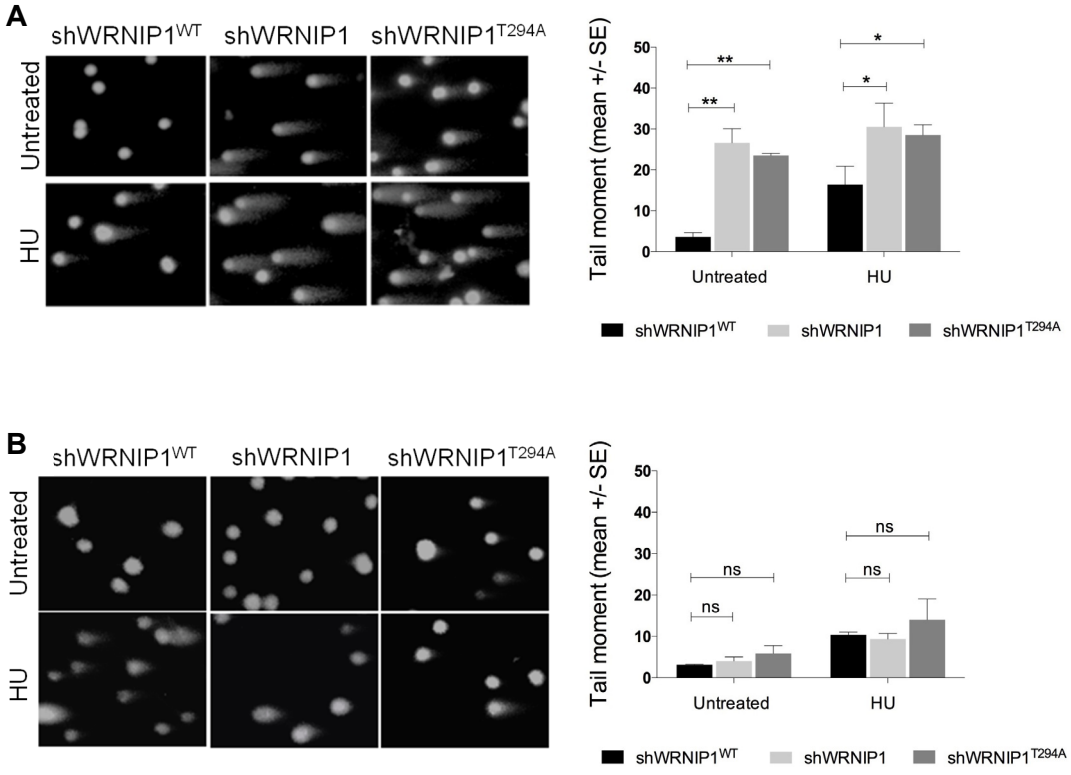

Figure 32. Loss of WRNIP1 or its ATPase activity produces DNA breakage, but not DSBs after replication fork stalling. (**A**) Analysis of DNA breakage accumulation evaluated by alkaline Comet assay. shWRNIP1^{WT}, shWRNIP1 and shWRNIP1^{T294A} cells were treated as in (A), then subjected to alkaline Comet assay. Graph shows data presented as mean tail moment SE from three independent experiments. Error bars represent standard error (*, $p < 0.1$; **, $p < 0.01$; two-tailed Student's t test). Representative images are shown. (**B**) Analysis of DSB formation evaluated by neutral Comet assay. Wild-type (shWRNIP1^{WT}), WRNIP1-deficient (shWRNIP1) or mutant (shWRNIP1^{T294A}) cells were treated with 4 mM HU for 4 h, then subjected to Comet assay. Graph shows data presented as mean tail moment SE from three independent experiments. Error bars represent standard errors. (ns, not significant; two-tailed Student's t test). Representative images are shown.

Furthermore, evaluation of cell viability by the fluorescence-based LIVE/DEAD assay confirmed that WRNIP1-deficient cells were more sensitive to HU, as the percentage of dead cells was higher than that of wild-type cells (Fig. 33). Similarly, expression of mutant form of WRNIP1 (shWRNIP1^{T294A}) led to enhanced cell death after HU exposure respect to shWRNIP1^{WT} cells (Fig. 33).

Thus, these experiments demonstrate that WRNIP1-deficient and mutant cells exhibit high sensitivity to HU-induced fork stalling, leading to DNA damage accumulation and cell death.

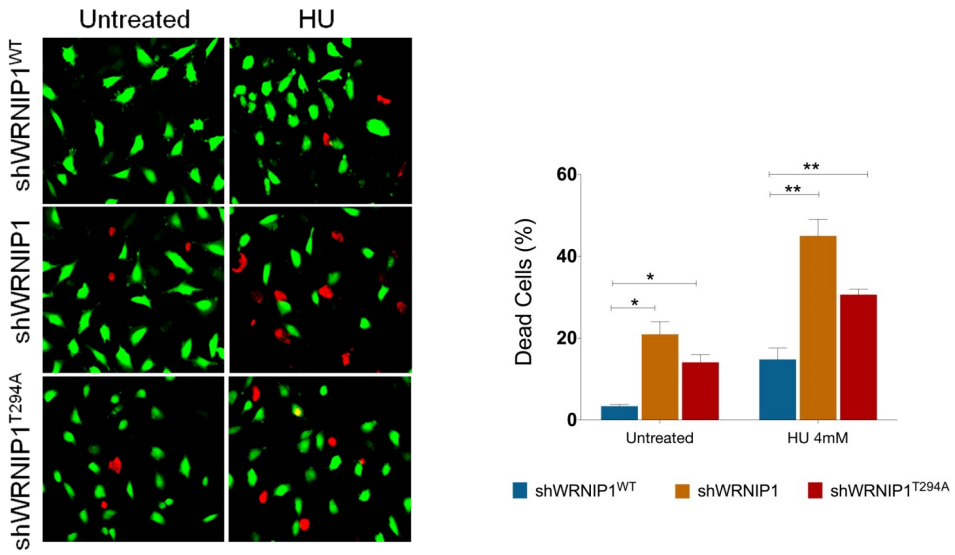

Figure 33. Loss of WRNIP1 or its ATPase activity increases cell death both in presence and absence of replication stress. shWRNIP1^{WT} shWRNIP1 and shWRNIP1^{T294A} cells were treated or not with 4 mM HU for 16 h. Cell viability was evaluated by LIVE/DEAD fluorescent assay. Data are expressed as mean of dead cells SE from three independent experiments. Error bars represent standard error (*, $p < 0.1$; **, $p < 0.01$; two-tailed Student's t test). Representative images of double-staining of viable (green) and dead (red) cells are shown.

UNPROTECTED STALLED FORKS LEAD TO CHROMOSOMAL INSTABILITY IN WRNIP1-DEFICIENT CELLS

To obtain further insights into the role of WRNIP1 in maintaining genome stability, we analysed the consequences of loss of WRNIP1 functions on chromosomal damage after HU-induced replication stress. To this aim, shWRNIP1^{WT}, shWRNIP1 and shWRNIP1^{T294A} cells were exposed to HU for 5 h, and released into drug-free medium for 16 h prior to the addition of colcemid for 3 h to collect metaphase chromosomes (Fig. 34A). Our analysis showed that WRNIP1-deficient as well as mutant cells, displayed higher spontaneous levels of chromosomal aberrations respect to wild-type cells (Fig. 34A), suggesting that loss of WRNIP1 by itself or of its ATPase activity can cause genome instability. Moreover, HU treatment significantly increased the mean number of total chromosomal aberrations per cell in shWRNIP1 cells, whereas, in both shWRNIP1^{WT} and shWRNIP1^{T294A} cells did not produce a similar effect (Fig. 34A). Next, we verified whether chromosomal damage formed after HU treatment in the absence of WRNIP1 could correlate with the MRE11-dependent nascent strand degradation. To do this, we

treated shWRNIP1 cells with HU and mirin or with mirin alone. Interestingly, we found that chemical inhibition of MRE11 activity during fork stalling led to attenuation of the level of chromosomal aberrations per cell in shWRNIP1 cells (Fig. 34B). In addition, the same analysis performed in cells in which MRE11 was downregulated by RNA interference (siMRE11) was comparable to that resulting from chemical inhibition of MRE11 (Fig. 34C).

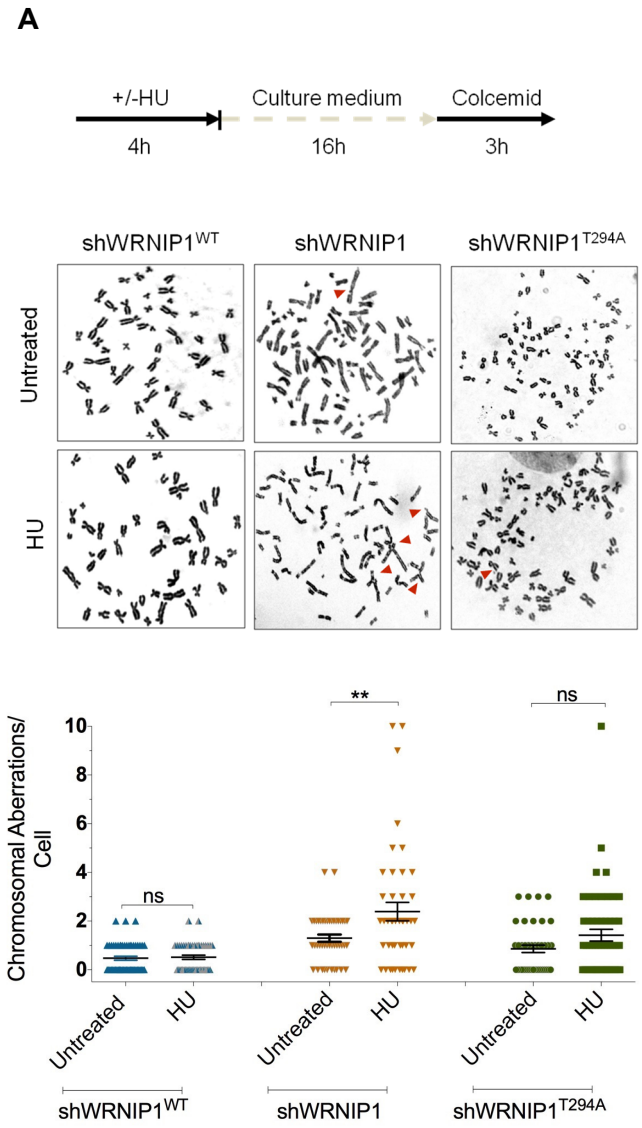

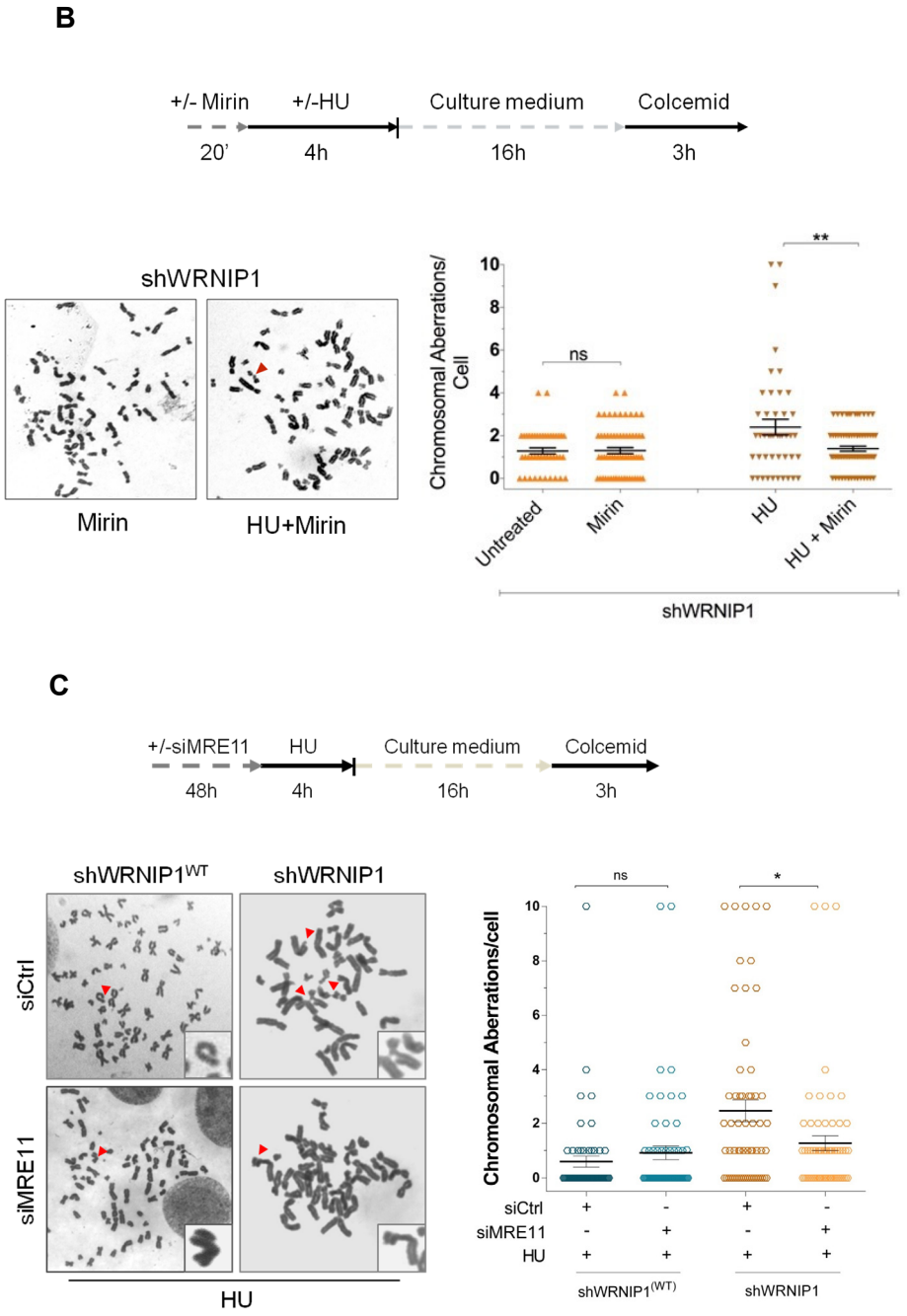

Figure 34. WRNIP1 stalled fork-protective function is required to limit chromosomal damage after HU-induced replication stress. (**A**) Experimental scheme for evaluation of the chromosomal aberrations is shown. shWRNIP1^{WT} shWRNIP1 and shWRNIP1^{T294A} cells were treated or not with 4 mM HU, then left to recover for 16h in drug-free medium and metaphases collected with colcemid. Next, cells were fixed and processed as reported in "Material and Methods" section. Dot plot shows the number of chromosomal aberrations per cell. Horizontal black lines represent the mean SE. Error bars represent standard error (ns, not significant; **, $p < 0.01$; two-tailed Student's t test). Representative Giemsa-stained metaphases of cells treated or not with 4 mM HU. Arrows indicate chromosomal aberrations. (**B**) Experimental scheme of the chromosomal aberration analysis is given. The experiment was carried out as in (A) but cells were pre-treated or not with 50 µM Mirin. Dot plot shows the effect of Mirin exposure on the number of chromosome aberrations per cell in shWRNIP1 cells. Horizontal black lines represent the mean SE. Error bars represent

standard error (ns, not significant; **, $p < 0.01$; two-tailed Student's t test). Representative Giemsa-stained metaphases of shWRNIP1 cells treated with Mirin alone or in combination with HU. Arrows indicate chromosomal aberrations.(**C**) Experimental scheme for evaluation of the chromosomal aberrations is shown. Wild-type (shWRNIP1^{WT}) or WRNIP1-deficient (shWRNIP1) cells were transfected with control siRNA (siCtrl) or *MRE11* siRNA (siMRE11), and 48 h thereafter treated with 4 mM HU, then left to recover for 16h in drug-free medium and metaphases collected with colcemid. Next, cells were fixed and processed as reported in "Material and Methods" section. Dot plot shows the number of chromosomal aberrations per cell. Horizontal black lines represent the mean SE. Error bars represent standard error (ns, not significant; *, $p < 0.1$; two-tailed Student's t test). Representative Giemsa-stained metaphases of HU-treated cells. Arrows indicate chromosomal aberrations.

Finally, the impact of RAD51-ssDNA filament stabilization by FBH1 depletion on chromosomal aberrations in shWRNIP1 cells was analysed. To this end, shWRNIP1 cells were depleted for FBH1 and treated as described in the scheme (Fig. 35). As shown in Fig. 35, inhibition of RAD51 dismantling from chromatin alleviated the level of chromosomal damage after HU treatment in WRNIP1-deficient cells.

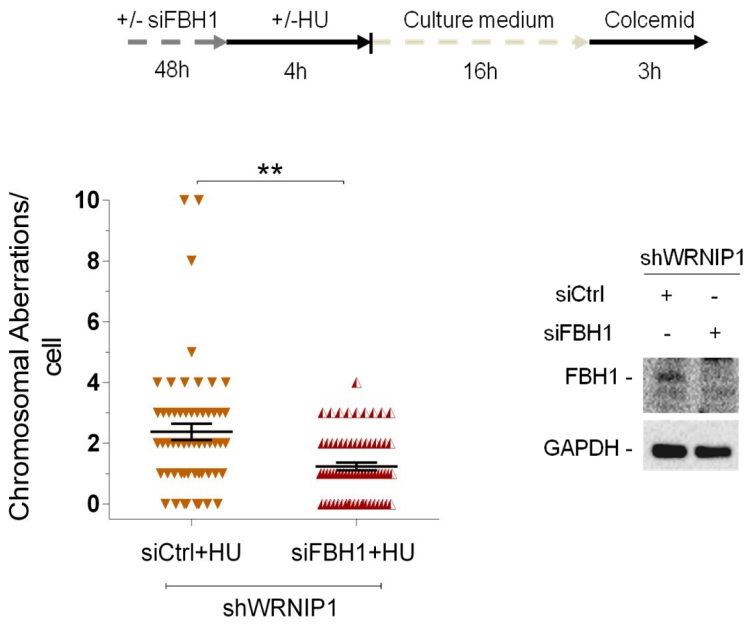

Figure 35. FBH1 depletion in WRNIP1-deficient cells alleviates the level of chromosomal damage after HU-induced replication stress. Experimental design of the chromosomal aberration assay is reported. shWRNIP1 cells were transfected with control siRNAs (siCtrl) or *FBH1* siRNA (siFBH1). Fourth-eight hours thereafter, cells were treated or not with 4 mM HU and then left to recover for 16 h. Metaphases were collected with colcemid and prepared as reported in "Material and Methods" section. Dot plot shows the number of chromosomal aberrations per cell. Western blot shows FBH1 depletion in the cells. The membrane was probed with an anti-FBH1. GAPDH was used as a loading control. Horizontal black lines represent the mean SE. Error bars represent standard error. (**, $p < 0.01$; two-tailed Student's t test).

In conclusion, our results suggest that loss of WRNIP1 as well as of its ATPase activity leads to a mild genomic instability. They also show that the WRNIP1-mediated fork protection function, rather than the role in restarting stalled forks, is responsible for chromosomal instability arising after fork stalling.

4. DISCUSSION

The ability to properly counteract replication stress is of paramount importance to ensure genome stability in living cells. Recently, it has emerged that some HR proteins, i.e. BRCA2 and RAD51, are essential components of a mechanism responsible for the defense against replication stress (Costanzo, 2011; Petermann and Helleday, 2010). Despite extensive research, it is still not completely understood how the HR proteins operate during the resolution of fork stalling, and which are their partners. In the present study, we have identified WRNIP1 as a factor working in conjunction with the RAD51 recombinase in response to replication stress.

Our experiments establish a function not previously described for WRNIP1 in maintaining the integrity of stalled forks, a behavior conserved among human cells. So far, clear data showing an involvement of WRNIP1 in the dynamics of replication fork progression were missing. Our DNA fiber analysis demonstrates that loss of WRNIP1 results in impaired fork progression under stressful conditions. Moreover, it shows that nascent DNA tracts undergo destabilization due to the nucleolytic activity of MRE11, which in turn causes marked genome instability in the absence of WRNIP1. We observed that WRNIP1-depleted cells exhibit increased fork degradation, envisaging a mechanism very similar to the pathological MRE11-mediated degradation of stalled replication intermediates reported in the absence of BRCA2 (Schlacher et al., 2011; Ying et al., 2012). In keeping with this, combined depletion of WRNIP1 and BRCA2 has no additional effect on the destabilization of newly synthesized DNA tracts compared to loss of the single genes. This observation indicates that WRNIP1 may function within the same pathway of BRCA2 to preserve stalled fork integrity. Our data reveal that loss of WRNIP1 results in a large amount of MRE11-dependent parental-strand ssDNA, but little nascent-strand ssDNA. It has been proposed that, in response to perturbed replication, MRE11 activity does not process parental DNA in eukaryotes, making impossible to expose ssDNA at nascent strand (Hashimoto et al., 2010). Consistently, accumulation of parental-strand ssDNA could derive from defects of the early stages of fork remodeling before regression, as probably occurs in the absence of BRCA2 (Schlacher et al., 2011; Ying et al., 2012). Alternatively, exposure of parental-strand ssDNA may result from over-processing of the extruded arm of a regressed fork, as opposed to the limited degradation reported in wild-type cells (Thangavel et al., 2015; Zellweger et al., 2015). Interestingly, further supporting the

hypothesis that WRNIP1 and BRCA2 can collaborate in a common pathway, WRNIP1 co-immunoprecipitates with BRCA2 and RAD51 under both unaltered and replication perturbed conditions, and physically interacts with RAD51. The fact that WRNIP1 is associated with these HR proteins, even under unperturbed conditions, raises the possibility that they may exist in a single complex ready to safeguard the integrity of the forks whenever they arrested. Previous studies have shown that WRNIP1 binds to forked DNA, which resembles stalled forks (Yoshimura et al., 2009). Our CldU-IP experiments reveal the association of WRNIP1 with replication forks upon replication stress, suggesting that WRNIP1 could be actually recruited to perturbed forks *in vivo*, also confirming recent observations from iPOND approaches (Dungrawala et al., 2015). In contrast, and consistently with the increased MRE11-mediated fork degradation, enhanced recruitment of MRE11 to chromatin and to stalled fork after replication stress is observed in WRNIP1-deficient cells.

BRCA2 is required for preserving stalled fork stability after replication perturbation, and this function is achieved by its direct interaction with RAD51, which is loaded on ssDNA (Jensen et al., 2010; Moynahan and Jasin, 2010). The inability to form RAD51-coated nucleofilament renders BRCA2-deficient cells susceptible to MRE11 nucleolytic degradation (Schlacher et al., 2011, 2012; Ying et al., 2012). Given that WRNIP1 directly interacts with RAD51, loss of this interaction may interfere with efficient nucleation of RAD51 on ssDNA, thus undermining nascent strand integrity. Interestingly, WRNIP1-deficient cells show increased accumulation of ssDNA, which is not accompanied by an excess of RAD51 loaded on chromatin. In addition, reduced fork recruitment and association between ssDNA and RAD51 is found in the absence of WRNIP1.

In line with this, co-depletion of WRNIP1 and RAD51 does not alter the excessive degradation occurring at stalled forks, but RAD51 over-expression effectively prevents the excessive fork destabilization in WRNIP1-defective cells. Defective accumulation of RAD51 at stalled forks in WRNIP1-deficient cells may be explained by the failure of proper relocalisation of RAD51 on ssDNA. Indeed, WRNIP1 could act as assisting factor for docking RAD51 recruitment to ssDNA through its association with the BRCA2/RAD51 complex. Alternatively, loss of WRNIP1 could result in the inability to retain RAD51 on chromatin. Interestingly, depletion of FBH1, which is involved in the removal of RAD51 from chromatin (Simandlova et al., 2013), restores RAD51 levels in chromatin and reverts both the fork degradation and chromosome instability phenotypes of

WRNIP1-deficient cells. In contrast, downregulation of FBH1 in BRCA2-deficient cells does not rescue fork degradation. Since BRCA2, which mediates RAD51 loading to chromatin, is recruited correctly in WRNIP1-deficient cells, these results support the hypothesis of a role for WRNIP1 in stabilizing or retaining RAD51 at stalled forks.

As a member of the AAA+ family proteins, human WRNIP1 possesses an ATPase activity that is stimulated by association with template/primer DNA (Tsurimoto et al., 2005). Interestingly, the catalytic activity of WRNIP1 would not be involved in the protection of nascent strand. Indeed, loss of ATPase activity of WRNIP1 does not hinder its interaction with RAD51, and consistently does not compromise the stability of nascent strand. However, we demonstrate that the ATPase activity of WRNIP1 is needed for restart of stalled forks. *In vitro* studies have indicated that WRNIP1 is able to bind DNA structures resembling stalled forks and template/primer DNA (Tsurimoto et al., 2005; Yoshimura et al., 2009). Similarly to MGS1, WRNIP1 associates with DNA polymerase delta (Polδ) (Kanamori et al., 2011), and by its ATPase activity promotes the Polδ-mediated DNA synthesis enhancing the frequency on template/primer DNA (Tsurimoto et al., 2005). Also WRN, a partner of WRNIP1 (Kawabe Yi et al., 2001; Kawabe et al., 2006), has shown the capacity to bind on template/primer DNA and to interact with Polδ increasing its activity in the elongation step of replication (Kamath-Loeb et al., 2000; Szekely et al., 2000). Interestingly, WRN is involved in the stability and restart of perturbed replication forks (Ammazzalorso et al., 2010; Franchitto, 2014; Sidorova et al., 2008). Thus, it is possible that WRNIP1, WRN and Polδ could form a complex, acting under replication stress to promote reinitiation of DNA synthesis at stalled forks, as it has been proposed *in vitro* (Tsurimoto et al., 2005).

It is worth noting that both WRNIP1 deficiency and loss of ATPase activity results in comparable levels of DNA damage and chromosomal instability under unperturbed conditions. As MGS1, the yeast homolog of WRNIP1, is essential for Okazaki fragment processing preventing genome instability (Kim et al., 2005), thus WRNIP1 could play a similar function. However, our results suggest that these phenotypes are not associated with any apparent impairment of normal replication. One possible explanation may be that specific replication defects are not detectable using our assays. Alternatively, the genome instability phenotype observed in untreated WRNIP1-deficient and ATPase mutant cells could be due to non-replicative events, such as the post-replication gap repair. The enhanced alkaline tail moment detected in untreated WRNIP1-deficient or ATPase mutant

cells could support both possibilities, but further investigations are necessary to address this point.

Taken together, previous works and the present study allow us to draw a model to explain how WRNIP1 could participate in the replication stress response (Fig. 36). Upon fork stalling, replication fork progression is arrested and extended ssDNA are generated. Thus, BRCA2 recruits RAD51, and WRNIP1 contributes to the stabilization of RAD51, in order to protect stalled forks and prevent their degradation by the nuclease MRE11. Once the reason of the stall is removed, the ATPase activity of WRNIP1, perhaps in association with other proteins, stimulates the restart of DNA synthesis, which can be completed, thus guaranteeing genome stability. However, when WRNIP1 or its ATPase activity is lost, cells undergo to a pathological process. The absence of WRNIP1 leads to extensive MRE11-dependent degradation of nascent DNA strand and uncontrolled action of the translocase, FBH1, resulting in enhanced accumulation of chromosomal damage and cell death. On the other hand, inhibition of the ATPase activity may abolish the binding of WRNIP1 with Polδ, as seen for MGS1 (Branzei et al., 2002; Hishida et al., 2001), making difficult the resumption of stalled forks.

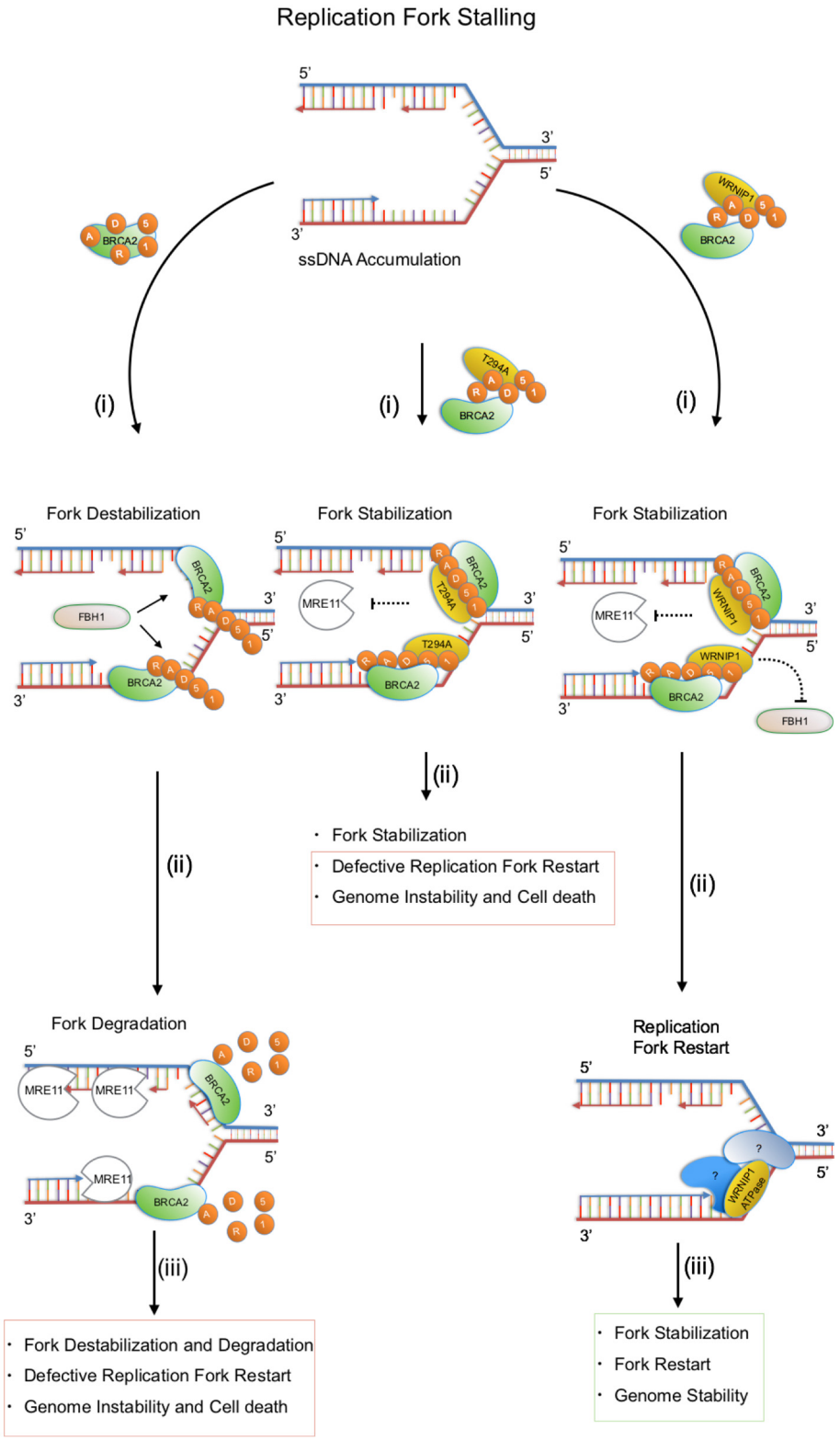

Figure 36. Model of WRNIP1 function during DNA replication fork stabilization and restart. See text for details.

Collectively, our data define a role for WRNIP1 in avoiding the pathological degradation of stalled forks, and contributes to explain how DNA damage accumulates in the absence of WRNIP1 in human cells. Stabilization of RAD51 at stalled forks is emerging as an essential function to preserve genome integrity upon replication stress(Higgs et al., 2015; Simandlova et al., 2013). These findings expand our understanding of the pathway required for the stabilization of stalled forks, identifying WRNIP1 as a novel crucial factor to the RAD51 function. As genomic instability is often associated with cancer development, our study can help to clarify how downregulation of WRNIP1 gene could give rise to several human tumours (Lukk et al., 2010).

5. MATERIALS AND METHODS

CELL LINES AND CULTURE CONDITIONS

The SV40-transformed MRC5 fibroblast cell line (MRC5SV) was a generous gift from Patricia Kannouche (IGR, Villejuif, France). MRC5SV were transduced with shRNA Lentiviral Transduction Particles targeting the UTR region of the mRNA (Sigma-Aldrich TRCN0000004526 PLKO.1-puro) and selected on puromycin (5 μg/ml; Invitrogen) to create the stable shWRNIP1 cell line. Cells were cultured in the presence of puromycin (100 ng/ml; Invitrogen) to maintain selective pressure for shRNA expression. By using the Neon^{TM} Transfection System Kit (Invitrogen) according to the manufacturer's instructions, shWRNIP1 cells were stably transfected with FLAG-tagged full-lenght cDNA encoding wild-type WRNIP1 plasmid (shWRNIP1^{WT}) or expressing a FLAG-tagged full-length WRNIP1 plasmid carrying Ala substitution at Thr294 site missense-mutant form of WRNIP1 with inactive ATPase activity (WRNIP1^{T294A}) (Tsurimoto et al., 2005). Cells were cultured in the presence of neomycin and puromycin (1 mg/ml and 100 ng/ml, respectively) to maintain selective pressure for expression. HEK293T cells were obtained from American Type Culture Collection (VA, USA). All cell lines were maintained in DMEM (Invitrogen) supplemented with 10% FBS (Boehringer Manheim) and incubated at 37°C in an humified 5% CO_2 atmosphere.

CHEMICALS

Chemicals used were commercially obtained for the replication stress-inducing drugs, hydroxyurea and aphidicolin (Sigma-Aldrich), the inibitor of RAD51 activity (B02; Calbiochem), the inibitor of MRE11 exonuclease activity (Mirin; Calbiochem), and the proteasome inhibitor (MG132; Sigma-Aldrich)

SITE-DIRECT MUTAGENESIS AND CLONING

Site-directed mutagenesis of the WRNIP1 full-lenght cDNA (Open Biosystems) was performed on the pCMV-FLAGWRNIP1 plasmid that contains the wild-type ORF sequence of WRNIP1. Substitution of Thr 294 to Ala in pCMV-FLAGWRNIP1 was introduced by the Quick-change XL kit (Stratagene) using mutagenic primer pairs

designed, according to the manufacturer's instructions. Each mutated plasmid was verified by full sequencing of the WRNIP1 ORF

PLASMIDS AND RNA INTERFERENCE

Plasmid expressing the wild-type human RAD51 (TU/T7-RAD51) was kindly provided by Maria Spies (University of Iowa, USA). The plasmid was transfected using the Neon^{TM} Transfection System Kit (Invitrogen), according to the manufacturer's instructions.
WRNIP1, BRCA2, MRE11, RAD51 and FBH1 genetic knockdown experiments were performed by Interferin (Polyplus), according to the manufacturer's instructions. siRNAs were used at 10 nM. As a control, a siRNA duplex directed against GFP was used. All depletions were achieved using siRNAs (QIAGEN) targeting the 3'UTR regions of the following human proteins: WRNIP1 (5'-ATGAATTAATGTTATAAGG-3'), BRCA2 (5'-CAGGACACAATTACAACTAAA-3'), MRE11 (5'-AAGGGTTATTTGAGCAAGTAA-3'), RAD51 (5'-CAGGATAAAGCTTCCGGGA-3') and FBH1 (5'-TAGGGCGGAAGTACCAGTCAA-3'). Depletion was confirmed by Western blot using the relevant antibodies (*see below*).

DNA FIBER ANALYSIS

Cells were pulse-labelled with 25 μM 5-chloro-2'-deoxyuridine (CldU) and 250 μM 5-iodo-2'-deoxyuridine (IdU) at specified times, with or without treatment as reported in the experimental schemes. Alternatively, cells were pulse-labelled with 250 μM IdU for the indicated times and treated or not as indicated. DNA fibres were prepared and spread out as previously reported (Franchitto, 2014). For immunodetection of labelled tracks the following primary antibodies were used: anti-CldU (rat-monoclonal anti-BrdU/CldU; BU1/75 ICR1 Abcam, 1:100) and anti-IdU (mouse-monoclonal anti-BrdU/IdU; clone b44 Becton Dickinson, 1:10). The secondary antibodies were: goat anti-mouse Alexa Fluor 488 or goat anti-rabbit Alexa Fluor 594 (Molecular Probes, 1:200). The incubation with antibodies were accomplished in a humidified chamber for 1 h at RT.
Images were acquired randomly from fields with untangled fibres using Eclipse 80i Nikon Fluorescence Microscope, equipped with a VideoConfocal (ViCo) system. The length of labelled tracks were measured using the Image-Pro-Plus 6.0 software, and values were converted into kilobase using the conversion factor 1μm = 2.59 kb as reported (Franchitto,

2014). A minimum of 100 individual fibres were analysed for each experiment and the mean of at least three independent experiments presented. Statistics were calculated using GraphPad Prism Software (*see* Appendix Tables 1 and 2).

IN SITU PLA ASSAY

The *in situ* proximity-ligation assay (PLA; Olink, Bioscience) was performed according to the manufacturer's instructions. Exponential growing cells were seeded into 24 multi-well plates at a density of 8×10^4 cells/well. After the indicated treatment, cells were permeabilized with 0.5% Triton X-100 for 10 min at 4°C, fixed with 3% formaldehyde/ 2% sucrose solution for 10 min, and then blocked in 3% BSA/PBS for 15 min. After washing with PBS, cells were incubated with the two relevant primary antibodies. Antibody staining was carried out in the standard immunofluorescence procedure. The primary antibodies used were: mouse-monoclonal anti-FLAG (Sigma-Aldrich, 1:1000), rabbit-polyclonal anti-WRNIP1 (GeneTex, 1:1000), rabbit-polyclonal anti-RAD51 (Santa Cruz Biotechnology, 1:500) and anti-IdU (mouse-monoclonal anti-BrdU/IdU; clone b44 Becton Dickinson, 1:10). The negative control consisted of using only one primary antibody. Samples were incubated with secondary antibodies conjugated with PLA probes MINUS and PLUS: the PLA Probe anti-Mouse PLUS and anti-Rabbit Minus (OLINK Bioscience). The incubation with all antibodies was accomplished in a humidified chamber for 1 h at 37°C. Next, the PLA probes MINUS and PLUS were ligated using two connecting oligonucleotides to produce a template for rolling-cycle amplification. After amplification, the products were hybridized with red fluorescence-labelled oligonucleotide. Samples were mounted in ProLong Gold antifade reagent with DAPI (blue). Images were acquired randomly using Eclipse 80i Nikon Fluorescence Microscope, equipped with a VideoConfocal (ViCo) system.

CO-IMMUNOPRECIPITATION, CELL FRACTIONATION AND WESTERN BLOT

Immunoprecipitation and chromatin fractionation experiments were performed as previously described (Franchitto, 2014). Briefly, for co-immunoprecipitation (co-IP) experiments, exponential growing HEK293T cells were cultured overnight at a density of 2.5×10^6 per 150 mm Petri dish, and treated or not as indicated. After treatment, cells were

collected and centrifuged. The cell pellets were resuspended in lysis co-IP buffer (1% Triton X-100, 0.5% Na-dehoxycolate, 150 mM NaCl, 1 mM EGTA, 20 mM Tris/HCl pH 8.0), freshly supplemented with protease inhibitor cocktail (Thermo Scientific), and sonicated on ice. After centrifugation, for each IP sample, lysate was incubated with 20 µl anti-FLAG M2 magnetic beads (Sigma-Aldrich) at 4°C overnight. The IP reaction was washed three times with the co-IP buffer, incubated in 2× sample loading buffer (100 mM Tris/HCl pH 6.8, 100 mM DTT, 4% SDS, 0.2% bromophenol blue and 20% glycerol) for 30 min at 90°C, then subjected to Western blot as described below.

Analysis of the distribution of proteins in the chromatin fraction was carried out by a standard protocol of chromatin fractionation (Méndez and Stillman, 2000). Briefly, 1.5×10^7 cells were harvested using a cell scraper, centrifuged (2 min, 1.300 × g, 4°C), and then pellet was washed twice with PBS (2 min, 1.300 × g, 4°C). Cell pellet were resuspended in buffer A (10 mM HEPES pH 7.9, 10 mM KCl, 1.5 mM $MgCl_2$, 0.34 M sucrose, 10% glycerol, 1 mM DTT, supplemented with protease inhibitor cocktail). Triton X-100 (0.1%) was added, and the cells were incubated for 5 min on ice. Nuclei were collected in pellet by centrifugation (4 min, 1.300 × g, 4°C). The supernatant was discarded, nuclei washed once in buffer A, and then lysed in buffer B (3 mM EDTA, 0.2 mM EGTA, 1 mM DTT, supplemented with protease inhibitor cocktail). Insoluble chromatin was collected by centrifugation (4 min, 1.700 × g, 4°C), washed once in buffer B, and centrifuged again under the same conditions. The final chromatin pellet was resuspended in 2× sample loading buffer (100 mM Tris/HCl pH 6.8, 100 mM DTT, 4% SDS, 0.2% bromophenol blue and 20% glycerol), sonicated on ice, and boiled for 30 min at 90°C, then subjected to Western blot as reported below.

The proteins were resolved on a 4 - 15% Mini-Protean TGX precast polyacrylamide gels (Bio-Rad), and transferred onto nitrocellulose membrane using the Trans-Blot Turbo Transfer System (Bio-Rad). The membranes were blocked using 5% NFDM in TBST (50 mM Tris/HCl pH 8, 150 mM NaCl, 0.1% Tween-20), and incubated with primary antibody for 2 h at RT. The primary antibodies used for WB were: rabbit-polyclonal anti-WRNIP1 (Novus Biologicals, 1:2000), mouse-monoclonal anti-FLAG (Sigma-Aldrich, 1:1000), mouse-polyclonal anti-GAPDH (Millipore, 1:5000), rabbit-polyclonal anti-RAD51 (Santa Cruz Biotechnology, 1:500), rabbit-polyclonal anti-LAMIN B1 (Abcam, 1:10000), rabbit-polyclonal anti-BRCA2 (Bethyl, 1:1000), mouse-monoclonal anti-MRE11 (Novus Biological, 1:2000) and mouse-monoclonal anti-FBH1 (Abcam, 1:200).

The membranes were incubated with horseradish peroxidase-conjugated goat specie-specific secondary antibodies (Santa Cruz Biotechnology, 1:20000), for 1 h at RT. Visualisation of the signal was accomplished using Super Signal West Dura substrate (Thermo Fisher Scientific), and developed by chemiluminescence and imaged using Chemidoc (GE healthcare LAS 4000).

CldU CO-IMMUNOPRECIPITATION OF PROTEINS AT STALLED FORKS

CldU co-immunoprecipitation of proteins present at replication forks was carry out according to the protocol reported elsewhere (Bryant et al., 2009). Exponential growing cells were seeded into plates at a density of 3×10^6 cells/plate. The day after, cells were labelled with 100 μM CldU for 30 min, then subjected to either no treatment or treatment with 4 mM HU for 4 h. Cells were cross-linked in 1% formaldehyde for 15 min at RT. The reaction was stopped by incubating cells with 125 mM glycine for 15 min at RT. Cells were washed twice with cold PBS and harvested in cold PBS using a cell scraper. The cytosolic protein fraction was removed by centrifugation (5 min, 1.500 × g, 4°C) of cells, after incubation with hypotonic buffer (10 mM HEPES pH 7.5, 50 mM NaCl, 0.3 M sucrose, 0.5% TX-100, supplemented with protease inhibitor cocktail (Thermo Scientific)) for 10 min on ice. Next, the nuclear soluble fraction was removed by centrifugation (2 min, 15.000 × g, 4°C) of cells, after incubation with nuclear buffer (10 mM HEPES pH 7.0, 200 mM NaCl, 1 mM EDTA, 0.5% NP-40, supplemented with protease inhibitor cocktail (Thermo Scientific)) for 10 min on ice. The pellets were resuspended in lysis buffer (10 mM HEPES pH 7.0, 500 mM NaCl, 1 mM EDTA, 1% NP-40, supplemented with protease inhibitor cocktail (Thermo Scientific)), sonicated, centrifuged (30 sec, 15.000 × g, 4°C). The supernatant was then collected. Total protein concentration was determined using the standard Bradford assay (BioRad). A total of 300 μg protein was used for IP reaction, and incubated with 6 μg of anti-CldU antibody (rat-monoclonal anti-BrdU/CldU; BU1/75 ICR1 Abcam) and 25 μl of Dynabeads Protein G (Novex). The IP reaction was washed 3 times with nuclear buffer and then 3 times with washing buffer (10 mM HEPES pH 7.0, 0,1 mM EDTA, supplemented with protease inhibitor cocktail). The reaction was resuspended in 2× sample loading buffer (100 mM Tris/HCl pH 6.8, 100 mM DTT, 4% SDS, 0.2% bromophenol blue and 20% glycerol), and boiled for 30 min at 90°C, then subjected to Western blot as previously described.

NEUTRAL AND ALKALINE COMET ASSAY

The occurrence of DNA double-strand breaks was evaluated by neutral Comet assay as described (Murfuni et al., 2012). Cell DNA was stained with a fluorescent dye GelRed (Biotium), and examined at 40× magnification with an Olympus fluorescence microscope. Slides were analyzed by a computerized image analysis system (Comet IV, Perceptive UK). To assess the amount of DNA damage, computer-generated tail moment values (tail length × fraction of total DNA in the tail) were used. A minimum of 200 cells was analyzed for each experimental point. Apoptotic cells (smaller comet head and extremely larger comet tail) were excluded from the analysis to avoid artificial enhancement of the tail moment.

DNA breakage induction was examined by alkaline Comet assay (single-cell gel electrophoresis) in denaturing conditions as described (Pichierri et al., 2001). Cell DNA was stained with a fluorescent dye GelRed (Biotium), and examined at 40× magnification with an Olympus fluorescence microscope. Slides were analyzed as described above.

IMMUNOFLUORESCENCE

Immunofluorescence analysis was performed as previously described (Murfuni et al., 2012). Briefly, exponential growing cells were seeded onto Petri dish, then treated (or mock-treated) as indicated, fixed in 2% formaldehyde for 10 min, and permeabilized using 0.4% Triton X-100 for 10 min before being incubated with 10% FBS for 1 h. After blocking, for γ-H2AX, BRCA2 and RAD51 detection, cells were incubated with the following primary antibodies: mouse-monoclonal anti-γ-H2AX (Millipore, 1:1000), rabbit-polyclonal anti-BRCA2 (Bethyl, 1:1000) or rabbit-polyclonal anti-RAD51 (Santa Cruz Biotechnology, 1:500), respectively. Cells were washed twice with PBS, and then incubated with the following secondary antibodies: goat anti-mouse Alexa Fluor 488 or goat anti-rabbit Alexa Fluor 594 (Molecular Probes, 1:200). The incubation with antibodies were accomplished in a humidified chamber for 1 h at RT. DNA was counterstained with 0.5 μg/ml DAPI (blue florescence). Images were acquired randomly using Eclipse 80i Nikon Fluorescence Microscope, equipped with a VideoConfocal (ViCo) system. For each time point, at least 200 nuclei were examined, and foci were scored at a 60× magnification. Only nuclei showing more than five bright foci were counted as positive. Parallel samples incubated with either the appropriate normal serum or only with

the secondary antibody confirmed that the observed fluorescence pattern was not attributable to artefacts.

To detect parental-strand ssDNA, cells were pre-labelled for 24 h with 10 μM IdU (Sigma-Aldrich), washed in drug-free medium, then treated with 4 mM HU for 4 h. To detect nascent-strand ssDNA, cells were pre-labelled for 20 min with 10 μM IdU (Sigma-Aldrich), then 4 mM HU was added for 4 h. Next, cells were washed with PBS, permeabilized with 0.5% Triton X-100 for 10 min at 4°C, fixed with 3% formaldehyde/ 2% sucrose solution for 10 min, and then blocked in 3% BSA/PBS for 15 min as previously described (Couch et al., 2013). Fixed cells were then incubated with anti-IdU antibody (mouse-monoclonal anti-BrdU/IdU; clone b44 Becton Dickinson, 1:10). Cells were washed twice with PBS, and then incubated with goat anti-mouse Alexa Fluor 488 (Molecular Probes, 1:200). The secondary antibodies were: goat anti-mouse Alexa Fluor 488 or goat anti-rabbit Alexa Fluor 594 (Molecular Probes, 1:200). The incubation with antibodies was accomplished in a humidified chamber for 1 h at RT. DNA was counterstained with 0.5 μg/ml DAPI. Images were acquired as described above.

LIVE/DEAD STAINING

Viability was evaluated by the fluorescence-based assay the LIVE/DEAD Cell Double Staining Kit (Sigma-Aldrich), according to the manufacturer's instructions. LIVE/DEAD assay is a short-term viability assay that allows direct evaluation of the number of live cells, stained in green with calcein-AM, and that of dead cells, stained in red with propidium iodide (PI). Since both calcein and PI-DNA can be excited with 490 nm light, simultaneous monitoring of live and dead cells is possible with a fluorescence microscope. Cell number was counted in randomly chosen fields and expressed as percent of dead cells (number of red nuclear stained cells/total cell number). For each time point, at least 1000 cells were counted.

CHROMOSOMAL ABERRATION ANALYSIS

Cells for metaphase preparations were collected according to standard procedure and as previously reported (Pirzio et al., 2008). Cell suspension was dropped onto cold, wet slides to make chromosome preparations. The slides were air dried overnight, then for each condition of treatment, the number of breaks and gaps was observed on Giemsa-stained

metaphases. For each time point, at least 50 chromosomes were examined by two independent investigators and chromosomal damage was scored at 100× magnification with an Olympus fluorescence microscope.

STATISTICAL ANALYSIS

Statistical differences in all case were determined by Student's t test, except for fork degradation, which was analysed by Mann-Whitney test (see Appendix Tables 1 and 2). In all case: ns, $p > 0.05$; * $p < 0.05$; ** $p < 0.01$; *** $p < 0.001$; **** $p < 0.0001$.

Appendix Table 1. Dataset and statistical information of DNA fibers spread

	Cell line	Treatment	Pulse-Labeling	Fiber analyzed	Median	* p-value (two-tailed)	* p-value (two-tailed)	Mean	SEM		Out of repeats	Total number of fibres
1.	shWRNIP1^{WT}	HU	CldU-IdU	IdU	7.72	< 0.0001 vs 3.	0.8049 vs 2.	7.84	0.18		3	520
2.	shWRNIP1^{WT}	Untreated	CldU-IdU	IdU	7.96	0.0512 vs 4.		7.82	0.14		3	612
3.	shWRNIP1	HU	CldU-IdU	IdU	4.70	< 0.0001 vs 5.	< 0.0001 vs 4.	4.90	0.09		3	590
4.	shWRNIP1	Untreated	CldU-IdU	IdU	7.43	0.0899 vs 6.		7.47	0.15		3	450
5.	shWRNIP1^{T294A}	HU	CldU-IdU	IdU	7.30	0.0672 vs 1.	0.5620 vs 6.	7.39	0.12		3	523
6.	shWRNIP1^{T294A}	Untreated	CldU-IdU	IdU	7.40	0.0511 vs 2.		7.55	0.14		3	465
7.	HEK293T ^{siCtrl}	HU	IdU	IdU	7.34		0.2766 vs 8.	7.48	0.15		2	481
8.	HEK293T ^{siCtrl}	Untreated	IdU	IdU	7.33	0.253 vs 10.		7.12	0.16		2	385
9.	HEK293T ^{siWRNIP1}	HU	IdU	IdU	4.42	< 0.0001 vs 7.		4.60	0.10		2	538
10.	HEK293T ^{siWRNIP1}	Untreated	IdU	IdU	7.49		< 0.0001 vs 9.	7.36	0.18		2	483
11.	shWRNIP1^{WT}	HU	CldU-IdU	IdU	8.51		0.524 vs 12.	8.51	0.25		3	412
12.	shWRNIP1^{WT}	HU+Mirin	CldU-IdU	IdU	7.90	0.637 vs 14.		7.87	0.18		3	393
13.	shWRNIP1	HU	CldU-IdU	IdU	4.95	< 0.0001 vs 11.		5.16	0.17		3	461
14.	shWRNIP1	HU+Mirin	CldU-IdU	IdU	7.89		< 0.0001 vs 13.	7.61	0.17		3	412
15.	shWRNIP1^{WT}	HU	IdU	IdU	7.40		0.381 vs 17.	7.77	0.15		3	620
16.	shWRNIP1^{WT}	Untreated	IdU	IdU	7.83	0.817 vs 20.	< 0.0001 vs 18.	7.91	0.16		3	513
17.	shWRNIP1^{WT}	HU+RAD51i	IdU	IdU	5.72		< 0.0001 vs 16.	5.75	0.14		3	335
18.	shWRNIP1	HU	IdU	IdU	5.31	< 0.0001 vs 16.	< 0.0001 vs 20.	5.45	0.07		3	1043
19.	shWRNIP1	Untreated	IdU	IdU	7.77		< 0.0001 vs 21.	7.91	0.12		3	583
20.	shWRNIP1	HU+RAD51i	IdU	IdU	5.36	0.329 vs 18.	0.275 vs 19.	5.67	0.13		3	629
21.	shWRNIP1$^{TV-RAD51}$	HU	IdU	IdU	7.89			7.78	0.17		3	773
22.	shWRNIP1	HU	IdU	IdU	5.11	< 0.0001 vs 22.		5.27	0.11		3	863
23.	shWRNIP1 ^{siMRE11}	HU	IdU	IdU	7.43			7.45	0.14		3	707
24.	shWRNIP1 ^{siCtrl}	HU	IdU	IdU	4.72	< 0.0001 vs 24.		5.14	0.10		3	816
25.	shWRNIP1^{WT}	Aph	IdU	IdU	7.45	< 0.0001 vs 27.		7.76	0.15		3	1345
26.	shWRNIP1^{WT}	Untreated	IdU	IdU	7.52		0.927 vs 25.	7.67	0.13		3	1155
27.	shWRNIP1	Aph	IdU	IdU	4.83		< 0.0001 vs 28.	5.28	0.10		3	1237
28.	shWRNIP1	Untreated	IdU	IdU	7.34	0.0551 vs 25.		7.35	0.19		3	1123
29.	shWRNIP1$^{WT\ siBRCA2}$	HU	IdU	IdU	4.67		< 0.0001 vs 30.	5.09	0.08		3	1054
30.	shWRNIP1$^{WT\ siBRCA2}$	Untreated	IdU	IdU	7.18	0.990 vs 32.		7.60	0.17		3	783
31.	shWRNIP1 ^{siBRCA2}	HU	IdU	IdU	4.56	0.136 vs 29.		4.86	0.09		3	886
32.	shWRNIP1 ^{siBRCA2}	Untreated	IdU	IdU	7.40		< 0.0001 vs 31.	7.65	0.18		3	1050
33.	shWRNIP1 ^{siCtrl}	Untreated	IdU	IdU	8.72	0.887 vs 35.		8.79	0.14		2	623
34.	shWRNIP1 ^{siCtrl}	HU	IdU	IdU	4.76		< 0.0001 vs 33.	5.12	0.10		2	952
35.	shWRNIP1 ^{siFBH1}	Untreated	IdU	IdU	8.69		0.463 vs 36.	8.71	0.14		2	677
36.	shWRNIP1 ^{siFBH1}	HU	IdU	IdU	7.69	< 0.0001 vs 34.		7.92	0.13		2	936
37.	shWRNIP1$^{WT\ siBRCA2}$	Untreated	IdU	IdU	7.20	0.5929 vs 39.					1	251
38.	shWRNIP1$^{WT\ siBRCA2}$	HU	IdU	IdU	4.87		< 0.0001 vs 37.				1	150
39.	shWRNIP1$^{WT\ siBRCA2/siFBH1}$	Untreated	IdU	IdU	7.41		< 0.0001 vs 40.				1	103
40.	shWRNIP1$^{WT\ siBRCA2/siFBH1}$	HU	IdU	IdU	4.70	0.2669 vs 38.					1	320
41.	shWRNIP1^{WT}	HU	IdU	IdU	7.11	< 0.0001 vs 43.					1	110
42.	shWRNIP1$^{WT/siRAD51}$	HU	IdU	IdU	4.97		< 0.0001 vs 41.				1	206
43.	shWRNIP1	HU	IdU	IdU	4.66		0.6122 vs 44.				1	173
44.	shWRNIP1^{siRAD51}	HU	IdU	IdU	4.48	0.0511 vs 42.					1	101

Medians and means are in µm. SEM, standard error of the mean. p-value derived from nonparametric test (Mann-Whitney test).

Appendix Table 2. DNA fibers lengths distributions data analysis information

	Cell line	Treatment	Pulse-Labeling	Fiber analyzed	IdU lengths distribution (in Percentage)										
					0	2	4	6	8	10	12	14	16	18	20
1.	shWRNIP1^{WT}	HU	CldU-IdU	IdU	0	1,27	8,23	28,48	31,65	21,52	6,96	1,9	0	0	0
2.	shWRNIP1^{WT}	Untreated	CldU-IdU	IdU	0,4	0,4	9,13	28,17	34,13	19,84	7,14	0,79	0	0	0
3.	shWRNIP1	HU	CldU-IdU	IdU	0	11,26	44,71	33,79	7,85	2,05	0,34	0	0	0	0
4.	shWRNIP1	Untreated	CldU-IdU	IdU	0,37	2,21	12,55	27,68	33,58	16,97	4,06	1,85	0,74	0	0
5.	shWRNIP1^{T294A}	HU	CldU-IdU	IdU	0	0,47	7,01	36,92	37,38	13,55	4,21	0,47	0	0	0
6.	shWRNIP1^{T294A}	Untreated	CldU-IdU	IdU	0	1,16	8,88	35,91	33,59	12,74	5,02	2,32	0,39	0	0
7.	HEK293T ^{siCtrl}	HU	IdU	IdU	0	1,25	14,64	29,6	28,97	17,13	4,98	2,49	0,62	0,31	0
8.	HEK293T ^{siCtrl}	Untreated	IdU	IdU	0,43	3,85	14,53	28,21	32,48	15,81	3,42	0,85	0,43	0	0
9.	HEK293T ^{siWRNIP1}	HU	IdU	IdU	0	16,97	49,46	23,47	7,58	2,17	0	0,36	0	0	0
10.	HEK293T ^{siWRNIP1}	Untreated	IdU	IdU	0	3,25	11,69	25,97	37,01	18,18	2,6	1,3	0	0	0
11.	shWRNIP1^{WT}	HU	CldU-IdU	IdU	0	0	10,61	21,97	41,67	18,94	6,06	0	0,76	0	0
12.	shWRNIP1^{WT}	HU+Mirin	CldU-IdU	IdU	0	1,63	8,13	18,7	28,46	26,83	9,76	4,07	2,44	0	0
13.	shWRNIP1	HU	CldU-IdU	IdU	0	13,11	38,52	33,61	10,66	3,28	0	0,82	0	0	0
14.	shWRNIP1	HU+Mirin	CldU-IdU	IdU	0	1,16	11,63	26,16	31,4	25	2,91	1,74	0	0	0
15.	shWRNIP1^{WT}	HU	IdU	IdU	0	0	13,91	29,7	27,82	17,29	7,89	2,26	1,13	0	0
16.	shWRNIP1^{WT}	Untreated	IdU	IdU	0	0,45	11,31	24,89	33,03	20,36	6,33	2,71	0,9	0	0
17.	shWRNIP1^{WT}	HU+RAD51i	IdU	IdU	0,68	3,42	33,56	35,62	23,29	3,42	0	0	0	0	0
18.	shWRNIP1	HU	IdU	IdU	0,36	6,08	38,46	36,14	14,31	4,11	0,54	0	0	0	0
19.	shWRNIP1	Untreated	IdU	IdU	0	1,13	7,61	29,3	30,14	21,41	9,01	1,41	0	0	0
20.	shWRNIP1	HU+RAD51i	IdU	IdU	0,65	7,82	33,55	31,6	18,89	4,89	2,61	0	0	0	0
21.	shWRNIP1$^{TV-RAD51}$	HU	IdU	IdU	0	1,26	14,29	18,91	37,39	16,81	7,56	2,94	0,42	0,42	0
22.	shWRNIP1	HU	IdU	IdU	0	5,23	42,86	31,01	15,68	4,53	0,7	0	0	0	0
23.	shWRNIP1 ^{siMRE11}	HU	IdU	IdU	0	2,87	16,91	28,08	20,92	22,64	5,73	2,58	0,29	0	0
24.	shWRNIP1 ^{siCtrl}	HU	IdU	IdU	0	9,73	45,72	26,25	15,34	1,77	1,18	0	0	0	0
25.	shWRNIP1^{WT}	Aph	IdU	IdU	0	3,63	15,98	23,97	26,63	16,46	7,75	2,18	2,91	0,24	0
26.	shWRNIP1^{WT}	Untreated	IdU	IdU	0	1,01	13,67	28,61	30,89	14,94	7,34	2,53	0,76	0,25	0
27.	shWRNIP1	Aph	IdU	IdU	0	15,74	37,56	26,73	12,52	3,89	1,86	1,18	0	0	0,17
28.	shWRNIP1	Untreated	IdU	IdU	0	2,42	19,38	25,95	27,68	12,46	7,96	2,77	1,04	0,35	0
29.	shWRNIP1$^{WT\ siBRCA2}$	HU	IdU	IdU	0	12,54	44,13	27,62	10,32	3,65	1,11	0,48	0,16	0	0
30.	shWRNIP1$^{WT\ siBRCA2}$	Untreated	IdU	IdU	0	2,13	16,41	29,18	24,92	16,72	5,47	2,43	1,52	0,91	0
31.	shWRNIP1 ^{siBRCA2}	HU	IdU	IdU	0	15,76	43,6	28,57	6,65	4,68	0,74	0	0	0	0
32.	shWRNIP1 ^{siBRCA2}	Untreated	IdU	IdU	0	2,42	20,85	24,17	22,66	15,11	8,76	3,93	0,91	0,91	0,3
33.	shWRNIP1 ^{siCtrl}	Untreated	IdU	IdU	0	0	7.77	20.27	27.50	24.44	14.17	4.17	1.11	0.28	0.27
34.	shWRNIP1 ^{siCtrl}	HU	IdU	IdU	0.26	15.10	41.14	27.60	10.67	4.68	0.52	0	0	0	0
35.	shWRNIP1 ^{siFBH1}	Untreated	IdU	IdU	0	0.84	8.45	18.30	29.29	26.19	12.39	2.81	1.40	0.28	0
36.	shWRNIP1 ^{siFBH1}	HU	IdU	IdU	0.49	1.74	12.18	29.10	27.36	16.91	7.71	2.98	0.99	0.49	0
37.	shWRNIP1$^{WT\ siBRCA2}$	Untreated	IdU	IdU	0	1.59	12.35	34.26	31.07	14.74	4.78	0.79	0.39	0	0
38.	shWRNIP1$^{WT\ siBRCA2}$	HU	IdU	IdU	0.66	6.66	47.33	36.66	6.66	0.66	1.33	0	0	0	0
39.	shWRNIP1$^{WT\ siBRCA2/siFBH1}$	Untreated	IdU	IdU	0	0	12.62	29.12	36.89	16.50	4.85	0	0	0	0
40.	shWRNIP1$^{WT\ siBRCA2/siFBH1}$	HU	IdU	IdU	0.31	9.37	51.25	31.56	5.93	1.56	0	0	0	0	0
41.	shWRNIP1^{WT}	HU	IdU	IdU	0.97	0.48	10.67	37.37	30.58	14.56	5.33	0	0	0	0
42.	shWRNIP1$^{WT/siRAD51}$	HU	IdU	IdU	0.90	1.81	50.90	31.81	12.72	1.81	0	0	0	0	0
43.	shWRNIP1	HU	IdU	IdU	0	10.98	53.75	27.16	6.90	1.15	0	0	0	0	0
44.	shWRNIP1^{siRAD51}	HU	IdU	IdU	0	12.35	59.95	25.85	2.24	0	0	0	0	0	0

IdU lengths are in µm. Distributions are in percentage. Red values represent the dominant rate of distribution.

6. REFERENCES

Abbas, T., Keaton, M.A., and Dutta, A. (2013). Genomic Instability in cancer development. Cold Spring Harb. Perspect. Biol. *5*, 1–18.

Abraham, R.T. (2001). Cell cycle checkpoint signaling through the ATM and ATR kinases. Genes Dev. *15*, 2177–2196.

Aguilera, A., and García-Muse, T. (2013). Causes of genome instability. Annu. Rev. Genet. *47*, 1–32.

Aguilera, A., and Gómez-González, B. (2008). Genome instability: a mechanistic view of its causes and consequences. Nat. Rev. Genet. *9*, 204–217.

Allen, C., Ashley, A.K., Hromas, R., and Nickoloff, J.A. (2011). More forks on the road to replication stress recovery. 4–12.

Altman, A.L., and Fanning, E. (2004). Defined sequence modules and an architectural element cooperate to promote initiation at an ectopic mammalian chromosomal replication origin. Mol. Cell. Biol. *24*, 4138–4150.

Ammazzalorso, F., Pirzio, L.M., Bignami, M., Franchitto, A., and Pichierri, P. (2010). ATR and ATM differently regulate WRN to prevent DSBs at stalled replication forks and promote replication fork recovery. EMBO J. *29*, 3156–3169.

Anglana, M., Apiou, F., Bensimon, A., and Debatisse, M. (2003). Dynamics of DNA replication in mammalian somatic cells: nucleotide pool modulates origin choice and interorigin spacing. Cell *114*, 385–394.

Ball, H.L., Myers, J.S., and Cortez, D. (2005). ATRIP binding to replication protein A-single-stranded DNA promotes ATR-ATRIP localization but is dispensable for Chk1 phosphorylation. Mol. Biol. Cell *16*, 2372–2381.

Baranovskiy, A.G., Babayeva, N.D., Suwa, Y., Gu, J., Pavlov, Y.I., and Tahirov, T.H. (2014). Structural basis for inhibition of DNA replication by aphidicolin. Nucleic Acids Res. *42*, 14013–14021.

Bartek, J., Lukas, C., and Lukas, J. (2004). Checking on DNA damage in S phase. Nat. Rev. Mol. Cell Biol. *5*, 792–804.

Baumann, P., Benson, F.E., and West, S.C. (1996). Human Rad51 protein promotes ATP-dependent homologous pairing and strand transfer reactions in vitro. Cell *87*, 757–766.

Bermejo, R., Lai, M.S., and Foiani, M. (2012). Preventing replication stress to maintain genome stability: resolving conflicts between replication and transcription. Mol. Cell *45*, 710–718.

Berti, M., and Vindigni, A. (2016). Replication stress: getting back on track. Nat. Struct. Mol. Biol. *23*, 103–109.

Berti, M., Ray Chaudhuri, A., Thangavel, S., Gomathinayagam, S., Kenig, S., Vujanovic, M., Odreman, F., Glatter, T., Graziano, S., Mendoza-Maldonado, R., et al. (2013). Human RECQ1 promotes restart of replication forks reversed by DNA topoisomerase I inhibition. Nat. Struct. Mol. Biol. *20*, 347–354.

Bétous, R., Mason, A.C., Rambo, R.P., Bansbach, C.E., Badu-Nkansah, A., Sirbu, B.M., Eichman, B.F., and Cortez, D. (2012). SMARCAL1 catalyzes fork regression and Holliday junction migration to maintain genome stability during DNA replication. Genes Dev. *26*, 151–162.

Bétous, R., Couch, F.B., Mason, A.C., Eichman, B.F., Manosas, M., and Cortez, D. (2013). Substrate-selective repair and restart of replication forks by DNA translocases. Cell Rep. *3*, 1958–1969.

Bish, R.A., and Myers, M.P. (2007). Werner helicase-interacting protein 1 binds polyubiquitin via its zinc finger domain. J. Biol. Chem. *282*, 23184–23193.

Bizard, A.H., and Hickson, I.D. (2014). The dissolution of double Holliday junctions. Cold Spring Harb. Perspect. Biol. *6*, a016477.

Blastyák, A., Pintér, L., Unk, I., Prakash, L., Prakash, S., and Haracska, L. (2007). Yeast Rad5 protein required for postreplication repair has a DNA helicase activity specific for replication fork regression. Mol. Cell *28*, 167–175.

Bochman, M.L., Paeschke, K., and Zakian, V.A. (2012). DNA secondary structures: stability and function of G-quadruplex structures. Nat. Rev. Genet. *13*, 770–780.

Branzei, D., and Foiani, M. (2005). The DNA damage response during DNA replication. Curr. Opin. Cell Biol. *17*, 568–575.

Branzei, D., and Foiani, M. (2009). The checkpoint response to replication stress. DNA Repair (Amst). *8*, 1038–1046.

Branzei, D., and Foiani, M. (2010). Maintaining genome stability at the replication fork. Nat. Rev. Mol. Cell Biol. *11*, 208–219.

Branzei, D., Seki, M., Onoda, F., Yagi, H., Kawabe, Y.I., and Enomoto, T. (2002). Characterization of the slow-growth phenotype of S. cerevisiae whip/mgs1 sgs1 double deletion mutants. DNA Repair (Amst). *1*, 671–682.

Brown, E.J. (2004). Analysis of cell cycle progression and genomic integrity in early lethal knockouts. Methods Mol. Biol. *280*, 201–212.

Bryant, H.E., Petermann, E., Schultz, N., Jemth, A., Loseva, O., Issaeva, N., Johansson, F., Fernandez, S., McGlynn, P., and Helleday, T. (2009). PARP is activated at stalled forks to mediate Mre11-dependent replication restart and recombination. EMBO J. *28*, 2601–2615.

Bugreev, D. V, Yu, X., Egelman, E.H., and Mazin, A. V (2007). Novel pro- and anti-recombination activities of the Bloom's syndrome helicase. Genes Dev. *21*, 3085–3094.

Bugreev, D. V, Rossi, M.J., and Mazin, A. V (2011). Cooperation of RAD51 and RAD54

in regression of a model replication fork. Nucleic Acids Res. *39*, 2153–2164.

Burrell, R.A., McClelland, S.E., Endesfelder, D., Groth, P., Weller, M.-C., Shaikh, N., Domingo, E., Kanu, N., Dewhurst, S.M., Gronroos, E., et al. (2013). Replication stress links structural and numerical cancer chromosomal instability. Nature *494*, 492–496.

Byun, T.S., Pacek, M., Yee, M., Walter, J.C., and Cimprich, K.A. (2005). Functional uncoupling of MCM helicase and DNA polymerase activities activates the ATR-dependent checkpoint. Genes Dev. *19*, 1040–1052.

Chan, K.-L., North, P.S., and Hickson, I.D. (2007). BLM is required for faithful chromosome segregation and its localization defines a class of ultrafine anaphase bridges. EMBO J. *26*, 3397–3409.

Chen, X., Bosques, L., Sung, P., and Kupfer, G.M. (2016). A novel role for non-ubiquitinated FANCD2 in response to hydroxyurea-induced DNA damage. Oncogene *35*, 22–34.

Chen, Y.-H., Jones, M.J.K., Yin, Y., Crist, S.B., Colnaghi, L., Sims, R.J., Rothenberg, E., Jallepalli, P. V, and Huang, T.T. (2015). ATR-mediated phosphorylation of FANCI regulates dormant origin firing in response to replication stress. Mol. Cell *58*, 323–338.

Chiolo, I., Saponaro, M., Baryshnikova, A., Kim, J.-H., Seo, Y.-S., and Liberi, G. (2007). The human F-Box DNA helicase FBH1 faces Saccharomyces cerevisiae Srs2 and postreplication repair pathway roles. Mol. Cell. Biol. *27*, 7439–7450.

Chu, W.K., Payne, M.J., Beli, P., Hanada, K., Choudhary, C., and Hickson, I.D. (2015). FBH1 influences DNA replication fork stability and homologous recombination through ubiquitylation of RAD51. Nat. Commun. *6*, 5931.

Ciccia, A., Nimonkar, A. V, Hu, Y., Hajdu, I., Achar, Y.J., Izhar, L., Petit, S.A., Adamson, B., Yoon, J.C., Kowalczykowski, S.C., et al. (2012). Polyubiquitinated PCNA recruits the ZRANB3 translocase to maintain genomic integrity after replication stress. Mol. Cell *47*, 396–409.

Cimprich, K.A., and Cortez, D. (2008). ATR: an essential regulator of genome integrity. Nat. Rev. Mol. Cell Biol. *9*, 616–627.

Claus Storgaard Sørensen, H.B.V.N.-K. and R.G.S. (2011). DNA Replication-Current Advances (InTech).

Cortez, D., Guntuku, S., Qin, J., and Elledge, S.J. (2001). ATR and ATRIP: partners in checkpoint signaling. Science *294*, 1713–1716.

Costa, A., Renault, L., Swuec, P., Petojevic, T., Pesavento, J.J., Ilves, I., MacLellan-Gibson, K., Fleck, R.A., Botchan, M.R., and Berger, J.M. (2014). DNA binding polarity, dimerization, and ATPase ring remodeling in the CMG helicase of the eukaryotic replisome. Elife *3*, e03273.

Costanzo, V. (2011). Brca2, Rad51 and Mre11: Performing balancing acts on replication forks. DNA Repair (Amst). *10*, 1060–1065.

Costanzo, V., and Gautier, J. (2003). Single-strand DNA gaps trigger an ATR- and Cdc7-dependent checkpoint. Cell Cycle *2*, 17.

Couch, F.B., Bansbach, C.E., Driscoll, R., Luzwick, J.W., Glick, G.G., Bétous, R., Carroll, C.M., Jung, S.Y., Qin, J., Cimprich, K. a., et al. (2013). ATR phosphorylates SMARCAL1 to prevent replication fork collapse. Genes Dev. *27*, 1610–1623.

Crosetto, N., Bienko, M., Hibbert, R.G., Perica, T., Ambrogio, C., Kensche, T., Hofmann, K., Sixma, T.K., and Dikic, I. (2008). Human Wrnip1 is localized in replication factories in a ubiquitin-binding zinc finger-dependent manner. J. Biol. Chem. *283*, 35173–35185.

Debatisse, M., Le Tallec, B., Letessier, A., Dutrillaux, B., and Brison, O. (2012). Common fragile sites: Mechanisms of instability revisited. Trends Genet. *28*, 22–32.

Dewar, J.M., Budzowska, M., and Walter, J.C. (2015). The mechanism of DNA replication termination in vertebrates. Nature *525*, 345–350.

Dobbelstein, M., and Sørensen, C.S. (2015). Exploiting replicative stress to treat cancer. Nat. Rev. Drug Discov. *14*, 405–423.

Dominguez-Sola, D., Ying, C.Y., Grandori, C., Ruggiero, L., Chen, B., Li, M., Galloway, D.A., Gu, W., Gautier, J., and Dalla-Favera, R. (2007). Non-transcriptional control of DNA replication by c-Myc. Nature *448*, 445–451.

Donoho, G., Brenneman, M.A., Cui, T.X., Donoviel, D., Vogel, H., Goodwin, E.H., Chen, D.J., and Hasty, P. (2003). Deletion of Brca2 exon 27 causes hypersensitivity to DNA crosslinks, chromosomal instability, and reduced life span in mice. Genes. Chromosomes Cancer *36*, 317–331.

Dungrawala, H., Rose, K.L., Bhat, K.P., Mohni, K.N., Glick, G.G., Couch, F.B., and Cortez, D. (2015). The Replication Checkpoint Prevents Two Types of Fork Collapse without Regulating Replisome Stability. Mol. Cell *59*, 998–1010.

Dupré, A., Boyer-Chatenet, L., Sattler, R.M., Modi, A.P., Lee, J.-H., Nicolette, M.L., Kopelovich, L., Jasin, M., Baer, R., Paull, T.T., et al. (2008a). A forward chemical genetic screen reveals an inhibitor of the Mre11-Rad50-Nbs1 complex. Nat. Chem. Biol. *4*, 119–125.

Dupré, A., Boyer-Chatenet, L., Sattler, R.M., Modi, A.P., Lee, J.-H., Nicolette, M.L., Kopelovich, L., Jasin, M., Baer, R., Paull, T.T., et al. (2008b). A forward chemical genetic screen reveals an inhibitor of the Mre11-Rad50-Nbs1 complex. Nat. Chem. Biol. *4*, 119–125.

Edwards, M.C., Tutter, A. V, Cvetic, C., Gilbert, C.H., Prokhorova, T.A., and Walter, J.C. (2002). MCM2-7 complexes bind chromatin in a distributed pattern surrounding the origin recognition complex in Xenopus egg extracts. J. Biol. Chem. *277*, 33049–33057.

Ekholm-Reed, S., Méndez, J., Tedesco, D., Zetterberg, A., Stillman, B., and Reed, S.I. (2004). Deregulation of cyclin E in human cells interferes with prereplication complex assembly. J. Cell Biol. *165*, 789–800.

Elvers, I., Johansson, F., Groth, P., Erixon, K., and Helleday, T. (2011). UV stalled replication forks restart by re-priming in human fibroblasts. Nucleic Acids Res. *39*, 7049–7057.

Esashi, F., Christ, N., Gannon, J., Liu, Y., Hunt, T., Jasin, M., and West, S.C. (2005). CDK-dependent phosphorylation of BRCA2 as a regulatory mechanism for recombinational repair. Nature *434*, 598–604.

Feijoo, C., Hall-Jackson, C., Wu, R., Jenkins, D., Leitch, J., Gilbert, D.M., and Smythe, C. (2001). Activation of mammalian Chk1 during DNA replication arrest: a role for Chk1 in the intra-S phase checkpoint monitoring replication origin firing. J. Cell Biol. *154*, 913–923.

Follonier, C., Oehler, J., Herrador, R., and Lopes, M. (2013). Friedreich's ataxia-associated GAA repeats induce replication-fork reversal and unusual molecular junctions. Nat. Struct. Mol. Biol. *20*, 486–494.

Franchitto, A. (2014). Checkpoint-dependent and independent roles of the Werner syndrome protein in preserving genome integrity in response to mild replication stress. Nucleic Acids Res. *42*, 12628–12639.

Franchitto, A., and Pichierri, P. (2011). Understanding the molecular basis of common fragile sites instability: role of the proteins involved in the recovery of stalled replication forks. Cell Cycle *10*, 4039–4046.

Franchitto, A., and Pichierri, P. (2014). Replication fork recovery and regulation of common fragile sites stability. Cell. Mol. Life Sci. *71*, 4507–4517.

Friedberg, E.C., Aguilera, A., Gellert, M., Hanawalt, P.C., Hays, J.B., Lehmann, A.R., Lindahl, T., Lowndes, N., Sarasin, A., and Wood, R.D. (2006). DNA repair: from molecular mechanism to human disease. DNA Repair (Amst). *5*, 986–996.

Fugger, K., Mistrik, M., Neelsen, K.J., Yao, Q., Zellweger, R., Kousholt, A.N., Haahr, P., Chu, W.K., Bartek, J., Lopes, M., et al. (2015). FBH1 Catalyzes Regression of Stalled Replication Forks. Cell Rep. *10*, 1749–1757.

Fumasoni, M., Zwicky, K., Vanoli, F., Lopes, M., and Branzei, D. (2015). Error-free DNA damage tolerance and sister chromatid proximity during DNA replication rely on the Polα/Primase/Ctf4 Complex. Mol. Cell *57*, 812–823.

Gaillard, H., García-Muse, T., and Aguilera, A. (2015). Replication stress and cancer. Nat. Rev. Cancer *15*, 276–289.

Gari, K., Décaillet, C., Delannoy, M., Wu, L., and Constantinou, A. (2008). Remodeling of DNA replication structures by the branch point translocase FANCM. Proc. Natl. Acad. Sci. U. S. A. *105*, 16107–16112.

Gelot, C., Magdalou, I., and Lopez, B.S. (2015). Replication stress in Mammalian cells and its consequences for mitosis. Genes (Basel). *6*, 267–298.

Georgescu, R.E., Schauer, G.D., Yao, N.Y., Langston, L.D., Yurieva, O., Zhang, D.,

Finkelstein, J., and O'Donnell, M.E. (2015). Reconstitution of a eukaryotic replisome reveals suppression mechanisms that define leading/lagging strand operation. Elife *4*, e04988.

Ghosal, G., and Chen, J. (2013). DNA damage tolerance: a double-edged sword guarding the genome. Transl. Cancer Res. *2*, 107–129.

Gorgoulis, V.G., and Halazonetis, T.D. (2010). Oncogene-induced senescence: the bright and dark side of the response. Curr. Opin. Cell Biol. *22*, 816–827.

Gottifredi, V., and Prives, C. (2005). The S phase checkpoint: when the crowd meets at the fork. Semin. Cell Dev. Biol. *16*, 355–368.

Harrigan, J.A., Belotserkovskaya, R., Coates, J., Dimitrova, D.S., Polo, S.E., Bradshaw, C.R., Fraser, P., and Jackson, S.P. (2011). Replication stress induces 53BP1-containing OPT domains in G1 cells. J. Cell Biol. *193*, 97–108.

Hashimoto, Y., Chaudhuri, A.R., Lopes, M., and Costanzo, V. (2010). Rad51 protects nascent DNA from Mre11-dependent degradation and promotes continuous DNA synthesis. Nat. Struct. Mol. Biol. *17*, 1305–1311.

Hekmat-Nejad, M., You, Z., Yee, M.C., Newport, J.W., and Cimprich, K.A. (2000). Xenopus ATR is a replication-dependent chromatin-binding protein required for the DNA replication checkpoint. Curr. Biol. *10*, 1565–1573.

Heller, R.C., and Marians, K.J. (2006). Replication fork reactivation downstream of a blocked nascent leading strand. Nature *439*, 557–562.

Helmrich, A., Ballarino, M., Nudler, E., and Tora, L. (2013). Transcription-replication encounters, consequences and genomic instability. Nat. Struct. Mol. Biol. *20*, 412–418.

Higgs, M.R., Reynolds, J.J., Winczura, A., Blackford, A.N., Borel, V., Miller, E.S., Zlatanou, A., Nieminuszczy, J., Ryan, E.L., Davies, N.J., et al. (2015). BOD1L Is Required to Suppress Deleterious Resection of Stressed Replication Forks. Mol. Cell *59*, 462–477.

Hills, S.A., and Diffley, J.F.X. (2014). DNA replication and oncogene-induced replicative stress. Curr. Biol. *24*, R435–R444.

Hishida, T., and Ohno, T. (2002). Saccharomyces cerevisiae MGS1 is essential in strains de ® cient in the RAD6 -dependent DNA damage tolerance pathway. *21*, 2019–2029.

Hishida, T., Iwasaki, H., Ohno, T., Morishita, T., and Shinagawa, H. (2001). A yeast gene, MGS1, encoding a DNA-dependent AAA(+) ATPase is required to maintain genome stability. Proc. Natl. Acad. Sci. U. S. A. *98*, 8283–8289.

Hishida, T., Ohno, T., Iwasaki, H., and Shinagawa, H. (2002). Saccharomyces cerevisiae MGS1 is essential in strains deficient in the RAD6-dependent DNA damage tolerance pathway. EMBO J. *21*, 2019–2029.

Hoang, M.L., Leon, R.P., Pessoa-Brandao, L., Hunt, S., Raghuraman, M.K., Fangman, W.L., Brewer, B.J., and Sclafani, R.A. (2007). Structural changes in Mcm5 protein bypass

Cdc7-Dbf4 function and reduce replication origin efficiency in Saccharomyces cerevisiae. Mol. Cell. Biol. *27*, 7594–7602.

Hoeijmakers, J.H.J. (2009). DNA damage, aging, and cancer. N. Engl. J. Med. *361*, 1475–1485.

Hu, Y., Raynard, S., Sehorn, M.G., Lu, X., Bussen, W., Zheng, L., Stark, J.M., Barnes, E.L., Chi, P., Janscak, P., et al. (2007). RECQL5/Recql5 helicase regulates homologous recombination and suppresses tumor formation via disruption of Rad51 presynaptic filaments. Genes Dev. *21*, 3073–3084.

Huang, F., Mazina, O.M., Zentner, I.J., Cocklin, S., and Mazin, A. V (2012). Inhibition of homologous recombination in human cells by targeting RAD51 recombinase. J. Med. Chem. *55*, 3011–3020.

Hyrien, O., Marheineke, K., and Goldar, A. (2003). Paradoxes of eukaryotic DNA replication: MCM proteins and the random completion problem. Bioessays *25*, 116–125.

Iannascoli, C., Palermo, V., Murfuni, I., Franchitto, A., and Pichierri, P. (2015). The WRN exonuclease domain protects nascent strands from pathological MRE11/EXO1-dependent degradation. Nucleic Acids Res. *43*, 9788–9803.

Ilves, I., Petojevic, T., Pesavento, J.J., and Botchan, M.R. (2010). Activation of the MCM2-7 helicase by association with Cdc45 and GINS proteins. Mol. Cell *37*, 247–258.

Issaeva, N., Schultz, N., Helleday, T., Petermann, E., and Lui, M. (2010). Article Hydroxyurea-Stalled Replication Forks Become Progressively Inactivated and Require Two Different RAD51-Mediated Pathways for Restart and Repair. 492–502.

Jensen, R.B., Carreira, A., and Kowalczykowski, S.C. (2010). Purified human BRCA2 stimulates RAD51-mediated recombination. Nature *467*, 678–683.

Jossen, R., and Bermejo, R. (2013). The DNA damage checkpoint response to replication stress: A Game of Forks. Front. Genet. *4*, 1–14.

Kamath-Loeb, A.S., Johansson, E., Burgers, P.M., and Loeb, L.A. (2000). Functional interaction between the Werner Syndrome protein and DNA polymerase delta. Proc. Natl. Acad. Sci. U. S. A. *97*, 4603–4608.

Kanamori, M., Seki, M., Yoshimura, A., Tsurimoto, T., Tada, S., and Enomoto, T. (2011). Werner interacting protein 1 promotes binding of Werner protein to template-primer DNA. Biol. Pharm. Bull. *34*, 1314–1318.

Kanu, N., Zhang, T., Burrell, R.A., Chakraborty, A., Cronshaw, J., Costa, C.D., Grönroos, E., Pemberton, H.N., Anderton, E., Gonzalez, L., et al. (2015). RAD18, WRNIP1 and ATMIN promote ATM signalling in response to replication stress. Oncogene.

Kawabata, T., Luebben, S.W., Yamaguchi, S., Ilves, I., Matise, I., Buske, T., Botchan, M.R., and Shima, N. (2011). Stalled fork rescue via dormant replication origins in unchallenged S phase promotes proper chromosome segregation and tumor suppression. Mol. Cell *41*, 543–553.

Kawabe, Y., Branzei, D., Hayashi, T., Suzuki, H., Masuko, T., Onoda, F., Heo, S.-J., Ikeda, H., Shimamoto, A., Furuichi, Y., et al. (2001). A Novel Protein Interacts with the Werner's Syndrome Gene Product Physically and Functionally. J. Biol. Chem. *276*, 20364–20369.

Kawabe, Y., Seki, M., Yoshimura, A., Nishino, K., Hayashi, T., Takeuchi, T., Iguchi, S., Kusa, Y., Ohtsuki, M., Tsuyama, T., et al. (2006). Analyses of the interaction of WRNIP1 with Werner syndrome protein (WRN) in vitro and in the cell. DNA Repair (Amst). *5*, 816–828.

Kawabe Yi, Branzei, D., Hayashi, T., Suzuki, H., Masuko, T., Onoda, F., Heo, S.J., Ikeda, H., Shimamoto, a, Furuichi, Y., et al. (2001). A novel protein interacts with the Werner's syndrome gene product physically and functionally. J. Biol. Chem. *276*, 20364–20369.

Kim, J.C., and Mirkin, S.M. (2015). Putting the Brakes on Huntington Disease in a Mouse Experimental Model. PLoS Genet. *11*, e1005409.

Kim, J.-H., Kang, Y.-H., Kang, H.-J., Kim, D.-H., Ryu, G.-H., Kang, M.-J., and Seo, Y.-S. (2005). In vivo and in vitro studies of Mgs1 suggest a link between genome instability and Okazaki fragment processing. Nucleic Acids Res. *33*, 6137–6150.

Kotsantis, P., Jones, R.M., Higgs, M.R., and Petermann, E. (2015). Cancer Therapy and Replication Stress: Forks on the Road to Perdition (Elsevier Inc.).

Kowalczykowski, S.C. (2015). An Overview of the Molecular Mechanisms of Recombinational DNA Repair. Cold Spring Harb. Perspect. Biol. *7*, a016410 – .

Krokan, H., Wist, E., and Krokan, R.H. (1981). Aphidicolin inhibits DNA synthesis by DNA polymerase alpha and isolated nuclei by a similar mechanism. Nucleic Acids Res. *9*, 4709–4719.

Leman, A.R., and Noguchi, E. (2013). The replication fork: understanding the eukaryotic replication machinery and the challenges to genome duplication. Genes (Basel). *4*, 1–32.

Liao, S., Guay, C., Toczylowski, T., and Yan, H. (2012). Analysis of MRE11's function in the 5'-->3' processing of DNA double-strand breaks. Nucleic Acids Res. *40*, 4496–4506.

Liu, J., Doty, T., Gibson, B., and Heyer, W.-D. (2010). Human BRCA2 protein promotes RAD51 filament formation on RPA-covered single-stranded DNA. Nat. Struct. Mol. Biol. *17*, 1260–1262.

Liu, Q., Guntuku, S., Cui, X.S., Matsuoka, S., Cortez, D., Tamai, K., Luo, G., Carattini-Rivera, S., DeMayo, F., Bradley, A., et al. (2000). Chk1 is an essential kinase that is regulated by Atr and required for the G(2)/M DNA damage checkpoint. Genes Dev. *14*, 1448–1459.

Lopes, M., Cotta-Ramusino, C., Pellicioli, A., Liberi, G., Plevani, P., Muzi-Falconi, M., Newlon, C.S., and Foiani, M. (2001). The DNA replication checkpoint response stabilizes stalled replication forks. Nature *412*, 557–561.

Lopes, M., Foiani, M., and Sogo, J.M. (2006). Multiple mechanisms control chromosome

integrity after replication fork uncoupling and restart at irreparable UV lesions. Mol. Cell *21*, 15–27.

Lord, C.J., and Ashworth, A. (2007). RAD51, BRCA2 and DNA repair: a partial resolution. Nat. Struct. Mol. Biol. *14*, 461–462.

Lukk, M., Kapushesky, M., Nikkilä, J., Parkinson, H., Goncalves, A., Huber, W., Ukkonen, E., and Brazma, A. (2010). A global map of human gene expression. Nat. Biotechnol. *28*, 322–324.

Madaan, K., Kaushik, D., and Verma, T. (2012). Hydroxyurea: a key player in cancer chemotherapy. Expert Rev. Anticancer Ther. *12*, 19–29.

Mailand, N., Gibbs-Seymour, I., and Bekker-Jensen, S. (2013). Regulation of PCNA-protein interactions for genome stability. Nat. Rev. Mol. Cell Biol. *14*, 269–282.

Masai, H., Matsumoto, S., You, Z., Yoshizawa-Sugata, N., and Oda, M. (2010). Eukaryotic chromosome DNA replication: where, when, and how? Annu. Rev. Biochem. *79*, 89–130.

McAllister, K.A., Bennett, L.M., Houle, C.D., Ward, T., Malphurs, J., Collins, N.K., Cachafeiro, C., Haseman, J., Goulding, E.H., Bunch, D., et al. (2002). Cancer susceptibility of mice with a homozygous deletion in the COOH-terminal domain of the Brca2 gene. Cancer Res. *62*, 990–994.

McMurray, C.T. (2010). Mechanisms of trinucleotide repeat instability during human development. Nat. Rev. Genet. *11*, 786–799.

Méndez, J., and Stillman, B. (2000). Chromatin association of human origin recognition complex, cdc6, and minichromosome maintenance proteins during the cell cycle: assembly of prereplication complexes in late mitosis. Mol. Cell. Biol. *20*, 8602–8612.

Meselson, M., and Stahl, F.W. (1958). THE REPLICATION OF DNA IN ESCHERICHIA COLI. Proc. Natl. Acad. Sci. U. S. A. *44*, 671–682.

Mirzoeva, O.K., and Petrini, J.H.J. (2003). DNA Replication-Dependent Nuclear Dynamics of the Mre11 Complex. Mol. Cancer Res. *1*, 207–218.

Moldovan, G.-L., Pfander, B., and Jentsch, S. (2007). PCNA, the Maestro of the Replication Fork. Cell *129*, 665–679.

Moldovan, G.-L., Dejsuphong, D., Petalcorin, M.I.R., Hofmann, K., Takeda, S., Boulton, S.J., and D'Andrea, A.D. (2012). Inhibition of homologous recombination by the PCNA-interacting protein PARI. Mol. Cell *45*, 75–86.

Mourón, S., Rodriguez-Acebes, S., Martínez-Jiménez, M.I., García-Gómez, S., Chocrón, S., Blanco, L., and Méndez, J. (2013). Repriming of DNA synthesis at stalled replication forks by human PrimPol. Nat. Struct. Mol. Biol. *20*, 1383–1389.

Moynahan, M.E., and Jasin, M. (2010). Mitotic homologous recombination maintains genomic stability and suppresses tumorigenesis. Nat. Rev. Mol. Cell Biol. *11*, 196–207.

Murfuni, I., De Santis, A., Federico, M., Bignami, M., Pichierri, P., and Franchitto, A. (2012). Perturbed replication induced genome wide or at common fragile sites is differently managed in the absence of WRN. Carcinogenesis *33*, 1655–1663.

Navarro, S., Meza, N.W., Quintana-Bustamante, O., Casado, J.A., Jacome, A., McAllister, K., Puerto, S., Surrallés, J., Segovia, J.C., and Bueren, J.A. (2006). Hematopoietic dysfunction in a mouse model for Fanconi anemia group D1. Mol. Ther. *14*, 525–535.

Neelsen, K.J., and Lopes, M. (2015). Replication fork reversal in eukaryotes: from dead end to dynamic response. Nat. Rev. Mol. Cell Biol. *16*, 207–220.

Neelsen, K.J., Zanini, I.M.Y., Herrador, R., and Lopes, M. (2013). Oncogenes induce genotoxic stress by mitotic processing of unusual replication intermediates. J. Cell Biol. *200*, 699–708.

Negrini, S., Gorgoulis, V.G., and Halazonetis, T.D. (2010). Genomic instability--an evolving hallmark of cancer. Nat. Rev. Mol. Cell Biol. *11*, 220–228.

Nick McElhinny, S.A., Kumar, D., Clark, A.B., Watt, D.L., Watts, B.E., Lundström, E.-B., Johansson, E., Chabes, A., and Kunkel, T.A. (2010). Genome instability due to ribonucleotide incorporation into DNA. Nat. Chem. Biol. *6*, 774–781.

Nimonkar, A. V, Genschel, J., Kinoshita, E., Polaczek, P., Campbell, J.L., Wyman, C., Modrich, P., and Kowalczykowski, S.C. (2011). BLM-DNA2-RPA-MRN and EXO1-BLM-RPA-MRN constitute two DNA end resection machineries for human DNA break repair. Genes Dev. *25*, 350–362.

O'Driscoll, M., Ruiz-Perez, V.L., Woods, C.G., Jeggo, P.A., and Goodship, J.A. (2003). A splicing mutation affecting expression of ataxia-telangiectasia and Rad3-related protein (ATR) results in Seckel syndrome. Nat. Genet. *33*, 497–501.

Paeschke, K., Bochman, M.L., Garcia, P.D., Cejka, P., Friedman, K.L., Kowalczykowski, S.C., and Zakian, V.A. (2013). Pif1 family helicases suppress genome instability at G-quadruplex motifs. Nature *497*, 458–462.

Paixão, S., Colaluca, I.N., Cubells, M., Peverali, F.A., Destro, A., Giadrossi, S., Giacca, M., Falaschi, A., Riva, S., and Biamonti, G. (2004). Modular structure of the human lamin B2 replicator. Mol. Cell. Biol. *24*, 2958–2967.

Patnaik, M.M., and Tefferi, A. (2016). Chronic Myelomonocytic Leukemia: Focus on Clinical Practice. Mayo Clin. Proc. *91*, 259–272.

Paull, T.T., and Gellert, M. (1998). The 3' to 5' exonuclease activity of Mre 11 facilitates repair of DNA double-strand breaks. Mol. Cell *1*, 969–979.

Petermann, E., and Helleday, T. (2010). Pathways of mammalian replication fork restart. Nat. Rev. Mol. Cell Biol. *11*, 683–687.

Petermann, E., Orta, M.L., Issaeva, N., Schultz, N., and Helleday, T. (2010). Hydroxyurea-stalled replication forks become progressively inactivated and require two different RAD51-mediated pathways for restart and repair. Mol. Cell *37*, 492–502.

Petrucelli, N., Daly, M.B., and Feldman, G.L. (2013). BRCA1 and BRCA2 Hereditary Breast and Ovarian Cancer.

Pichierri, P., Franchitto, A., Mosesso, P., Palitti, F., and Molecolare, C. (2001). Werner ' s Syndrome Protein Is Required for Correct Recovery after Replication Arrest and DNA Damage Induced in S-Phase of Cell Cycle. Mol. Biol. Cell *12*, 2412–2421.

Pirzio, L.M., Pichierri, P., Bignami, M., and Franchitto, A. (2008). Werner syndrome helicase activity is essential in maintaining fragile site stability. J. Cell Biol. *180*, 305–314.

Poli, J., Tsaponina, O., Crabbé, L., Keszthelyi, A., Pantesco, V., Chabes, A., Lengronne, A., and Pasero, P. (2012). dNTP pools determine fork progression and origin usage under replication stress. EMBO J. *31*, 883–894.

Rajaram, M., Zhang, J., Wang, T., Li, J., Kuscu, C., Qi, H., Kato, M., Grubor, V., Weil, R.J., Helland, A., et al. (2013). Two Distinct Categories of Focal Deletions in Cancer Genomes. PLoS One *8*, e66264.

Ray Chaudhuri, A., Hashimoto, Y., Herrador, R., Neelsen, K.J., Fachinetti, D., Bermejo, R., Cocito, A., Costanzo, V., and Lopes, M. (2012). Topoisomerase I poisoning results in PARP-mediated replication fork reversal. Nat. Struct. Mol. Biol. *19*, 417–423.

Richardson, C. (2005). RAD51, genomic stability, and tumorigenesis. Cancer Lett. *218*, 127–139.

Sale, J.E., Lehmann, A.R., and Woodgate, R. (2012). Y-family DNA polymerases and their role in tolerance of cellular DNA damage. Nat. Rev. Mol. Cell Biol. *13*, 141–152.

Santamaria, D. (2000). Bi-directional replication and random termination. Nucleic Acids Res. *28*, 2099–2107.

Schlacher, K., Christ, N., Siaud, N., Egashira, A., Wu, H., and Jasin, M. (2011). Double-Strand Break Repair-Independent Role for BRCA2 in Blocking Stalled Replication Fork Degradation by MRE11. Cell *145*, 529–542.

Schlacher, K., Wu, H., and Jasin, M. (2012). A Distinct Replication Fork Protection Pathway Connects Fanconi Anemia Tumor Suppressors to RAD51-BRCA1/2. Cancer Cell *22*, 106–116.

Sclafani, R.A. (2000). Cdc7p-Dbf4p becomes famous in the cell cycle. J. Cell Sci. *113*, 2111–2117.

Shechter, D., Costanzo, V., and Gautier, J. (2004). ATR and ATM regulate the timing of DNA replication origin firing. Nat. Cell Biol. *6*, 648–655.

Shiloh, Y. (1997). Ataxia-telangiectasia and the Nijmegen breakage syndrome: related disorders but genes apart. Annu. Rev. Genet. *31*, 635–662.

Shiloh, Y., and Kastan, M.B. (2001). ATM: genome stability, neuronal development, and cancer cross paths. Adv. Cancer Res. *83*, 209–254.

Sidorova, J.M., Li, N., Folch, A., and Monnat, R.J. (2008). The RecQ helicase WRN is required for normal replication fork progression after DNA damage or replication fork arrest. Cell Cycle *7*, 796–807.

Simandlova, J., Zagelbaum, J., Payne, M.J., Chu, W.K., Shevelev, I., Hanada, K., Chatterjee, S., Reid, D.A., Liu, Y., Janscak, P., et al. (2013). FBH1 helicase disrupts RAD51 filaments in vitro and modulates homologous recombination in mammalian cells. J. Biol. Chem. *288*, 34168–34180.

Söderberg, O., Leuchowius, K.-J., Gullberg, M., Jarvius, M., Weibrecht, I., Larsson, L.-G., and Landegren, U. (2008). Characterizing proteins and their interactions in cells and tissues using the in situ proximity ligation assay. Methods *45*, 227–232.

Somyajit, K., Saxena, S., Babu, S., Mishra, A., and Nagaraju, G. (2015). Mammalian RAD51 paralogs protect nascent DNA at stalled forks and mediate replication restart. Nucleic Acids Res. *43*, 9835–9855.

Sørensen, C.S., Syljuåsen, R.G., Falck, J., Schroeder, T., Rönnstrand, L., Khanna, K.K., Zhou, B.-B., Bartek, J., and Lukas, J. (2003). Chk1 regulates the S phase checkpoint by coupling the physiological turnover and ionizing radiation-induced accelerated proteolysis of Cdc25A. Cancer Cell *3*, 247–258.

Su, F., Mukherjee, S., Yang, Y., Mori, E., Bhattacharya, S., Kobayashi, J., Yannone, S.M., Chen, D.J., and Asaithamby, A. (2014). Nonenzymatic role for WRN in preserving nascent DNA strands after replication stress. Cell Rep. *9*, 1387–1401.

Szekely, A.M., Chen, Y.H., Zhang, C., Oshima, J., and Weissman, S.M. (2000). Werner protein recruits DNA polymerase delta to the nucleolus. Proc. Natl. Acad. Sci. U. S. A. *97*, 11365–11370.

Tercero, J.A., Longhese, M.P., and Diffley, J.F.X. (2003). A central role for DNA replication forks in checkpoint activation and response. Mol. Cell *11*, 1323–1336.

Thangavel, S., Berti, M., Levikova, M., Pinto, C., Gomathinayagam, S., Vujanovic, M., Zellweger, R., Moore, H., Lee, E.H., Hendrickson, E.A., et al. (2015). DNA2 drives processing and restart of reversed replication forks in human cells. J. Cell Biol. *208*, 545–562.

Toledo, L.I., Altmeyer, M., Rask, M.-B., Lukas, C., Larsen, D.H., Povlsen, L.K., Bekker-Jensen, S., Mailand, N., Bartek, J., and Lukas, J. (2013). ATR prohibits replication catastrophe by preventing global exhaustion of RPA. Cell *155*, 1088–1103.

Tsurimoto, T., Shinozaki, A., Yano, M., Seki, M., and Enomoto, T. (2005). Human Werner helicase interacting protein 1 (WRNIP1) functions as a novel modulator for DNA polymerase delta. Genes Cells *10*, 13–22.

Veaute, X., Jeusset, J., Soustelle, C., Kowalczykowski, S.C., Le Cam, E., and Fabre, F. (2003). The Srs2 helicase prevents recombination by disrupting Rad51 nucleoprotein filaments. Nature *423*, 309–312.

Vijeh Motlagh, N.D., Seki, M., Branzei, D., and Enomoto, T. (2006). Mgs1 and

Rad18/Rad5/Mms2 are required for survival of Saccharomyces cerevisiae mutants with novel temperature/cold sensitive alleles of the DNA polymerase delta subunit, Pol31. DNA Repair (Amst). *5*, 1459–1474.

Wang, L.C., and Gautier, J. (2010). The Fanconi anemia pathway and ICL repair: implications for cancer therapy. Crit. Rev. Biochem. Mol. Biol. *45*, 424–439.

Ward, I.M., and Chen, J. (2001). Histone H2AX Is Phosphorylated in an ATR-dependent Manner in Response to Replicational Stress. J. Biol. Chem. *276*, 47759–47762.

Watanabe, Y., and Maekawa, M. (2010). Spatiotemporal regulation of DNA replication in the human genome and its association with genomic instability and disease. Curr. Med. Chem. *17*, 222–233.

Wyrick, J.J., Aparicio, J.G., Chen, T., Barnett, J.D., Jennings, E.G., Young, R.A., Bell, S.P., and Aparicio, O.M. (2001). Genome-wide distribution of ORC and MCM proteins in S. cerevisiae: high-resolution mapping of replication origins. Science *294*, 2357–2360.

Yang, Y., Liu, Z., Wang, F., Temviriyanukul, P., Ma, X., Tu, Y., Lv, L., Lin, Y.-F., Huang, M., Zhang, T., et al. (2015). FANCD2 and REV1 cooperate in the protection of nascent DNA strands in response to replication stress. Nucleic Acids Res. *43*, 8325–8339.

Yarbro, J. (1992). Mechanism of action of hydroxyurea. Semin. Oncol. *19*, 1–10.

Yeeles, J.T.P., Poli, J., Marians, K.J., and Pasero, P. (2013). Rescuing Stalled or Damaged Replication Forks. Cold Spring Harb. Perspect. Biol. *5*, a012815–a012815.

Ying, S., Hamdy, F.C., and Helleday, T. (2012). Mre11-Dependent Degradation of Stalled DNA Replication Forks Is Prevented by BRCA2 and PARP1. *72*, 2814–2822.

Yoshimura, A., Seki, M., Kanamori, M., Tateishi, S., Tsurimoto, T., Tada, S., and Enomoto, T. (2009). Physical and functional interaction between WRNIP1 and RAD18. Genes Genet. Syst. *84*, 171–178.

Zellweger, R., Dalcher, D., Mutreja, K., Berti, M., Schmid, J.A., Herrador, R., Vindigni, A., and Lopes, M. (2015). Rad51-mediated replication fork reversal is a global response to genotoxic treatments in human cells. J. Cell Biol. *208*, 563–579.

Zeman, M.K., and Cimprich, K.A. (2014). Causes and consequences of replication stress. Nat. Cell Biol. *16*, 2–9.

Zhou, B.-B.S., and Bartek, J. (2004). Targeting the checkpoint kinases: chemosensitization versus chemoprotection. Nat. Rev. Cancer *4*, 216–225.

Zhou, B.B., and Elledge, S.J. (2000). The DNA damage response: putting checkpoints in perspective. Nature *408*, 433–439.

Zhu, W., Ukomadu, C., Jha, S., Senga, T., Dhar, S.K., Wohlschlegel, J.A., Nutt, L.K., Kornbluth, S., and Dutta, A. (2007). Mcm10 and And-1/CTF4 recruit DNA polymerase alpha to chromatin for initiation of DNA replication. Genes Dev. *21*, 2288–2299.

Zou, L., and Elledge, S.J. (2003). Sensing DNA damage through ATRIP recognition of RPA-ssDNA complexes. Science *300*, 1542–1548.

Zou, L., Cortez, D., and Elledge, S.J. (2002). Regulation of ATR substrate selection by Rad17-dependent loading of Rad9 complexes onto chromatin. Genes Dev. *16*, 198–208.

Zou, L., Liu, D., and Elledge, S.J. (2003). Replication protein A-mediated recruitment and activation of Rad17 complexes. Proc. Natl. Acad. Sci. U. S. A. *100*, 13827–13832.

7. ACKNOWLEDGMENTS

I would like to express my sincere gratitude to my group leaders Dr.ssa Annapaola Franchitto and Dr. Pietro Pichierri for giving me the opportunity to pursue my doctoral studies in their labs.

In particular, I am deeply grateful to my supervisor Dr.ssa Annapaola Franchitto who has been a great source of motivation, and under her guidance I have learned and achieved a lot both scientifically and personally. The Ph.D. project has been particularly challenging and I really appreciate her scientific guidance and patience through tough times. Her flexibility in scheduling, gentle encouragement and relaxed demeanor made for a good working relationship and the impetus for me to produce good results. I acknowledge the scientific freedom she has provided, which allowed me to develop my independent thinking. I am also very grateful to Dr. Pietro Pichierri for his scientific advice and knowledge and many insightful discussions and suggestions.

My gratitude is also extended to all my colleagues of the *Genome Stability Group* for their support: Anita Palma, Eva Malacaria, Monia Pugliese, Valentina Palermo, Giorgia Basile, Ivana Murfuni, Chiara Iannascoli, Francesca Cremona and Francesca Grillini. I would also like to give a special thanks to Veronica Marabitti, who has contributed not only to some experiments of this work, but also she has turned out to be a friend and supporter.

I am also grateful to Dr.ssa Eugenia Dogliotti, for welcoming me into the whole group of the Molecular Epidemiology lab. Especially thanks to Filomena Mazzei Marco Crescenzi, Margherita Bignami, Riccardo Crebelli, Fiorella Malchiodi, Pompeo Macioce and Marina Ceccarini for their hospitality in their labs for my experiments. I express my thanks to Professor Giorgio Prantera. I gratefully acknowledge the AIRC funding sources that made my doctoral studies possible.

On a personal note, I extend my deepest regards and love to my parents for shaping me into the individual that I have become. Heartfelt thanks to my sister for cheering me up. I am also grateful to my friends Federica, Diletta, Andrea, Alberto and Ianna. Last, but certainly not least, I must acknowledge with tremendous and deep thanks my partner, Paola. Her love, support, and belief in me are a treasure, which allows me to overcome the obstacles of the life with lightness.

Thank you all.